

Magnetic Resonance

HST.584J / 22.561

**Compiled and Written By:
Faith Van Nice 1992, Mark Haig Khachaturian 2002**

**Instructors: Bruce Rosen M.D., Ph.D.
Larry Wald Ph.D.**

TABLE OF CONTENTS

Acronyms & Symbols	1
Chapter 1: Introduction	2
Chapter 2: Basic NMR	4
Chapter 3: Relaxation	16
Chapter 4: Liquid Spectroscopy	26
Chapter 5: Fourier Transform Theorems	36
Chapter 6: Introduction to Imaging	38
Chapter 7: NMR Imaging	45
Chapter 8: Chemical Shift Imaging	66
Chapter 9: Flow Imaging	71
Chapter 10: Microscopic Motions	78
Chapter 11: Rapid Imaging	81

ACRONYMS & SYMBOLS

NMR – Nuclear Magnetic Resonance

MRI – Magnetic Resonance Imaging

μ - Magnetic Dipole Moment

F{ } – Fourier Transform

TR – Repetition Time

TE – Echo Time

TI – Inversion Time

STIR – Short TI Inversion Recovery

CHAPTER 1: INTRODUCTION

Substances respond to magnetic fields in varying degrees. For instance, if we measure the force on a material in a magnetic field \mathbf{B} , we get the following ($\mathbf{B} = 1.8 \text{ T}$):

Water	-22 dynes
Cu	-2.6 dynes
CuCl ₂	+280 dynes
InO ₂	+7500 dynes
Fe	+4x10 ⁵ dynes

Magnetic fields interact with one another, but they also induce magnetism in matter. Force on a magnetic dipole

$$\mathbf{F} = \mu \frac{d\mathbf{B}}{dz}$$

μ = magnetic dipole moment (for a current loop, $\mu = \pi r^2 I$; I = current, r = radius of loop).

This helps understand the table above. It implies that in a magnetic field, for most materials,

$$\mu \propto \pm B.$$

Thus, as \mathbf{B} decreases, $\frac{d\mathbf{B}}{dz}$ decreases, μ decreases, and the force decreases by both terms.

An applied magnetic field, \mathbf{B} , induces a magnetic moment in material, but the direction of the magnetic moment depends on the type of material. For instance, a **diamagnetic** material (e.g. water) is repelled in a magnetic field, implying that the direction of μ is opposite that of \mathbf{B} . Magnetic fields cause the orbital electrons to speed up or slow down depending on the orientation, or direction of the electron spins. This induces a current (Lenz's Law) such that the magnetic field of the induced current is opposite that of the applied field. The resulting magnetic moment, μ , opposes \mathbf{B}

$$\mu = \frac{ne^2 r^2 \mathbf{B}}{6m_e c^2}$$

where n = number of electrons per gram, e is the elementary charge, and m_e is the mass of the electron. (Note: assume cancellation of the average orbital angular momentum).

Paramagnetic materials, on the other hand, are attracted to a stronger magnetic field. The magnetic moment aligns with the applied magnetic field (as a compass needle does). Examples of paramagnetic materials includes atoms or molecules that possess an odd number of electrons so that the total spin of the system is not zero (e.g. organic free radicals, or nitric oxide, NO). Transition elements such as manganese and gadolinium, and some metals are also paramagnetic.

The **net magnetization**, \mathbf{M} , ($\mathbf{M} = \sum \mu$) is a function of the **magnetic susceptibility**, χ , which is defined as

$$\chi = \frac{\mathbf{M}}{\mathbf{B}}.$$

A diamagnetic material has a negative χ , while a paramagnetic material has a positive magnetic susceptibility.

Ferromagnetism refers to materials with a spontaneous magnetic moment, such as iron. This suggests that even in zero magnetic field, the electron spins and magnetic moments are arranged in some regular pattern. We will limit our discussion to diamagnetic and paramagnetic materials in this course.

CHAPTER 2: BASIC NMR

We will refer to three different magnetic fields in this course:

- (1) \mathbf{B}_0 – large, static field (> 1 Tesla typically; $1 \text{ T} = 10,000$ Gauss)
- (2) \mathbf{B}_1 – oscillating radio frequency (rf) field (1-100 Gauss)
- (3) $\boldsymbol{\mu}$ - magnetic moment of a nucleus (few Gauss)

Nuclei with nonzero nuclear spin quantum numbers (e.g. if the nucleus possesses an odd number of protons or neutrons) have angular momentum. Examples are ^1H , ^{13}C , ^{19}F , and ^{31}P . The concept of nuclear spin is a result of quantum mechanics. We need not worry about the details of this theory, but it is helpful to highlight some of the important physical features of a nuclear spin. Since the nucleus is charged and is spinning (or rotating due to angular momentum), it creates a small magnetic field which we call the **nuclear magnetic moment**. It can be thought of as a tiny bar magnet with north and south poles. The ratio of the magnetic moment to the angular momentum, \mathbf{J} , is called the gyromagnetic ratio, γ (or sometimes the magnetogyric ratio). Each type of nucleus has a unique γ .

$$\gamma = \left| \frac{\boldsymbol{\mu}}{\mathbf{J}} \right| \quad \boldsymbol{\mu} = \gamma \mathbf{I}$$

where \mathbf{I} is the dimensionless angular momentum operator with eigenvalues of the z-component being $m = I, I - 1, \dots, -I$.

If you put some nuclei in a magnetic field, \mathbf{B}_0 , the interaction energy is

$$E = \boldsymbol{\mu} \cdot \mathbf{B}$$

We define \mathbf{B}_0 to be along the z-axis and the energy is

$$E = \gamma \hbar \mathbf{B}_0$$

where m is defined above.

Protons have spin quantum number $I = \frac{1}{2}$ so that energy levels available to the spin system are $E = \pm \gamma \hbar B_0$ and the energy level difference (or frequently called the **resonance frequency**) is (allowed transitions are $\Delta m = \pm 1$)

$$\Delta E = \gamma \hbar B_0.$$

A sketch of the energy level dependence is shown in Figure 1.

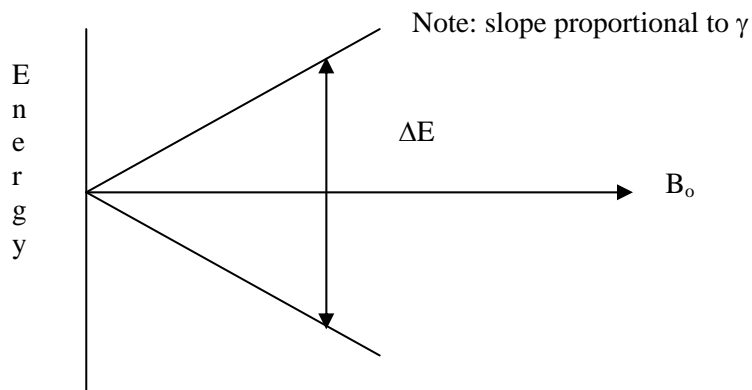


Figure 1 – Energy Level Dependence of Energy Split vs. B_0

Thus, the energy level difference is related to the gyromagnetic ratio and the applied static magnetic field. Some gyromagnetic ratios are given below

Atom	γ (MHz/T)	γ (rad·MHz/T); $\gamma = 2\pi\gamma$
^1H ($I = 1/2$)	42.6	267.7
^{13}C ($I = 1/2$)	10.7	67.2
^{19}F ($I = 1/2$)	40.1	252
^{31}P ($I = 1/2$)	17.2	108

The resonance frequency is referred to as the **Lamor frequency**, ω_L (since $\Delta E = \hbar\omega$)

$$\omega_L = \gamma |\mathbf{B}_0|.$$

This is important because if we want to study the spin system we must use energy at the Lamor frequency of the allowed energy transition. For example, in a 1.5 T field, the resonance frequency for protons is about 63 MHz. If we put in energy at 100 MHz, nothing will happen to the system, since photons can neither be absorbed nor emitted at this frequency. (A note about frequencies, i.e. in Hz, because it is easier to say, and write, than radians/second).

Now, when a spin system (or ensemble of protons) is not in the presence of a large magnetic field, there is no preferred orientation of the individual magnetic moments and consequently no net magnetization is generated. The reason for this is that the magnitude of the magnetic moments and the earth's magnetic field are two small to do any work on the system. On the other hand, when we apply a strong field, we cause the magnetic moments to align with or against the direction of the field (parallel or anti-parallel), in the case of protons. The magnetic field is strong enough to put torque on the spins to do the alignment. The spins (or magnetic moments) do not have equal populations in the two states and the result is a net macroscopic magnetization in the direction of the field since it is the lower energy state (Boltzmann's law). We commonly use arrows to depict a nuclear magnetic moment, since then we can see the magnitude and direction of the moment.

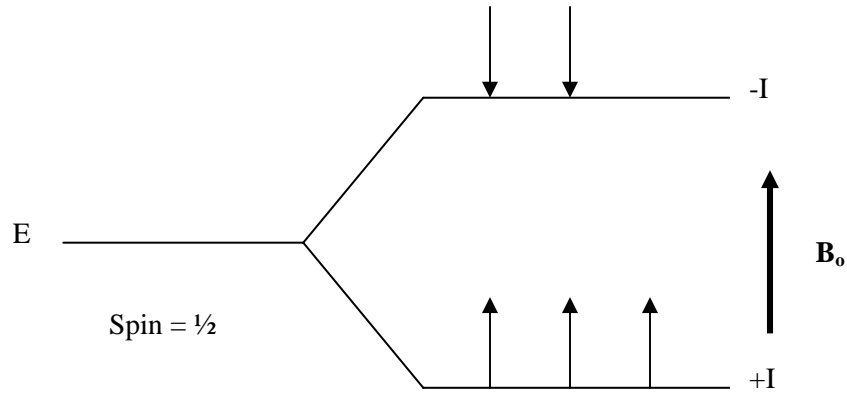


Figure 2 – Energy Level Splitting in a Magnetic Field

We can explain the NMR experiment easily using classical mechanics. We begin with the classical equation of motion that says that the rate of change of angular momentum of a nuclear dipole depends upon the torque exerted on the dipole by the applied magnetic field.

$$\text{Torque} = \frac{d\mathbf{J}}{dt} = \boldsymbol{\mu} \times \mathbf{B}; \quad \boldsymbol{\mu} = \gamma\mathbf{J}$$

Taking $\mathbf{M} = \sum \boldsymbol{\mu}$ and manipulating the equations above we have that:

$$\frac{d\mathbf{M}}{dt} = \gamma\mathbf{M} \times \mathbf{B}$$

where we call \mathbf{M} the net macroscopic magnetization for an ensemble.

A cross-product in mathematics is equivalent to a rotation in the physical world. Thus, what is happening here is that the large static magnetic field puts a torque on the magnetic moments and moments precess, or rotate, around the applied magnetic field (Figure 3). For simplicity, only one magnetic moment is shown in 3a. It follows that an ensemble of spins would inscribe a cone as shown in 3b since there would be no phase coherence between individual magnetic moments. A way to think about this process is to envision a gyroscope. You wind up the gyroscope and set it on the floor and it precesses while it spins. It is that motion that we are dealing with here.

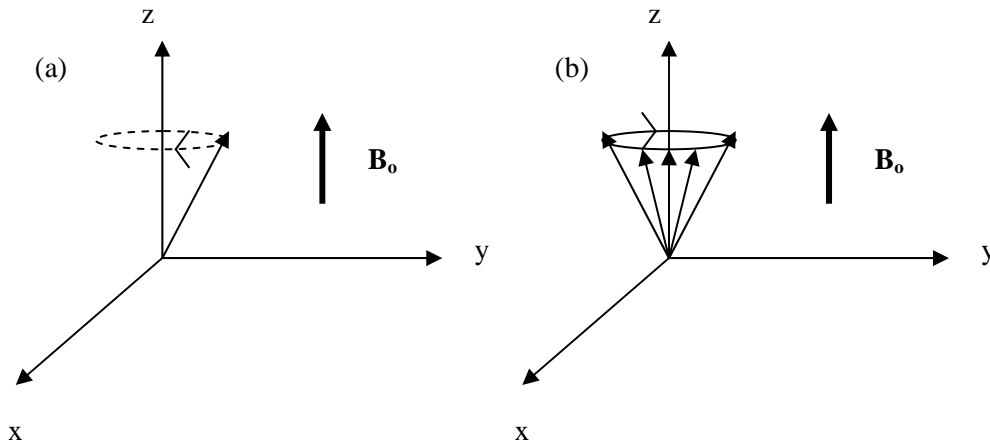


Figure 3 – (a) Precession of a Single Magnetic Moment about the z-axis Due to a Static Magnetic Field and (b) Precession of a Number of Magnetic Moments Along the z-axis Due to a Static Magnetic Field

We can expand the cross-product into matrix form. Remember that $\mathbf{M} = iM_x + jM_y + kM_z$ and same for \mathbf{B} .

$$\frac{d\mathbf{M}}{dt} = \gamma \mathbf{M} \times \mathbf{B} = \gamma \det \begin{pmatrix} i & j & k \\ M_x & M_y & M_z \\ B_x & B_y & B_z \end{pmatrix}$$

$$\frac{d\mathbf{M}}{dt} = i(M_y B_z - M_z B_y) + j(M_z B_x - M_x B_z) + k(M_x B_y - M_y B_x)$$

This an equivalent form of

$$\frac{d\mathbf{M}}{dt} = i \frac{dM_x}{dt} + j \frac{dM_y}{dt} + k \frac{dM_z}{dt}$$

We can break the equation into its pieces and show the time dependence of the motion for each component of \mathbf{M} . First define the components of the magnetic field, \mathbf{B} .

$$\mathbf{B} = \mathbf{B}_o + \mathbf{B}_1 = \text{static} + \text{oscillating}$$

We can create a \mathbf{B}_1 field (oscillating rf field that produces a small magnetic field in a specified direction) that rotates in the x-y plane at a frequency ω . Then

$$B_x = B_1 \cos(\omega t)$$

$$B_y = B_1 \sin(\omega t)$$

$$B_z = B_o$$

Substitute these into the components of $d\mathbf{M}/dt$ and see that:

$$\frac{dM_x}{dt} = \gamma(M_y B_o + M_z B_1 \sin(\omega t)) - \frac{M_x}{T_2}$$

$$\frac{dM_y}{dt} = \gamma(M_z B_1 \cos(\omega t) - M_x B_o) - \frac{M_y}{T_2}$$

$$\frac{dM_z}{dt} = -\gamma(M_x B_1 \sin(\omega t) + M_y B_1 \cos(\omega t)) - \frac{(M_z - M_o)}{T_1}$$

Note that I have added in the relaxation terms from a phenomenological standpoint. The x and y components of \mathbf{M} must go to zero and I have arbitrarily given the time constant for that process T_2 . On the other hand, M_z must return to the equilibrium magnetization which we call M_o or M_{eq} and I have that that time the constant value T_1 . Note that at equilibrium, $M_z = M_o$. These equations are formally called the Bloch equations after Felix Bloch.

Up to this point we have described the system in the **laboratory frame of reference**. As we will see later, it is much easier conceptually to work in a different reference frame called the **rotating frame**. It is quite simple. Imagine grabbing hold of the z-axis of the system in Figure 3b and spinning the x-y plane at the Larmor frequency of the system. Think of it like this: the laboratory frame is like watching a record turn on a turntable, while the rotating frame is like standing on the record itself and rotating with it – now you are able to read the songs on the label without getting dizzy! If we do this to our ensemble of nuclei, we can add up the vector components of the magnetic moment and see that the x and y components cancel each other, while the z-components add (Figure 4).

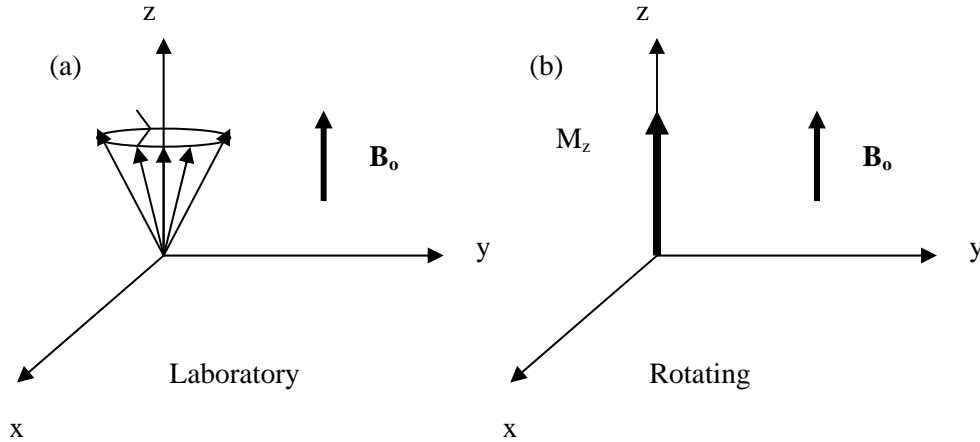


Figure 4- Illustration of the Magnetic Moments in the (a) Laboratory and (b) Rotating Frame

Now we must derive the equations of motion for the components of \mathbf{M} in the rotating frame. The total time derivative of \mathbf{M} is given by

$$\frac{d\mathbf{M}}{dt} = i \frac{dM_x}{dt} + j \frac{dM_y}{dt} + k \frac{dM_z}{dt} + M_x \frac{\partial i}{\partial t} + M_y \frac{\partial j}{\partial t} + M_z \frac{\partial k}{\partial t}$$

The unit vectors i, j, k rotate in the rotating frame, but cannot change length. As we have seen before, a rotation is a cross-product in mathematics. Thus,

$$\begin{aligned} \frac{\partial i}{\partial t} &= \omega \times i \\ \frac{\partial j}{\partial t} &= \omega \times j \\ \frac{\partial k}{\partial t} &= \omega \times k \end{aligned}$$

If we substitute this into the total time derivative, we get

$$\begin{aligned}\left(\frac{d\mathbf{M}}{dt}\right)_{\text{fixed}} &= \frac{\partial\mathbf{M}}{\partial t} + \omega \times (M_x i + M_y j + M_z k) \\ &= \left(\frac{\partial\mathbf{M}}{\partial t}\right)_{\text{rotating}} + \omega \times \mathbf{M}\end{aligned}$$

We know that the left hand side is equal to $\gamma\mathbf{M} \times \mathbf{B}$. Rearranging and substituting

$$\begin{aligned}\left(\frac{\partial\mathbf{M}}{\partial t}\right)_{\text{rotating}} &= \gamma\mathbf{M} \times \mathbf{B} - \omega \times \mathbf{M} \\ &= \gamma\mathbf{M} \times \mathbf{B} - \gamma\mathbf{M} \times \frac{\omega}{\gamma} \\ &= \gamma\mathbf{M} \times \left(\mathbf{B} - \frac{\omega}{\gamma}\right)\end{aligned}$$

We call $\mathbf{B} + \omega/\gamma$ the effective magnetic field, or \mathbf{B}_{eff} . It is apparent then that the magnetization precesses around the effective field in the rotating frame just as the magnetic moments precess around the applied magnetic field in the laboratory frame.

Let's look at the limiting case and see if the total time derivative makes sense with our situation in the rotating frame. If the frequency of the rotating frame equals the frequency of precession

($\omega_{\text{rotating}} = \omega_{\text{precession}} = -\gamma\mathbf{B}_o$), then

$$\left(\frac{\partial\mathbf{M}}{\partial t}\right)_{\text{rotating}} = 0$$

Thus, if the frame of reference rotates at the Larmor frequency, the magnetization is static in the rotating frame, which is what we see in Figure 4b. This simplifies the problem immensely as we try to envision the NMR experiment. For those of you who are still uncomfortable with the idea of the rotating frame, remember that we live in a rotating frame. The earth spins on its axis and precesses around the sun. If you throw a ball in the air, it is a simple problem to describe its trajectory while on earth, but it would be quite a difficult proposition to describe it if you were in outer space.

If we want information about the characteristics of any physical system, we must perturb the system from equilibrium and then measure the energy that is emitted from the system as it returns to equilibrium. In our case, we want to study the magnetization generated by the nuclear spin system in a large static magnetic field. We must figure out a way to perturb the net magnetization away from equilibrium, or the z-axis. We can do this by using another magnetic field, \mathbf{B}_1 . Define

$$\begin{aligned}\mathbf{B}_{\text{lab}} &= \mathbf{B}_o + \mathbf{B}_1 \cos(\omega t)i - \mathbf{B}_1 \sin(\omega t)j \\ \mathbf{B}_{\text{rot}} &= \mathbf{B}_o k + \mathbf{B}_1 i \quad (\text{rotating at } \omega_o)\end{aligned}$$

where we choose only one of the rotating components of the \mathbf{B}_1 field (along the x-axis). This gives

$$\left(\frac{\partial \mathbf{M}}{\partial t}\right)_{\text{rotating}} = \gamma \mathbf{M} \times \left(\mathbf{B}_0 - \frac{\omega}{\gamma} + \mathbf{B}_1\right)$$

If \mathbf{B}_1 is rotating at the Larmor frequency, or $-\gamma \mathbf{B}_0$ (in the opposite direction), then

$$\left(\frac{\partial \mathbf{M}}{\partial t}\right)_{\text{rotating}} = \gamma \mathbf{M} \times \mathbf{B}_1$$

This shows that if we apply an oscillating field, \mathbf{B}_1 , at the Larmor frequency, the magnetization will rotate about the x-axis at $\omega = \gamma \mathbf{B}_1$. (Note: it turns out to be in the clockwise direction about the x-axis. Use the left hand rule and let your thumb be the x-axis). This action tilts the magnetization off the z-axis, i.e. away from equilibrium. Figure 5 summarizes the basic process. We generate a \mathbf{B}_1 field using a radio frequency transmitter and a tuned resonant circuit (Figure 6) where the power is delivered to a solenoid coil (where the sample resides) in a pulse fashion. The amount of precession, θ , of the magnetization about \mathbf{B}_1 depends on the magnitude (power) of the applied field and the duration of the pulse, t.

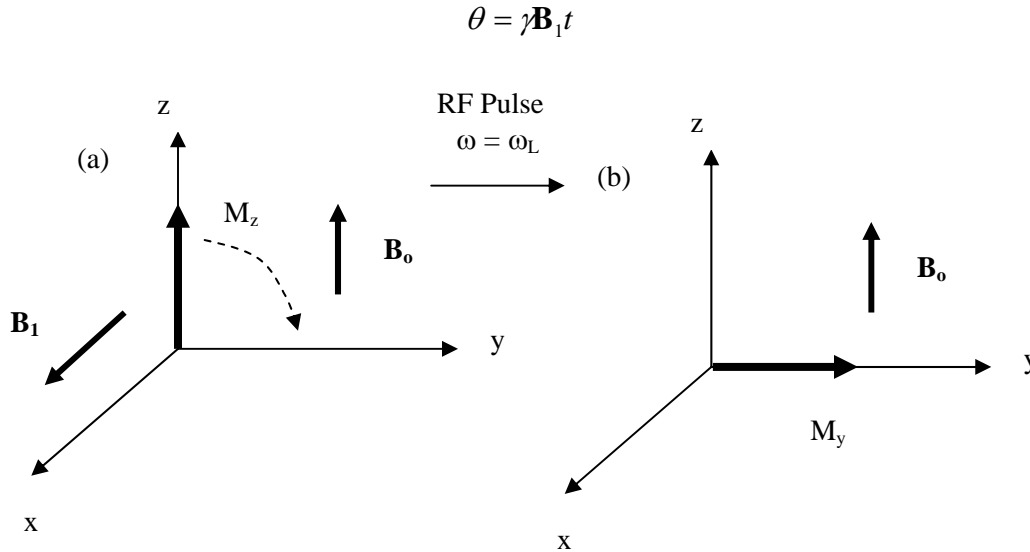


Figure 5 – Motion of the Net Magnetization After a 90° RF Pulse

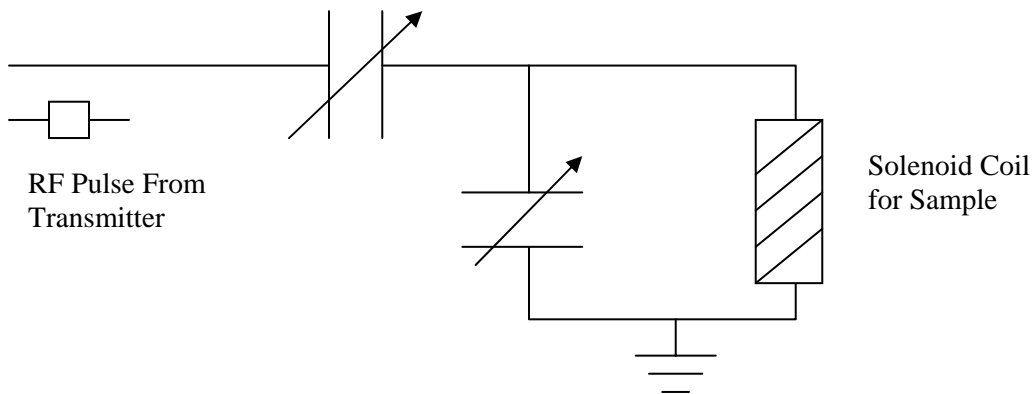


Figure 6 – Common NRM Probe Circuit

Before going on, let us explore the other avenue of applying a \mathbf{B}_1 field that off resonance, i.e. if

$$\frac{\omega_{rf}}{\gamma} \neq \mathbf{B}_o. \text{ Then}$$

$$\begin{aligned} \mathbf{B}_{eff} &= k \left(\mathbf{B}_o - \frac{\omega_{rf}}{\gamma} \right) + i\mathbf{B}_1 \\ &= \sqrt{|\mathbf{B}_1|^2 + \left| \frac{\omega_{rf}}{\gamma} - \mathbf{B}_o \right|^2} \end{aligned}$$

Figure 7 shows the magnetization precession around the effective magnetic field as opposed to precession in the y-z plane when we are on resonance (Figure 5). When ω_{rf} is well below resonance, the effective field is parallel to \mathbf{B}_o . As ω_{rf} approaches resonance, the effective field is perpendicular to \mathbf{B}_o and finally, when ω_{rf} continues above resonance, the \mathbf{B}_{eff} is anti-parallel to \mathbf{B}_o .

An interesting note: In the “old” days of NMR before Fourier transforms and pulse spectroscopy, the experiment was done in “cw” of continuous wave mode. This was done by either varying the frequency of the transmitter, or by varying \mathbf{B}_o . The latter turned out to be technically easier at the time. In the adiabatic slow passage experiment, the magnetization follows the effective field (i.e. continues to align with it) as long as the change in ω_{rf} is much less than the Larmor frequency. That is what is meant by slow passage. In this way one could manipulate the magnetization and study the chemical environment of the spin system. These days virtually all NMR spectroscopy is done using the pulse technique followed by a Fourier transform, but it is important to understand the effective field concept because it is a common to conduct pulse experiments off resonance. This complicates where the magnetization ends up after a pulse and one cannot assume perfect 90° or 180° rotations of the magnetization. This is true the farther off resonance the transmitter frequency is (for small differences in frequency, the effect is negligible).

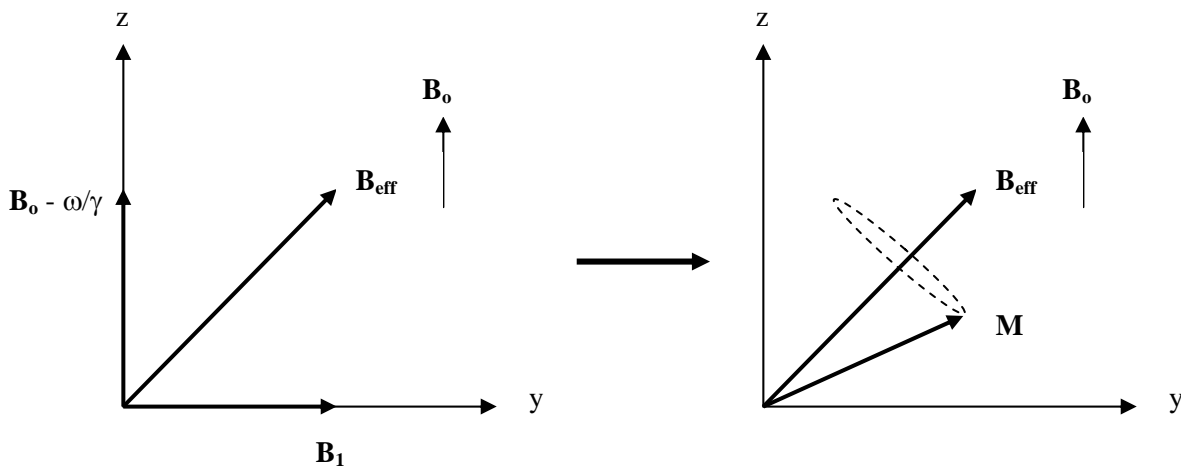


Figure 7 – Precession About the Effective Field

Now we are ready to examine what happens after the radio frequency (rf) pulse is applied and we have rotated the magnetization to the y-axis shown in Figure 5 (assuming resonance conditions). We know

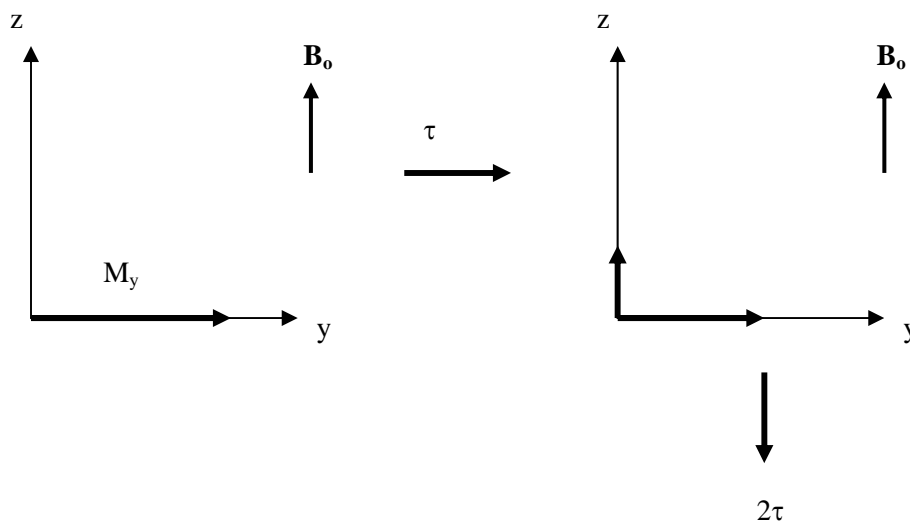
from Thermodynamics that the system will return to thermal equilibrium. The spin system does this through two types of relaxation processes: **longitudinal and transverse relaxation**. The time constants characterizing these processes are T_1 and T_2 , respectively. Longitudinal relaxation is the return of the z-component of the magnetization to the equilibrium value, \mathbf{M}_0 (Figure 8). Following the rf pulse, the z-component of \mathbf{M} is zero. As time elapses, M_z increases exponentially until the equilibrium value is restored.

$$M_z(t) = M_o \left(1 - e^{-\frac{t}{T_1}} \right)$$

Transverse relaxation involves the dephasing of the magnetization in the x-y plane (Figure 9). The reason for this type of dephasing is that the absolute magnitude of the magnetic field is not identical at each nucleus, causing each nucleus to precess at a slightly different frequency than its neighbor. We actually differentiate between the causes of this net loss of coherence into two groups. The time constant T_2 is used when describing the transverse relaxation due to processes intrinsic to the sample, for example, the dipolar interaction among magnetic moments (discussed in detail later). On the other hand, there are causes of transverse relaxation that are the result of experimental error, such as the impossible task of creating a \mathbf{B}_0 field that is absolutely perfect at each point in the sample. This type of relaxation due to inhomogeneities in the experimental environment is given the time constant T_2^* . At any rate, the dephasing of the x-y components of \mathbf{M} cause the generation of tiny current in the sample coil (refer to Figure 6) and the result is a **free induction decay** (FID). The FID is detected with an oscilloscope as a fluctuating voltage (Figure 10). This means that after the rf pulse, M_x and M_y will have the same amplitude as \mathbf{M}_0 and then decay exponentially to zero with time constant T_2^* .

$$M_{x,y}(t) = M_o e^{-\frac{t}{T_2^*}}$$

(Note: the FID shown in Figure 10 is a damped cosine wave which means that the transmitter frequency was slightly off resonance – the oscillations (or beats) are the protons going in and out of phase with the carrier frequency. If the transmitter were exactly on resonance, we would get a smooth exponential without oscillations).



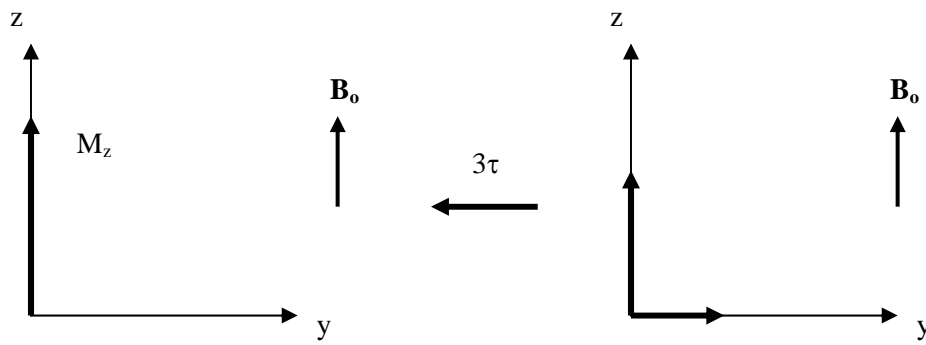


Figure 8 – Longitudinal Relaxation (τ is a time interval)

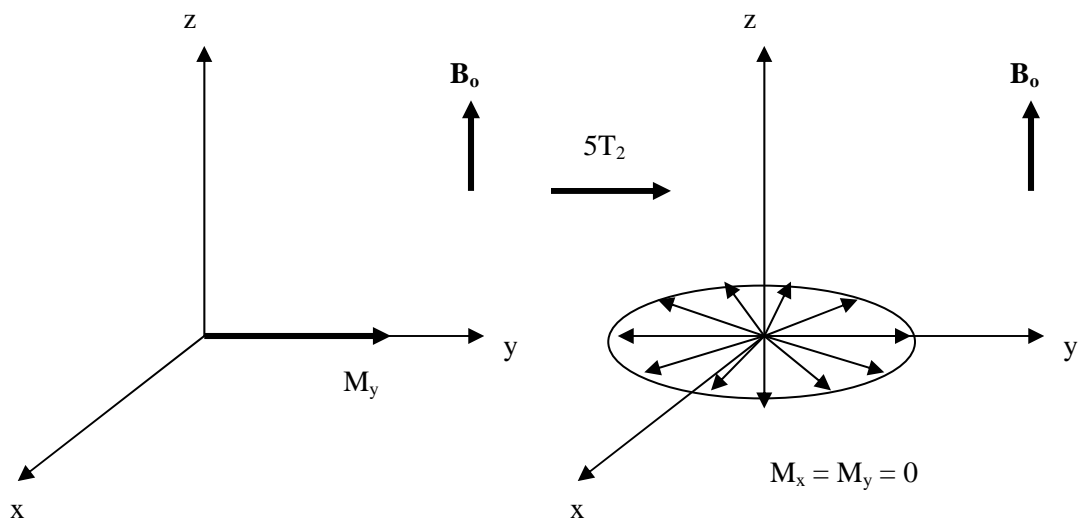


Figure 9 – Transverse Relaxation

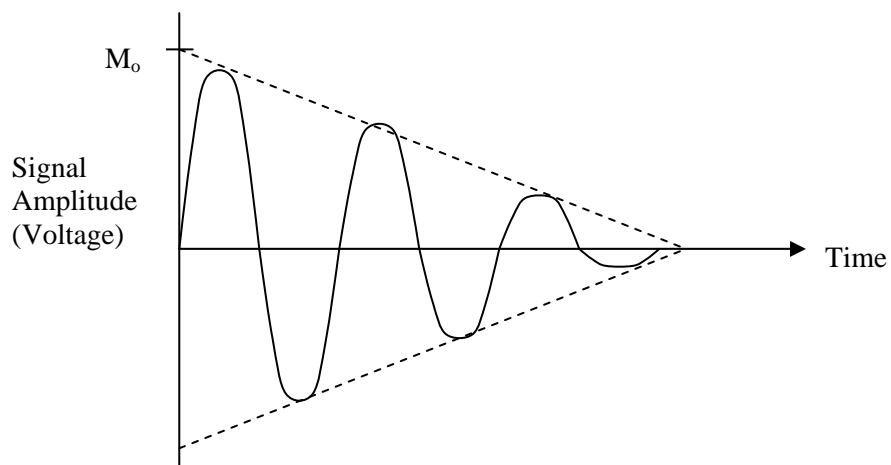


Figure 10 – Signal FID with Decay Envelop

In order to visualize the traverse and longitudinal relaxation, the Bloch equations were solved and Figure 10b shows the path of the net magnetic moment, \mathbf{M} , position as a function of time.

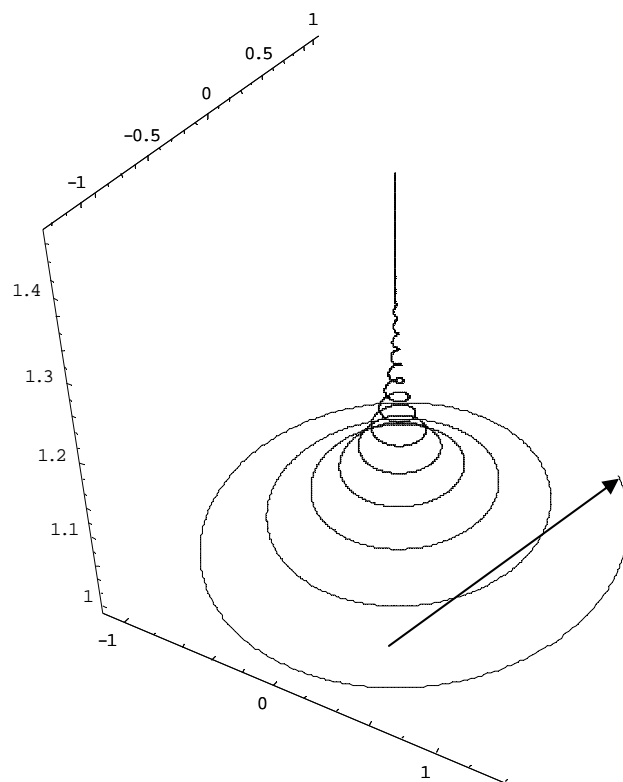


Figure 10b – Path of Net Magnetization Under Both Transverse and Longitudinal Relaxation

Let us estimate the approximate signal amplitude for a 1 cm^3 sample of water in a solenoid consisting of $N = 10$ turns and surface area (A) of 1 cm^2 . The magnetic flux caused by the relaxing nuclei in a 1 T field is on the order of $4 \times 10^{-10} \text{ T}$ (remember $\mathbf{M} = \chi \mathbf{B}$). The voltage induced in the coil is given by

$$emf = NAM\omega \sin(\omega t)$$

which gives an answer on the order of 1 mV. We can see that the signal voltage is proportional to ω^2 (the other ω comes from M). Noise is trickier to evaluate. The amplitude of noise goes anywhere from the fourth root of ω for small samples to ω for large samples. Thus the signal to noise ratio is proportional to ω in the range of ω to $\omega^{7/4}$. The important point here is that the signal in NMR spectroscopy at room temperature is quite small.

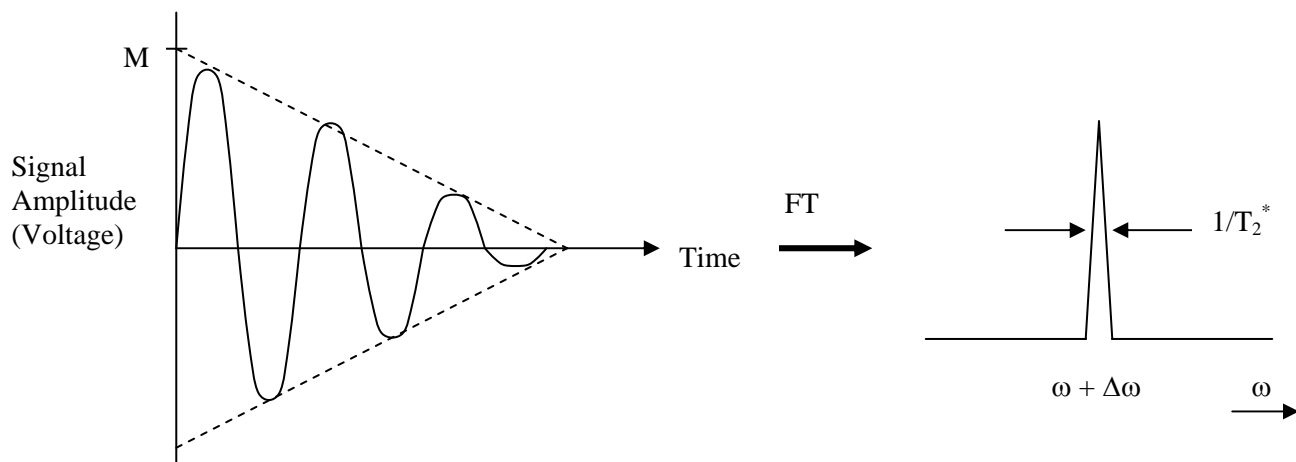
We are now at the point where we have collected the FID, which is a time domain signal. It is difficult to extract information about the system in the time domain and we are often more interested in the frequency components of the signal. We use the Fourier transform (FT) to give us this information

$$A(t) = \frac{1}{2\pi} \int_{-\infty}^{\infty} A(\omega) e^{i\omega t} d\omega$$

and

$$A(\omega) = \frac{1}{2\pi} \int_{-\infty}^{\infty} A(t) e^{-i\omega t} dt$$

where $A(t)$ is the signal function and $A(\omega)$. Conversely, $A(t)$ is the inverse FT (or FT^{-1}) of $A(\omega)$. Figure 11 shows the FT of an FID obtained from a pure water sample. The FT of an exponential is a Lorentzian lineshape. Note that one peak is the result as all the protons in water are essentially equal. Also, the peak is shifted slightly ($\Delta\omega$) since the transmitter frequency was off resonance (thus giving beats in the FID). The width of the peak at half height approximates $1/T_2^*$. Later we will see that NMR and the Fourier transformed spectrum does an excellent job at distinguishing between different types of protons contained within a molecule.



CHAPTER 3: RELAXATION

It is helpful to examine the longitudinal and transverse relaxation in more detail and understand some of the fundamental processes that give rise to relaxation. In NMR spectroscopy, relaxation back to thermal equilibrium is caused by fluctuating local magnetic fields. The term “local” refers to the immediate environment of a nucleus. Since nuclear spins are essentially tiny bar magnets, there exist certain interactions between them. We have all played with bar magnets and felt the forces when two are brought together – this is analogous to the dipolar interaction between magnetic moments, or dipoles. Molecules are continually moving (i.e. translating, rotating, and vibrating) and these motions modulate the interactions among the nuclei. In other words, the molecular motions cause the local magnetic fields to fluctuate and allow the nuclear spins to relax via some well known interaction, like the dipolar interaction, which is most important in spin = ½ systems. Other interactions can be the basis for relaxation such as the electric quadrupole, chemical shift anisotropy, scalar coupling, and spin-rotation interactions. The effectiveness of the relaxation as measured by the relaxation time depends on the magnitude of the interaction, i.e. for large interactions, the relaxation is generally faster.

Consider a water molecule with protons 1 and 2 in a static magnetic field \mathbf{B}_0 (Figure 12). The total magnetic field at proton 1 is due not only to the static field, but also the local field created by the presence of proton 2. The local field due to the dipolar interaction is

$$|b_{loc}| = \mu_2 \frac{(3 \cos^2 \theta - 1)}{r_{12}^3}$$

where r_{12} is the distance between the two spins, θ is the angle between r_{12} and the direction of the static field, \mathbf{B}_0 , μ_2 is the magnetic moment of proton 2. We can see that certain variables change when the water molecules moves, thus causing the local field to fluctuate. The angle θ changes when the molecule rotates or translates, while r_{12} varies as the molecule vibrates.

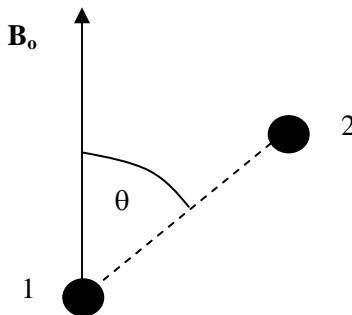


Figure 12 – The dipolar interaction and the local magnetic field.

In order to understand the dynamics of the relaxation process due to local field fluctuations, we must return to the original equation of motion for magnetization in a magnetic field. Instead of looking at the effect of the \mathbf{B}_0 and \mathbf{B}_1 fields, let us define the components of the local magnetic field as b_x , b_y , and b_z . We get

$$\frac{d\mathbf{M}}{dt} = \gamma \mathbf{M} \times \mathbf{b}$$

$$\frac{dM_x}{dt} = \gamma (M_y b_z - M_z b_y)$$

$$\frac{dM_y}{dt} = \gamma (M_z b_x - M_x b_z)$$

$$\frac{dM_z}{dt} = \gamma (M_x b_y - M_y b_x)$$

These equations tell us something very important. First, the change in the z-component of the magnetization is unaffected by the z-component of the local field b_z . This means that b_z has no effect on T_1 since T_1 relaxation is described by $\frac{dM_z}{dt}$. Similarly, we can see that all three components of the local field affect the change in M_x and M_y , or the transverse relaxation. Go back to the laboratory and rotating reference frames and compare the components of the local field. Remember that in the rotating frame, the static components are rotating at the Larmor frequency. The z-component of the local field is stationary in both frames, since in the rotating frame, we are rotating about the z-axis, and in the lab frame, the system precesses about the z-axis. On the other hand, we know that b_x and b_y are stationary in the rotating frame, which means they must be rotating at the Larmor frequency in the lab frame. All this is saying is that b_x and b_y signify fast dynamic processes, while b_z , being stationary, signifies slow dynamic processes. Since T_1 depends only on b_x and b_y , it is affected only by fast molecular motions, while T_2 is affected by both fast and slow molecular motions. This is an important difference between T_1 and T_2 , causing T_2 always to be equal to or shorter than T_1 . You should be able to convince yourself of this last fact simply by using a vector diagram. Later, when we learn about spectral density functions and molecular correlation times, it will hopefully become more clear.

We have seen that when we put a spin system ($I = 1/2$) in a static magnetic field, the magnetic moments go from a state of random orientation with no net magnetization, to a more ordered state where there are two distinct energy levels, parallel and anti-parallel to the direction of the static field. In order for this thermal equilibrium to be established, energy must be transferred from the spin system to the surrounding, or lattice. In the jargon of NMR, we say that a common temperature is established. A universal condition for energy difference for the spin system is $\gamma \hbar \mathbf{B}_0$. In the lattice, many energy levels are available and because there are so many degrees of freedom, we assume a proper energy level exists for energy transfer. Furthermore, since the surroundings at room temperature have essentially infinite heat capacity, we assume that the temperature remains constant. This means that the spin system “cools” to the lattice temperature and a population difference between the spin energy levels is established, thus generating a macroscopic net magnetization. Figure 13 summarizes the energy transfer process. It shows a spin energy level $|1\rangle$ “flipping” down to energy level $|2\rangle$, while the lattice accepts the quantum of energy and goes from energy level $|b\rangle$ to $|a\rangle$. This is the only allowed transition.

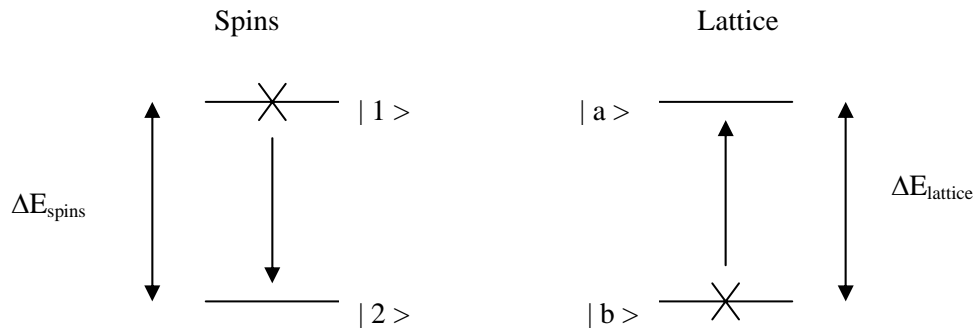


Figure 13 – Spin-Lattice Energy Transfer

Requiring the energy levels to match is synonymous with saying that the frequencies must be equal. It follows, then, that some molecular motion on the time scale of the Larmor frequency must exist for relaxation, or the establishment of thermal equilibrium, to occur. Thermal equilibrium is, by definition, a state whereby dynamic processes are happening (i.e. “spin-flips”), but the net energy change is always zero.

Let us describe an entire system soaking in a static magnetic field. Define the four populations: the spin system will have populations n_1 and n_2 , while the lattice will be N_a and N_b . The number of transitions per second is

$$\text{Transitions / sec} = n_1 N_b W_{1b \rightarrow 2a}$$

where $W_{1b \rightarrow 2a}$ is the rate of transition from states $|1\rangle$ and $|b\rangle$ to states $|2\rangle$ and $|a\rangle$, as shown in Figure 13. Define the spin system populations as

$$\text{Pop. difference} = n = n_1 - n_2$$

$$\text{Total Pop} = N = n_1 + n_2$$

and the corresponding transition rates (“up” and “down” are with reference to the spin system with the assumption that the lattice does the opposite) are

$$\text{Rate Up} = W \uparrow = N_a W_{2a \rightarrow 1b}$$

$$\text{Rate Down} = W \downarrow = N_b W_{1b \rightarrow 2a}$$

The change in the spin population difference, n , is the number of transitions per second minus those up, or

$$\frac{dn}{dt} = n_1 W \downarrow - n_2 W \uparrow$$

Note that dn/dt is zero at thermal equilibrium. Substitute

$$n_1 = \frac{1}{2}(n + N) \text{ and } n_2 = \frac{1}{2}(N - n)$$

to obtain

$$\frac{dn}{dt} = N(W \downarrow - W \uparrow) - n(W \downarrow + W \uparrow)$$

We define the equilibrium population difference, n_o , as

$$n_o = N \left[\frac{W \downarrow - W \uparrow}{W \downarrow + W \uparrow} \right]$$

and substitute this into dn/dt to arrive at the equation for the rate of change of the population difference

$$\frac{dn}{dt} = \frac{n_o - n}{T_1}$$

where we define the rate $R_1 = \frac{1}{T_1} = W \downarrow + W \uparrow$. The solution for the above differential equation is the familiar result

$$n(t) = n_o \left(1 - e^{-\frac{t}{T_1}} \right)$$

as we have seen this for the relaxation of the z-component of the net magnetization, or T_1 relaxation.

At thermal equilibrium, the rate up equals the rate down and we get a ratio of the two spin populations following a Boltzman distribution

$$\frac{n_1}{n_2} = e^{-\frac{\Delta E}{kT}} = e^{-\frac{\gamma \hbar \mathbf{B}_o}{kT}}$$

From the Boltzman distribution, we can see that it is possible to alter the ratio of the spin populations. The ratio decreases (n_2 increases) as \mathbf{B}_o increases, or the temperature decreases. This allows for a greater net magnetization and hence, better signal to noise. This is why the field of NMR spectroscopy has seen the development of very high magnetic fields (10 to 15 T can be standard) and the systems that can cool the sample to the millikelvin region (obviously not suitable when the sample is a human being!).

The next item to study in more detail is molecular motions. We need to introduce the concept of a correlation function and its corresponding correlation time. The correlation function describes the average behavior of a molecular motion in a system. Most correlation functions (for our purposes) can be approximated by an exponential function

$$G(\tau) = A e^{-\frac{\tau}{\tau_c}}$$

and thus have a characteristic time scale defined by the correlation time τ_c . Go back to Figure 12 and think about the rotating and vibrating water molecule. The molecule rotates at some frequency, but not at

the same frequency all the time because it is also busy vibrating, translating and colliding with other molecules. What we mean by the correlation time for the rotational motion, is that time necessary for the molecule to rotate in order to change the angle θ , appreciably. Similarly for the vibrational correlation time – it is the time interval in which r_{12} will change appreciable due to the vibrations.

The correlation function is a time domain function and if we wish to know that rate of motion, we are looking for the frequency range. It is no surprise that the rate is equal to the Fourier transform of the correlation function. We call the resulting function the spectral density function, $J(\omega)$. It is the range of frequencies at which the motion exists.

$$J(\omega) = \int_{-\infty}^{\infty} G(\tau) e^{-i\omega\tau} d\tau$$

$$G(\tau) = \frac{1}{2\pi} \int_{-\infty}^{\infty} J(\omega) e^{-i\omega\tau} d\omega$$

Let us assume we have a random step function with amplitude, A (Figure 14)

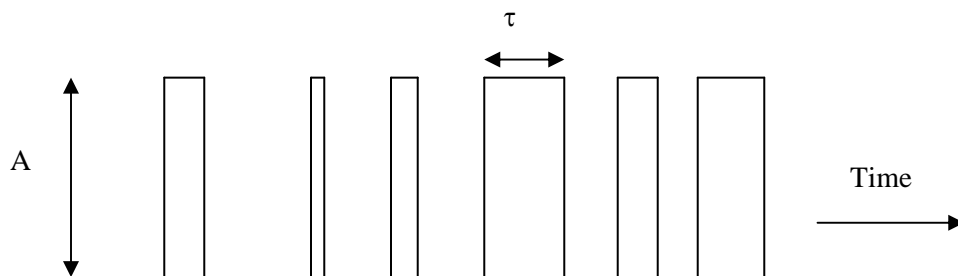


Figure 14 – A Random Step Function Process With Amplitude A.

We can assume that the correlation function for the motion is an exponential and is written as

$$G(\tau) = A^2 e^{-\frac{\tau}{\tau_c}}$$

Solve for the spectral density function

$$J(\omega) = \int_{-\infty}^{\infty} A^2 e^{-\frac{\tau}{\tau_c}} e^{-i\omega\tau} d\tau$$

$$\propto A^2 \frac{\tau_c}{1 + \omega^2 \tau_c^2}$$

The spectral density function tells us that for a motion described by an exponential, the spectral density maximum occurs when $\tau_c = \frac{1}{\omega}$. This is yet another way of stating that efficient relaxation in NMR occurs when a motion has frequency components at the Larmor frequency.

We can experimentally vary the correlation times that give rise to relaxation. An approach to increase the correlation time (i.e. slow down the system) is to increase the viscosity of a solution by lowering the temperature. Conversely, to speed up the system (lower the correlation time), we can increase the temperature. This obviously causes the molecules to move faster. It is important to realize that up altering the temperature of the system, we only alter the frequency distribution of the motions, not the total power available for molecular motions. This means that the area under the spectral density curve remains constant (Figure 15).

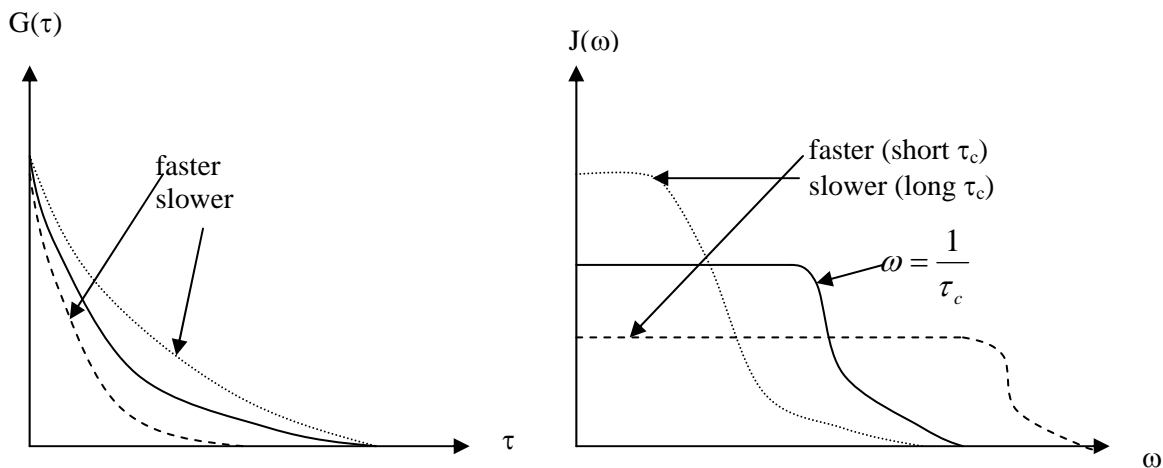


Figure 15 – Correlation and Spectral Density Functions

As was mentioned previously, many interactions exist that the molecular motions could modulate and cause T_1 and T_2 relaxation. The primary interaction responsible for relaxation in proton systems is the dipolar interaction. The dipolar Hamiltonian gives us an idea as to the magnitude of the interaction. We have seen part of it before, but here is the entire equation

$$\hat{H}_{dipolar} = \frac{\gamma_1 \gamma_2 h}{r_{12}^3} (A + B + C + D + E + F)$$

where the letter are mostly orientationally dependent terms like we have seen before (i.e. $3 \cos^2 \theta - 1$). Using the dipolar interaction, we can derive expressions for the relaxation rates (the particulars here are not important, just the result)

$$R_1 = \frac{1}{T_1} \propto \frac{\gamma^4}{r^6} [J(\omega_o) + J(2\omega_o)]$$

$$R_2 = \frac{1}{T_2} \propto \frac{\gamma^4}{r^6} [J(0) + J(\omega_o) + J(2\omega_o)]$$

where the spectral density functions indicate the magnitude of the frequency component at the specified frequency. This shows that T_1 relaxation depends on frequency components at the Larmor frequency and twice the Larmor frequency (a higher order term that is much smaller than the first one), or fast dynamic processes. T_2 relaxation has the same terms with the addition of a zero frequency term, corresponding to the slow dynamic processes. The addition of this term automatically makes T_2 equal to or less than T_1 .

This relates back to the Bloch equations where we saw that T_2 relaxation depended on all three components of the local field, while T_1 relaxation depended on b_x and b_y .

We can look at the spectral density function in Figure 15 and anticipate the effect of changing the static magnetic field on the relaxation rates. On the middle curve, a point where the relaxation rate is most efficient is shown. If we have a static magnetic field such that the Larmor frequency is at that point, we will have the fastest relaxation. If we go to the right of that point, the spectral density falls off, thus making the relaxation slower. If we continue this exercise, we find that T_1 changes more than T_2 if we vary \mathbf{B}_0 (unless we stay in the flat part of the curve). Later on we will see that T_1 and T_2 govern the contrast obtained in an NMR image. It is important to realize that images obtained on different machines will look the same only if the magnetic fields are identical.

For completeness, a rough idea of the magnitude of the other interactions among spins is given. Paramagnetic interactions become important when molecules have unpaired electrons. The dominating factor in the relaxation rate is the γ for an electron which is 1000 times greater than that for a nucleus.

$$rate \propto \frac{\gamma_{nucleus}^2 \gamma_{electron}^2}{r^6}$$

The quadrupolar interaction is important for nuclei with spin $> 1/2$. It is an interaction between the electric fields generated at the nucleus due to nuclear anisotropies. It is a quite large interaction resulting in very fast T_2 's and T_1 's. The chemical shift anisotropy interaction arises when the Larmor frequency changes with the orientation of the molecule relative to \mathbf{B}_0 . The next interaction is scalar relaxation which occurs in systems with different nuclei, such as ^1H and ^{13}C . In these systems, each type of spin has its own energy levels and relaxation mechanisms, but one relaxing can affect the other by causing a local field fluctuation. As you can imagine, this is an extremely small effect. The final interaction is the spin-rotation interaction where the rotation of the molecule and the electronic distribution couple to cause a fluctuating local field at the nucleus. In summary, relaxation occurs by any of the above possible mechanisms, but we tend to simplify the problem and concentrate on the dominant process, the dipolar interaction.

The last part of this section deals with the measurement of the relaxation times. We will begin with T_2 . We saw that the FID decayed with the time constant T_2^* because of inhomogeneities in the magnetic fields. We can minimize this effect by shimming the static field and causing T_2^* to approach T_2 . We can also do a tricky experiment called the spin echo that capitalizes on the static inhomogeneities. We use the two pulses in the experiment, a 90° and a 180° . Figure 16 shows that after the 90° pulse, the spins are allowed to dephase in the x-y plane. They dephase because each spin precesses at a slightly different frequency due to magnetic field inhomogeneities (static) and local field fluctuations (dynamic) intrinsic to the spins. Thus, some spins go faster than the Larmor frequency, while others go slower and get behind. We let the spins dephase for some time τ and then apply a 180° pulse. At τ seconds after the 180° pulse, the spin system refocuses along the $-y$ axis. The effect of the 180° pulse is to put the slow spins ahead of the fast ones and then the fast ones catch up and the magnetization refocuses. Since there is nothing to keep the spins in phase, they dephase again. This rephasing and dephasing gives rise to what is called an echo – it is essentially a back to back FID. An analogy to this process goes as follows. You are a runner in a road race and everyone is lining up at the starting line. The gun goes off and the race begins. Now, there are fast people and slow people, and pretty soon runners are distributed along the race course. Let the race proceed for one minute, freeze the runners, and then flip them 180° so that the fast ones are behind the slow ones. Now start the race again and after one minute everyone is at the starting line. The runners keep going and again become distributed along the course.

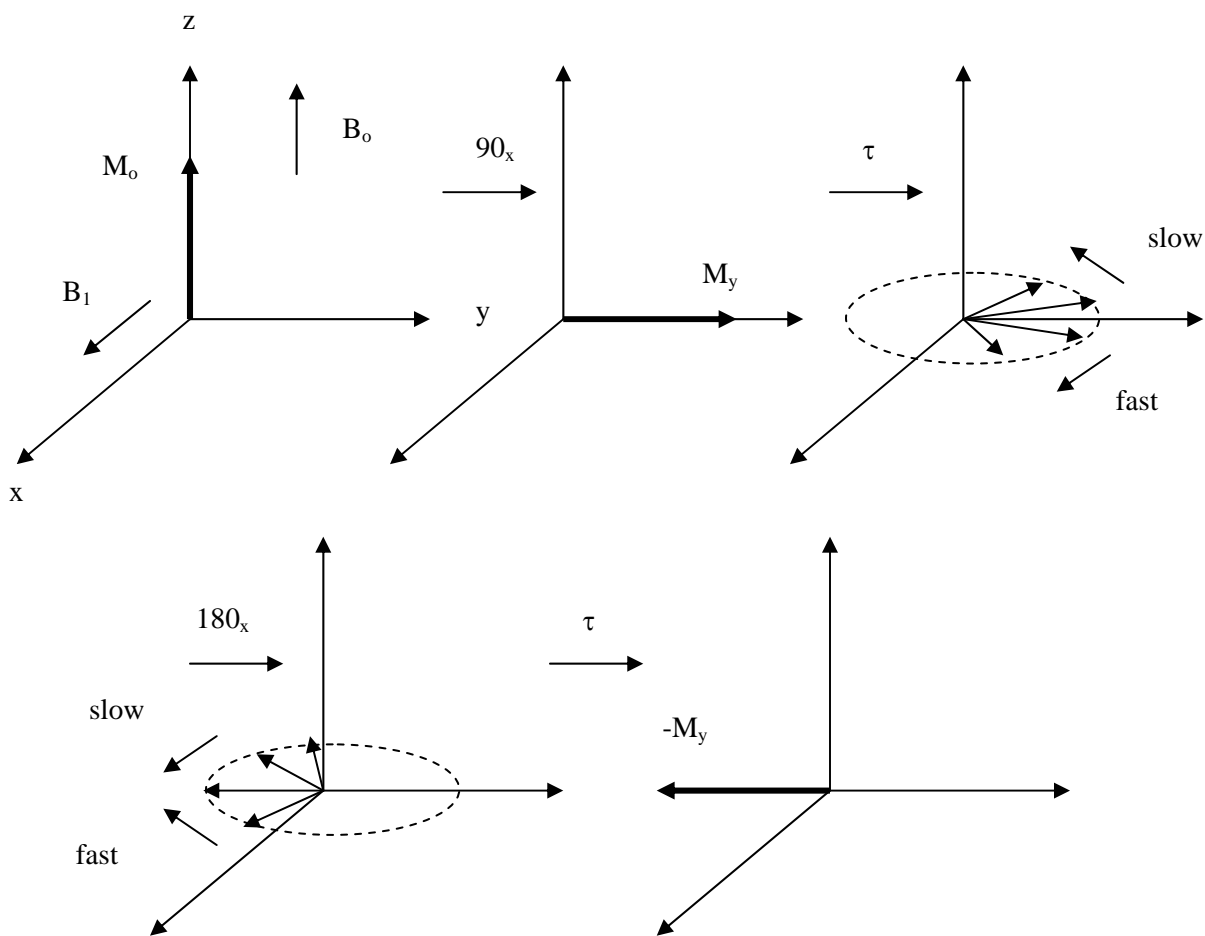


Figure 16 – The Spin Echo Experiment

The way we write a pulse sequence like the spin echo is shown in Figure 17, along with the resulting signal echo. Note that the polarity of the FID and echo signals depends on the phases of the 90° and 180° pulses (which direction B_1 field points) and the type of receiver in the spectrometer. In the above example, the echo rephases along the $-y$ axis and would give us an upside down echo. In Figure 17, I have phase shifted 180° pulse so that the echo is formed on the y axis. Remember, the magnetization rotates around the axis of the rf field according to the left hand rule.

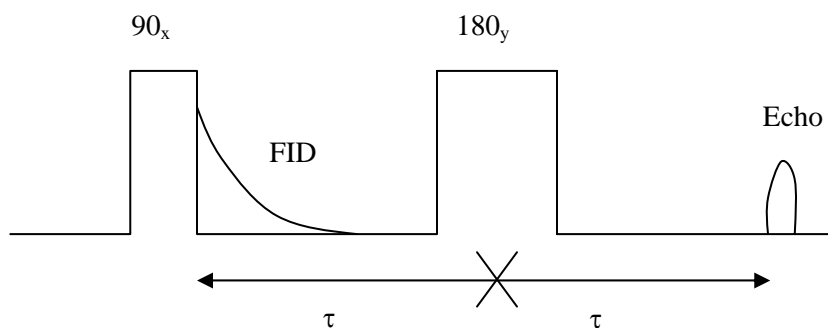


Figure 17 – Spin Echo Sequence. Note phase of 180°

You can see in Figure 17 that the amplitude of the echo is less than that of the FID. If we did a series of experiments where we increased τ each time, we would see a gradual decline in the echo amplitude. In fact it decays as an exponential, with a time constant T_2 . This is exactly how we measure the intrinsic T_2 relaxation time. In the spin echo experiment, only the dephasing due to the static inhomogeneities is refocused, thereby leaving the dephasing done by dynamic inhomogeneities. Instead of doing several experiments where we vary τ , we can do the entire experiment in one shot. All we do is to keep repeating the 180° pulse ($90^\circ - \tau - 180^\circ - \tau - 180^\circ - \tau \dots$). Figure 18 shows the resulting echo train. If we plot the absolute values of the echo amplitudes, we could extract T_2 by the equation

$$M_{x,y}(t) = M_o e^{-t/T_2}$$

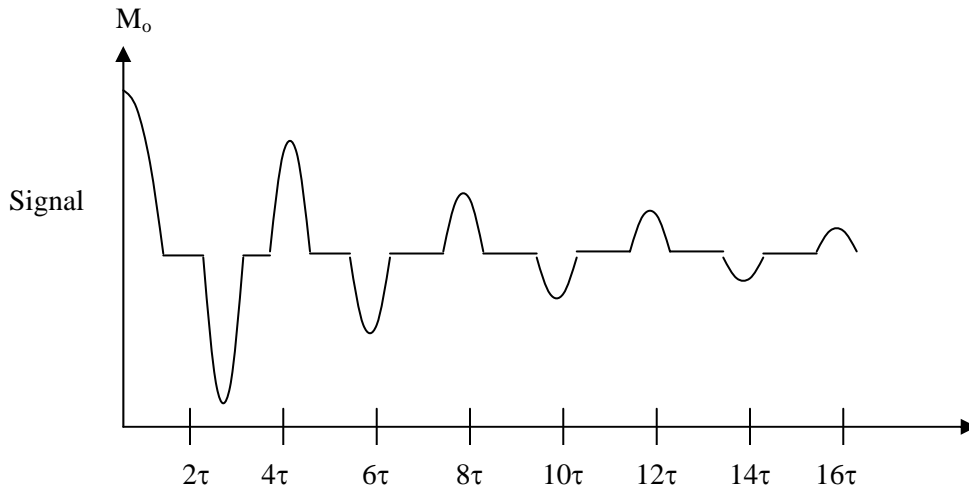


Figure 18 - Spin Echo Train

There are two basic experiments for measuring T_1 . One is called **saturation recovery** and the other is **inversion recovery**. The first involves saturating the spin system with a series of 90° pulses which eliminates all components of \mathbf{M} . The magnetization then returns to its equilibrium value with time constant T_1 . We can do a series of experiments where we saturate the system, wait τ seconds, and then apply a 90° pulse and collect the FID. As τ gets longer, the amplitude of the FID begins to approach M_o . Refer back to Figure 8 for a vector diagram of the process. We have seen relaxation equation before and Figure 19 shows the plot of signal amplitudes (by plotting the signal amplitudes we mean the initial point of the FID).

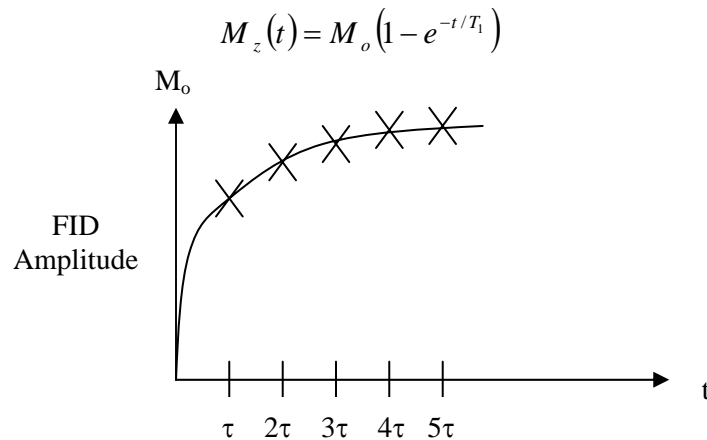
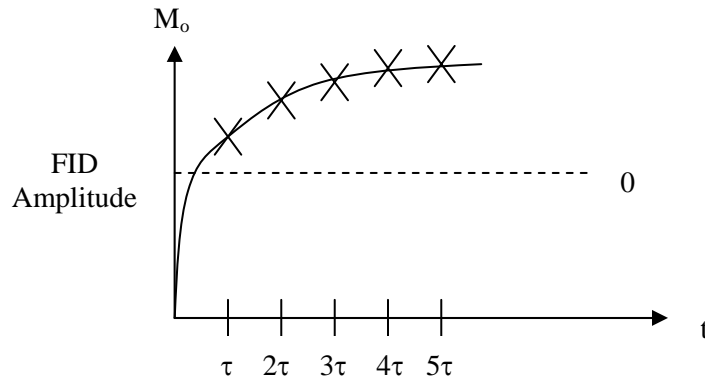


Figure 19 – Saturation Recovery

The inversion recover pulse sequence contains a 180° pulse, a wait of some time τ , followed by a 90° pulse. The phase of the rf pulses is not important in this experiment. Since we begin with an inversion of the magnetization we measure the recovery from $-\mathbf{M}_o$ to \mathbf{M}_o , thus doubling the dynamic range which reduces experimental error (Figure 20). The relaxation equation is

$$M_z(t) = M_o(1 - 2e^{-t/T_1})$$



CHAPTER 4: LIQUID SPECTROSCOPY

The most important application of NMR spectroscopy is in the field of organic chemistry. It is one of the most powerful tools used in molecular structure determination and has allowed the field to advance at lightening speed. The reason for this is that NMR is exquisitely sensitive to the atomic environment in a molecule in the liquid state, or a compound dissolved in some solvent. The resonances in a spectrum reflect subtle differences (i.e. a few hertz) in the environment of the protons in a molecule. Using a few rules, we can come to a basic understanding of how these spectra are interpreted, and explore other types of experiments that are useful in liquid spectroscopy.

First let us begin with the information contained in a resonance line. Remember the line is obtained through a FT of the FID. The resonance line reflects whatever relaxation mechanism is used by the system to cause T_2 relaxation. In solids, the dominant process involves the dipolar interaction which goes as $\frac{\gamma^4}{r^6}$, and thus can give us information about the distance between interacting dipoles. Another important relaxation mechanism in solids and less mobile molecules is the chemical shift anisotropy. These interactions cause the width of the line to be quite large – on the order of several kilohertz. Any smaller interactions are “covered up” and consequently lost. Liquids, on the other hand, contain mobile molecules which cause an averaging of any orientationally dependent interactions and a remarkable narrowing of the resonance lines. This is formally called **motional narrowing**.

Let us compare the NMR spectrum of ice and water. A typical line width for a sample of ice can be estimated at

$$(\Delta\omega)_o \propto \frac{1}{T_2} \approx 10^5 \text{ radians / sec}$$

T_2 can be defined as the time in which an individual spin dephases by one radian due to a perturbation, \mathbf{B}_i or synonymously, $\gamma\mathbf{B}_i \approx (\Delta\omega)_o$ is the local frequency deviation due to the perturbation, \mathbf{B}_i . Assume the perturbation, \mathbf{B}_i is due to the dipolar interaction. If the molecules are moving rapidly (short τ_c), then \mathbf{B}_i seen by a given spin fluctuates rapidly in time. In time τ , the spin will precess an extra phase angle, $\Delta\phi$ relative to steady precession in \mathbf{B}_o . Note this is no different than applying a \mathbf{B}_1 field and having the magnetization precess around it.

$$\begin{aligned} \Delta\phi &= \pm\gamma\mathbf{B}_i\tau \\ &= (\Delta\omega)_o \end{aligned}$$

If τ is short such that $\Delta\phi \ll 1$, then motional narrowing occurs. We can see this using the simple random walk theory of diffusion. The mean square displacement due to diffusion of a molecule is

$$\langle r^2 \rangle = nL^2$$

where L is the average length of a single step and n is the number of steps taken. In our example, the mean square dephasing angle after n intervals of duration τ in \mathbf{B}_o is

$$\langle \phi^2 \rangle = n(\Delta\phi)^2 = n\gamma^2 \mathbf{B}_i^2 \tau^2$$

The average number of steps required to dephase one radian is

$$n = \frac{1}{\gamma^2 \mathbf{B}_i^2 \tau^2}$$

By definition

$$n\tau = \frac{1}{T_2} = \frac{1}{\gamma^2 \mathbf{B}_i^2 \tau}$$

Now, the line width for water (since the criterion of $\Delta\phi \ll 1$ is met with $\tau \approx 10^{-10}$ seconds in water) is

$$\Delta\omega_{liquid} = T_2 = (\gamma\mathbf{B}_i)^2 \tau = (\Delta\omega_o)^2 \tau$$

which gives a line width on the order of one radian per second as compared to 10^5 radians per second for ice. Thus, the T_2 for solids is quite short, while that for liquids is long. T_1 is about the same as T_2 for liquids, while in solids T_1 can be short or long.

In liquid spectroscopy, the Larmor frequency of an individual nucleus is determined by the electronic distribution in the chemical bonds. Different electronic distributions give rise to different **chemical shifts** and **J coupling**, the two main interactions that are not averaged out by the molecular motion. The chemical shift in liquids is an isotropic phenomenon. Because the line widths in liquids are very small, the static magnetic field must be extremely homogeneous. Shimming the magnetic field provides homogeneities on the order of 1ppm or less. In addition to this, the liquid sample is put into a long cylindrical tube and is spun inside the static field to further average our inhomogeneities.

The chemical shift of a particular proton, or group of equivalent protons, is determined by the **shielding constant, σ** , where

$$\omega = \gamma(\mathbf{H}_o + \Delta\mathbf{H})$$

and

$$\Delta\mathbf{H} = -\sigma\mathbf{H}_o$$

$\Delta\mathbf{H}$ is referred to the chemical shift relative to some standard chemical shift that is accepted as zero. The most common “zero” is the resonance arising from the 12 equivalent protons of tetramethyl silane. The reasons that this compound is used as a standard is that it is one of the most shielded, is essentially inert, and is easy to insert and remove from samples. Shielding means that much of the electron density exists in the vicinity of the protons, corresponding to a large σ . Before going into this detail, let us go over the rules of liquid NMR spectrum (Figure 21). The units for reporting resonances are in ppm, where

$$ppm = \frac{\Delta\nu \text{ from reference (Hz)}}{\text{Spectrometer frequency (MHz)}}$$

The reason for this scale is that it eliminates the field dependence of the resonance as the magnetic fields on no two spectrometers are exactly identical. We use the symbol δ to report chemical shifts in ppm.

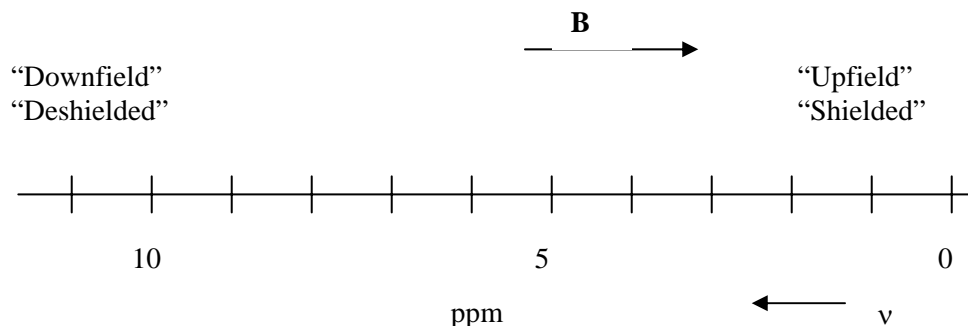


Figure 21 – Spectrum Basics

Figure 21 shows what seems to be an error: the frequency and magnetic field are going in opposite directions. You are also wondering why the spectrum goes from 0 to 10 from right to left. Tradition is at play here. We must go back and examine the way spectra were taken when NMR jumped on the scene. In CW NMR, the field, $\mathbf{B}_{\text{sweep}}$. The Larmor frequency can be written

$$\omega_L = \gamma(\mathbf{B}_o + \Delta\mathbf{B} + \mathbf{B}_{\text{sweep}})$$

A resonance occurs when $\Delta\mathbf{B}$ and $\mathbf{B}_{\text{sweep}}$ cancel. A large shielding constant requires a larger sweep field and we say that the resonance appears “upfield” and that the nucleus is “shielded”. Shielded nuclei, then, resonate at lower Larmor frequencies since frequency increases going left. This is a confusing convention, but over time, it will make sense.

Chemical bonds are responsible determining the electronic distribution within a molecule. The shielding constant is a result of the character of the bond. Begin with a hydrogen atom (Figure 22). For diamagnetic materials, Lenz’s Law states that in a magnetic field, an induced current will flow in the electron field such that a local magnetic field will arise at the nucleus in a direction opposite that of the applied field (use the right hand rule here). Therefore, the total field seen at the nucleus is always less than the applied field. The hydrogen atom has the largest shielding constant, given by

$$\sigma = \frac{\mu_o e^2}{3m_e} \int_0^\infty r \rho(r) dr$$

where μ is the permittivity of free space, e is the elementary charge, m_e is the mass of an electron, and $\rho(r)$ is the electron distribution.

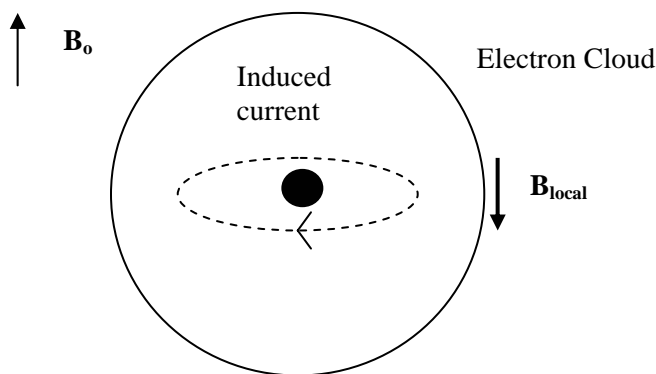


Figure 22 – Schematic of the Hydrogen Atom

We speak of the hydrogen atom as being purely diamagnetic. Its resonance is the farthest upfield. Adding atoms to a molecule causes a reduction in the “pure” diamagnetic effect and the resonances are shifted downfield. For molecules, the shielding constant is the sum of different electronic effects

$$\sigma_{molecule} = \sigma_{hydrogen} + \sigma'$$

where σ' is the shielding effect due to other atoms in the molecule. The determining factors of σ' are the type of atom in the vicinity, the character of the chemical bond (i.e. single, double, or triple bonds), the electron circulates within the substituents which can cause secondary field effects, van der Waals effects, and the effects of the surrounding medium (i.e. hydrogen bonding, etc.).

The hydrogen halides, HF, HCl, HBr, and HI, can be used as an example of the inductive effect of the electronegativity of the halides to reduce the pure diamagnetic shielding constant. The most electronegativity element, fluorine, has the largest effect and essentially sucks away the electron density from the hydrogen nucleus to deshield it. Chlorine follows, then bromine, and finally iodine, so that the hydrogen nucleus in HI is the most shielded series.

More important in organic chemistry are hydrogen atoms attached to carbon skeletons. The electron density at the carbon atom usually defines the effects on the hydrogen nucleus and its Larmor frequency. The effects of halide substituents on a carbon skeleton parallel the effects in the hydrogen halide series – it follows electronegativity. Figure 23 summarizes the effect of a halide in small alkanes. The arrows above the protons on the right identify which protons are targeted in the plot. In series' A and B, a purely inductive effect is seen. In B, an added effect of another carbon is seen. In series C, the effect is more complicated due to secondary magnetic fields generated because of the large size of the electron clouds (or, in other words, the increased polarizability). This effect is called magnetic anisotropy.

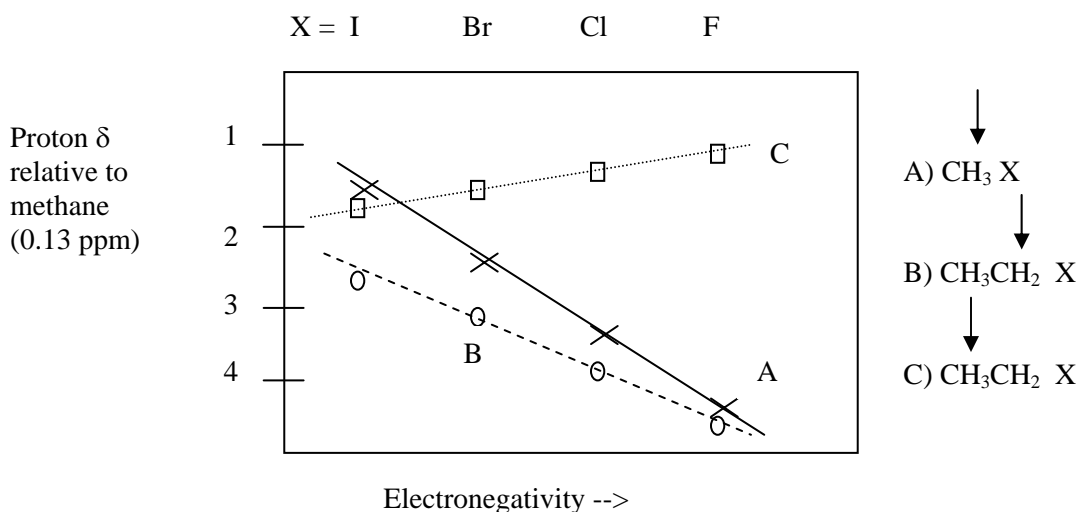


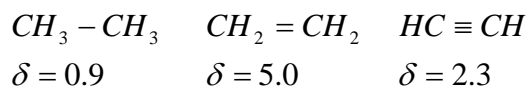
Figure 23 – Effect of Halides on the Protons in a Carbon Skeleton

The effect of an $-\text{NO}_2$ group is seen in Figure 24. This is purely an inductive effect that decreases with distance as can be seen in the $\Delta\delta$ column.

	1	2	3		1	2	3	
	$\text{CH}_3\text{CH}_2\text{CH}_3$				$\text{O}_2\text{NCH}_2\text{CH}_2\text{CH}_3$			$\Delta\delta$
1	δ_{CH_3}	0.91 ppm			δ_{CH_2}	4.36 ppm		3.45
2	δ_{CH_2}	1.33 ppm			δ_{CH_2}	2.05 ppm		0.72
3	δ_{CH_3}	0.91 ppm			δ_{CH_3}	1.03 ppm		0.12

Figure 24 – Effect of a Nitro Group on Proton Chemical Shift

Carbon cations and anions can cause a loss or gain of electron density around the neighboring protons. It is easy to see this effect. One way to clarify where the electron density is in a molecule is to draw the resonance structures. This is especially true in molecules that have multiple bonds in them. It becomes more difficult to predict the chemical shifts in carbon skeletons with double and triple bonds. For instance, the chemical shift values for the protons in three examples, ethane, ethylene, and ethyne, are shown below. We must actually look at the geometry of the electron density to account for these values.



Vinyl protons actually sit in the plane of the molecule (Figure 25) where the electron density is at a minimum since the π -electrons of the double bond hover above and below the plane. This causes the deshielding effect and accounts for the chemical shift of 5.0.

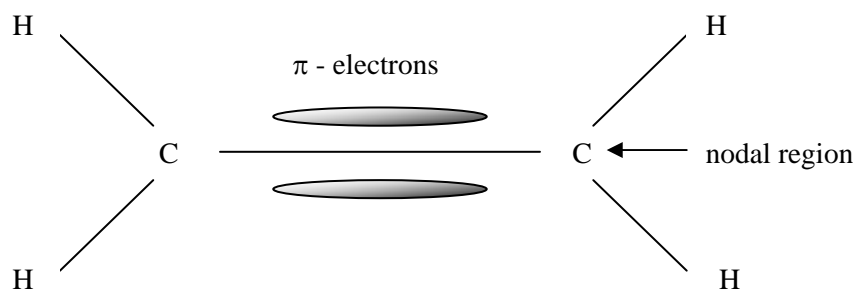


Figure 25 – Vinyl protons deshielding in the plane of the molecule

A similar effect is seen in a carbonyl group where the C-O bond forms the plane of the molecule with π -electrons above and below. Any protons in the plane are deshielded. A molecule with a double bond can have a geometry so that a proton from another part of the molecule hangs near the π -electron density and can be actually be shielded.

A triple bond must also be examined geometrically. Here the π -bond electrons are perpendicular to each other, forming a cylinder of electron density about the axis of the molecule. Within this cylinder these electrons can circulate, generating a current, and thus a local field in the opposite direction to the applied field (Figure 26). This causes a shielding effect on the protons.

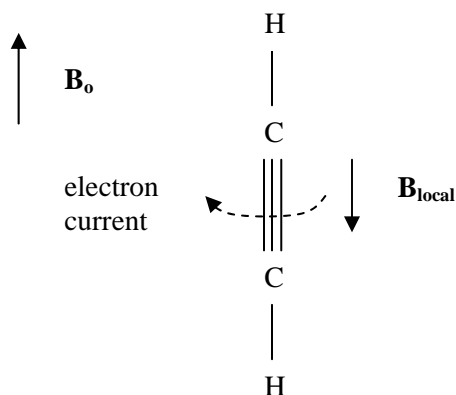


Figure 26 – Shielding Effect in Ethyne

The last major effect for our purposes is the generation of ring currents in cyclic conjugated systems (those with $4n + 2 \pi$ - electrons). The chemical shift for the protons in benzene is 6.9 ppm. We ask why this is farther down field than the vinyl protons. The reason is that a diamagnetic ring current is generated in the benzene ring (Figure 27), which results in a local field opposing the applied field **in the center of the ring**.

If we follow the field lines out and around to the protons on the outer part of the ring, we see that the direction of the local field is in the same direction as the applied field. This is a deshielding effect and the resonance is downfield.

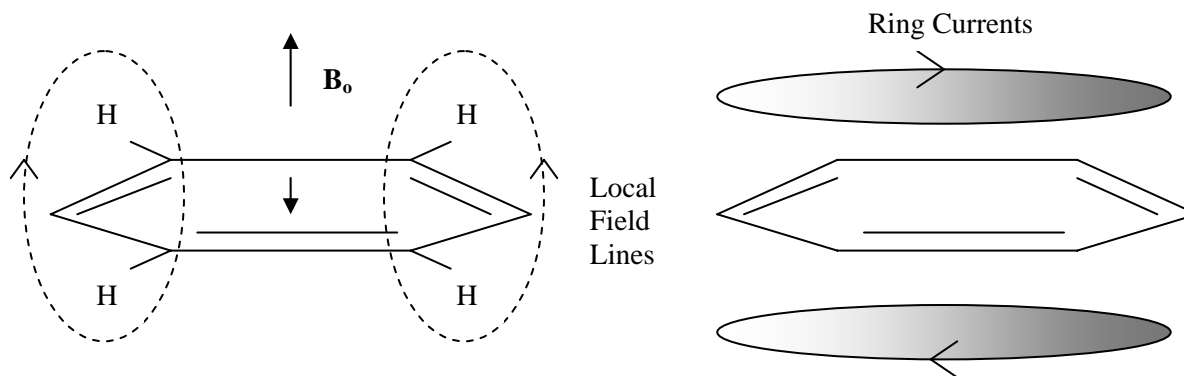


Figure 27 – Ring Currents and Local Field in Benzene

We have examined some of the effects of chemical shift in basic organic molecules. The following is a short summary of approximate chemical shifts:

Alkanes: $\delta = 0.9 - 1.5$

Cycloalkanes: $\delta = 1.0 - 1.8$

Alkenes: $\delta = 4.5 - 6.0$

Alcohols: $\delta = 3.4 - 4.0$ (-OH proton can be anywhere)

Ethers: $\delta = 3.3 - 4.0$

Ketones and Aldehydes: $\delta = 2.0 - 2.7$

Carboxylic Acids: $\delta = 2.0 - 2.7$

Amines: $\delta = 2.0 - 2.8$ (-NH protons wide $\delta = 1.0 - 5.0$)

Aromatic Compounds: $\delta = 6.0 - 8.5$ (aromatic protons)

$\delta = 2.3 - 3.0$ (attached alkyl groups)

Another aspect of the NMR spectrum is helpful in determining molecule structure. The area under each resonance peak is proportional to the number of protons that gave rise to the peak. Next we will see that a resonance may not only be a single peak, but may also have multiplicity.

Multiplicity arises because of another interaction left in liquid NMR spectroscopy J-coupling. This is a small scalar effect and leads to hyperfine splitting of a single peak. It is a consequence of the orientation of the nuclear spins on the electronic wavefunction. The only reason we see it is that the motion in liquids eliminates everything else. It is the smallest isotropic effect.

J-coupling is a magnetic interaction not transmitted through space, but rather by bonding electrons through which the protons are indirectly coupled. We will only consider first order effects – the distance of transmission is through 3 bonds.

Consider the ethanol molecule, $\text{CH}_3\text{CH}_2\text{OH}$. If you are the $-\text{CH}_3$ group, you see 3 different possible spin states (a triplet) for the CH_2 group next door (Figure 28). The frequency shift of the states is $\pm J$, the spin coupling constant.

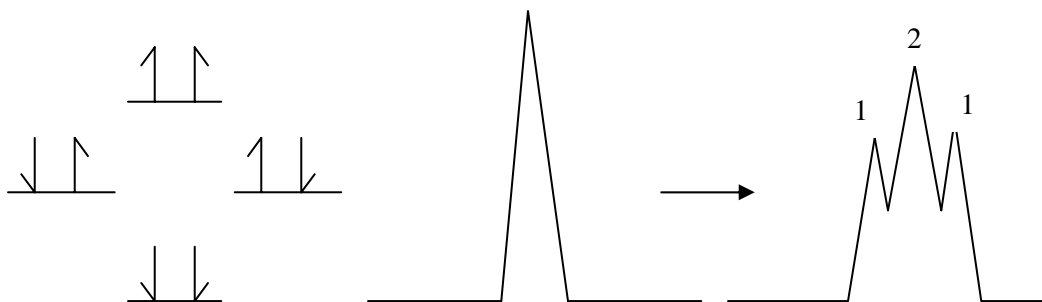


Figure 28 – Possible Spin States for $-\text{CH}_2$

Likewise if you are the $-\text{CH}_2$ group looking at the $-\text{CH}_3$ (Figure 29) and the result is a quartet instead of a singlet.

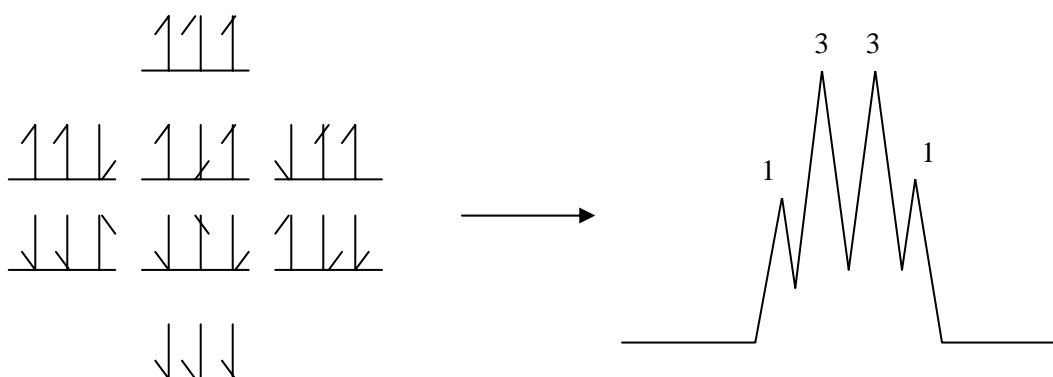


Figure 29 – Multiplet from $-\text{CH}_3$

The intensity distribution within a multiplet is related to the relative probabilities of the different spin combinations, or

$$\text{Multiplicity} = 2nI + 1$$

where $I = \frac{1}{2}$ for protons and n is the number of neighboring protons. Multiplicity for protons is $n + 1$. The relative intensity of each peak in the multiplet goes as the coefficient of the binomial expansion $(a + b)^n$ (Pascal's Triangle) (Figure 30).

$n = 0$				1						
$n = 1$			1		1					
$n = 2$			1		2		1			
$n = 3$			1		3		3	1		
$n = 4$			1		4		6		4	1

Figure 30 – Pascal's Triangle

A few examples follow. The protons on the second carbon in n-butane ($\text{CH}_3\text{CH}_2\text{CH}_2\text{CH}_3$) will give a multiplet with 6 peaks since there are a total of 5 protons on the two adjacent neighboring carbon atoms. Remember, we are only concerned with a distance of 3 bonds. In t-butane ($(\text{CH}_3)_3\text{CH}$), the tertiary carbon has one proton that will give rise to a multiplet of 10 peaks due to the nine protons on adjacent carbons. The methyl protons are considered chemically and magnetically equivalent and will give rise to a simple doublet since there is only one neighboring proton. We will do many examples in class – practice is the only way to master these principles.

In π -bond systems, there are higher order, longer range effects and the expected multiplet may have yet finer splittings. This is due to the ability of π -electrons to “transmit” magnetic information more effectively and coupling occurs farther than the 3 bonds as in saturated systems.

Another useful aspect of liquid spectroscopy is that it can give us information about molecular kinetics. For instance, N, N-dimethylformamide is shown in Figure 31 as two resonance structures.

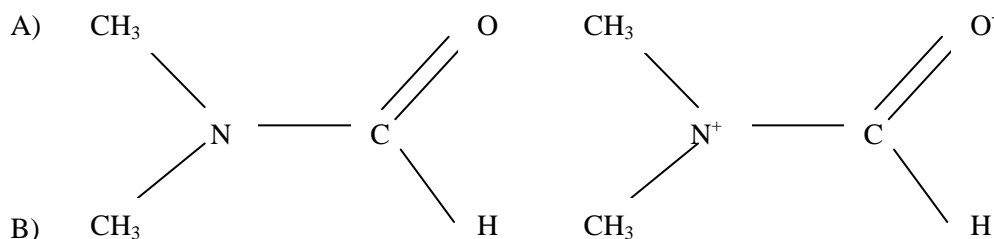


Figure 31 – Resonance Structures of N, N-dimethylformamide

The structure on the right tells us that the N-C bond has some double bond character which causes a rather high barrier to rotation at room temperature. This barrier to rotation then causes the protons on the methyl groups (labeled A and B) to have different chemical shifts, since the chemical environments are different. The protons on A, see carbonyl oxygen across the way, while those on B see a lone proton. Thus, at lower temperatures, two singlets result – one from A and one from B. Consider the two states, A and B, which exchange with the corresponding rate constants, k and k_{-1}



and protons A and B give rise to peaks at ω_A and ω_B . The separation between the peaks is then $|\omega_A - \omega_B| = \Delta\omega$. Now, if the correlation time for the rotational process is such that $\tau\Delta\omega \gg 1$, then we see two peaks. As $\tau\Delta\omega$ approaches 1, the two peaks begin to coalesce to form one peak. We can do this by increasing the temperature which makes the correlation time decrease (the molecules are moving faster). We can increase the temperature farther and the one peak now becomes sharper. What is happening is that we are seeing the time average of the two different environments when the molecule is rotating faster than the “NMR time scale”, or $\tau\Delta\omega \ll 1$. In other words, in order for the protons to give off two separate peaks, they must remain in one environment long enough to satisfy $\tau\Delta\omega > 1$.

One final aspect of liquid spectroscopy to discuss is the use of decoupling experiments. If you are an organic chemist and you build a new molecule, but the NMR spectrum is complicated and you are unsure of the peak assignments, you do a decoupling experiment to identify adjacent protons. This requires the use of a separate transmitter set at a frequency to saturate and give rise to no peak. Also, the multiplets

from protons on neighboring carbon atoms would collapse into singlets. Thus, you can walk you way through a molecule and determine neighboring protons. Decoupling may also be used to eliminate unwanted peaks. For example, if a large water peak is covering up information about other molecules, it is possible to saturate the water protons so that the water peak disappears and leaves the information desired underneath it. This is especially useful in biological systems where water is everywhere.

This chapter has been a brief explanation of liquid spectroscopy, hopefully enough to understand the basic principles. It is important as the field of MRI advances since spatially localized spectroscopy is becoming a fascinating way to look at biochemical processes in the body. We will see more of this later.

CHAPTER 5: FOURIER TRANSFORM THEOREMS

Image processing involves several of the FT theorems. Here we list and describe the important ones for our purposes. The FT in two dimensions yields spatial frequencies. We define the FT and FT^{-1} in two dimensions

$$G(k_x, k_y) \equiv F(g) = \iint g(x, y) e^{-2\pi i(k_x x + k_y y)} dx dy$$

$$F^{-1}(G) = \iint G(k_x, k_y) e^{2\pi i(k_x x + k_y y)} dk_x dk_y$$

The FT theorems are listed below:

- (1) Linearity: $F(\alpha g + \beta h) = \alpha F(g) + \beta F(G)$
- (2) Similarity: if $F(g(x, y)) \equiv G(k_x, k_y)$, then $F\{g(ax, by)\} = \frac{1}{ab} G\left(\frac{k_x}{a}, \frac{k_y}{b}\right)$. Stretching space is equivalent to contraction in frequency.
- (3) Shift Theorem: if $F(g(x, y)) \equiv G(k_x, k_y)$, then $F\{g(x-a, y-b)\} = G(k_x, k_y) e^{-2\pi i(k_x a + k_y b)}$. Translation in space is equivalent to a linear phase shift in frequency.
- (4) Parseval's Theorem: $\iint |g(x, y)|^2 dx dy = \iint |G(k_x, k_y)|^2 dk_x dk_y$.
- (5) Convolution Theorem: $F\left\{\iint g(a, b) h(x-a, y-b) da db\right\} = G(k_x, k_y) H(k_x, k_y)$ where $G = F(g)$ and $H = F(h)$.
- (6) Autocorrelation Function: if $F(g(x, y)) \equiv G(k_x, k_y)$, then $F\left\{\iint g(a, b) g^*(a-x, b-y) da db\right\} = |G(k_x, k_y)|^2$. Similarly, $F\left\{|g(a, b)|^2\right\} = \iint G(a, b) G^*(a-k_x, b-k_y) da db$.
- (7) Fourier Integral Theorem: $FF^{-1}\{g(x, y)\} = F^{-1}F\{g(x, y)\} = g(x, y)$

Commonly Used FT's:

- (1) Rectangle: $rect(x) = \begin{cases} 1 & |x| < \frac{1}{2} \\ 0 & elsewhere \end{cases}$. The FT is $F\{rect(x), rect(y)\} = \text{sinc}(k_x) \text{sinc}(k_y)$, where $\text{sinc}(x) = \frac{\sin(\pi x)}{\pi x}$.

(2) Triangle: $tri(x) = \begin{cases} 1-|x| & |x| \leq 1 \\ 0 & \text{elsewhere} \end{cases}$. The FT is $F\{tri(x), tri(y)\} = \text{sinc}^2(k_x) \text{sinc}^2(k_y)$.

Note that $tri(x) = \text{rect}(x) * \text{rect}(x)$, a convolution.

(3) Delta Function: $\delta(x) = \lim_{N \rightarrow \infty} (N e^{-N^2 x^2})$. The FT is $F\{\delta(x), \delta(y)\} = 1$. The FT is constant overall frequencies.

(4) Comb Function: $comb(x) = \sum_{n=-\infty}^{\infty} \delta(x-n)$. The FT is

$F\{comb(x), comb(y)\} = comb(k_x) comb(k_y)$. The similarity theorem applied here is

$F\{comb(ax), comb(by)\} = \frac{1}{ab} comb\left(\frac{k_x}{a}\right) comb\left(\frac{k_y}{b}\right)$.

CHAPTER 6: INTRODUCTION TO IMAGING

We are interested in the relation between the physical properties of an object and the image and its properties. The object is usually something in three dimensions, while the image has been compressed into two. The properties reflected in an object are listed below.

Conventional x-ray $\rightarrow \mu$, the mapping attenuation
 CT scan $\rightarrow \mu$, and atomic number
 Digital subtraction angiography $\rightarrow \mu$ (iodine)
 Nuclear scanning, PET, SPECT \rightarrow Concentration of emitting nuclei
 Ultrasound \rightarrow interfaces, velocity
 NMR \rightarrow Spin density, T_1 , T_2 , chemical shift (σ)

The relationship between object and image can be linear or have spatial invariance. A space invariant, or stationary process is where the object is moved and the image is shifted without change. A linear process means

$$S[as(x_1, y_1) + bt(x_1, y_1)] = aSs(x_1, y_1) + bSt(x_1, y_1)$$

where s and t are the input functions and S is the operator function.

The image is usually intensity, or optical density, reflecting spatial frequencies. The noise in the image can be continuous or digital. The resolution of an image is important and defined to be the ability of an imaging system to reproduce spatial variation of the object in the image plane. It should be stressed that resolution is **not** the smallest object that you see. Use the point spread function (PSF), or impulse response function

$$h(x_2, y_2, a, b) = S\{\delta(x_1 - a, y_1 - b)\}$$

which is the output response at (x_2, y_2) of δ at (a, b) . This tells how well the points get transferred from object to image. Think of an input function

$$g_1(x_1, y_1) = \iint g_1(a, b)\delta(x_1 - a, y_1 - b)dadb$$

where $g_1(a, b)$ is essentially a weighting factor for the elementary δ 's. The output function reflects the "sifting" property of the delta functions

$$\begin{aligned} g_2(x_2, y_2) &= S\left\{\iint g_1(a, b)\delta(x_1 - a, y_1 - b)dadb\right\} \\ &= \iint g_1(a, b)S[\delta(x_1 - a, y_1 - b)]dadb \\ &= \iint g_1(a, b)h(x_2, y_2, a, b)dadb \end{aligned}$$

If the system is space invariant, then

$$h(x_2, y_2, a, b) = h(x_2 - a, y_2 - b)$$

and only the distances $x_2 - a$ and $y_2 - b$ contribute causing h to change in location and not form. Thus,

$$g_2(x_2, y_2) = \iint g_1(a, b)h(x_2 - a, y_2 - b)dad b$$

$$g_2(x_2, y_2) = g_1 * h$$

where $*$ denotes a convolution. In other words, the output function is convolution of the input function and the PSF (go back to review of FT theorems). The response to a unit impulse is characterized by the full width at half height (FWHH) of the PSF. If the system has many sources of spread in the PSF, then, in general

$$\mu_{total} = \sqrt{\mu_1^2 + \mu_2^2 + \mu_3^2 + ..}$$

by the Central Limit Theorem.

Another important function to describe the resolution of an image is the **modulation transfer function** (MTF). It is the ratio of the output modulation to the input modulation (Figure 32).

$$MTF(\nu) = \frac{Output(\nu)}{Input(\nu)}$$

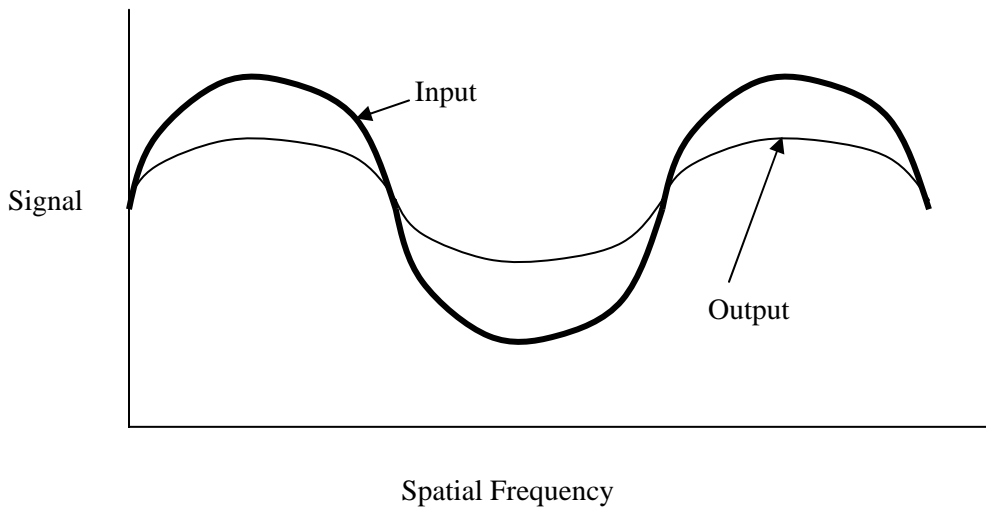


Figure 32 – Frequency Modulation

The MTF is normalized such that $MTF(0) = 1$. Thus, $MTF(\nu) \leq MTF(0)$. Digital imaging involves discrete sampling of an object, for example, in a CT scan, the signal detectors are aligned in discrete banks. If the signal is digitized, we must determine how rapidly to sample the data in order to get an accurate reflection of the analogue signal. The Nyquist theorem states that we must sample at twice the highest frequency to accurately reconstruct a sinusoidal signal, i.e. we must sample at least twice per cycle (or we will have aliasing).

For a certain class of object function, it is possible to reconstruct the sample data exactly. The objects must be band limited, i.e. their Fourier Transform must be non-zero over a finite region of frequency space. This is known as the Whittaker-Shannon sampling theorem. Consider a rectangle lattice of samples of g :

$$g_s(x, y) = \text{comb}\left(\frac{x}{X}\right) \text{comb}\left(\frac{y}{Y}\right) g(x, y)$$

where $g_s(x,y)$ is the sampled object $g(x,y)$ is the object itself, $\text{comb}(x) = \sum_{n=-\infty}^{\infty} \delta(x - n)$ and X and Y are sample spacing. The object is therefore sampled on a grid which is separated by X and Y . By the convolution theorem,

$$G_s(k_x, k_y) = FT\left\{\text{comb}\left(\frac{x}{X}\right) \text{comb}\left(\frac{y}{Y}\right)\right\} * G(k_x, k_y)$$

where

$$\begin{aligned} FT\left\{\text{comb}\left(\frac{x}{X}\right) \text{comb}\left(\frac{y}{Y}\right)\right\} &= XY \text{comb}(Xk_x) \text{comb}(Yk_y) \\ &= \sum_{m=-\infty}^{\infty} \sum_{n=-\infty}^{\infty} \delta\left(k_x - \frac{n}{X}, k_y - \frac{m}{Y}\right) \end{aligned}$$

therefore,

$$G_s(k_x, k_y) = \sum_m \sum_n G\left(k_x - \frac{n}{X}, k_y - \frac{m}{Y}\right)$$

i.e. G_s is just $G = FT\{g\}$ about each point n/X and m/Y in the $k_x - k_y$ plane.

Since we assume $g(x,y)$ to be band limited, G is finite over a region T (see Figure 33). If X and Y are sufficiently small, then $1/X$ and $1/Y$ are large enough to avoid any overlap. It is therefore possible to obtain G from G_s by passing g_s through a filter that only transmits the $n = 0$ and $m = 0$ term. By excluding all the other terms, the output of this filter is exactly $g(x,y)$, the desired object.

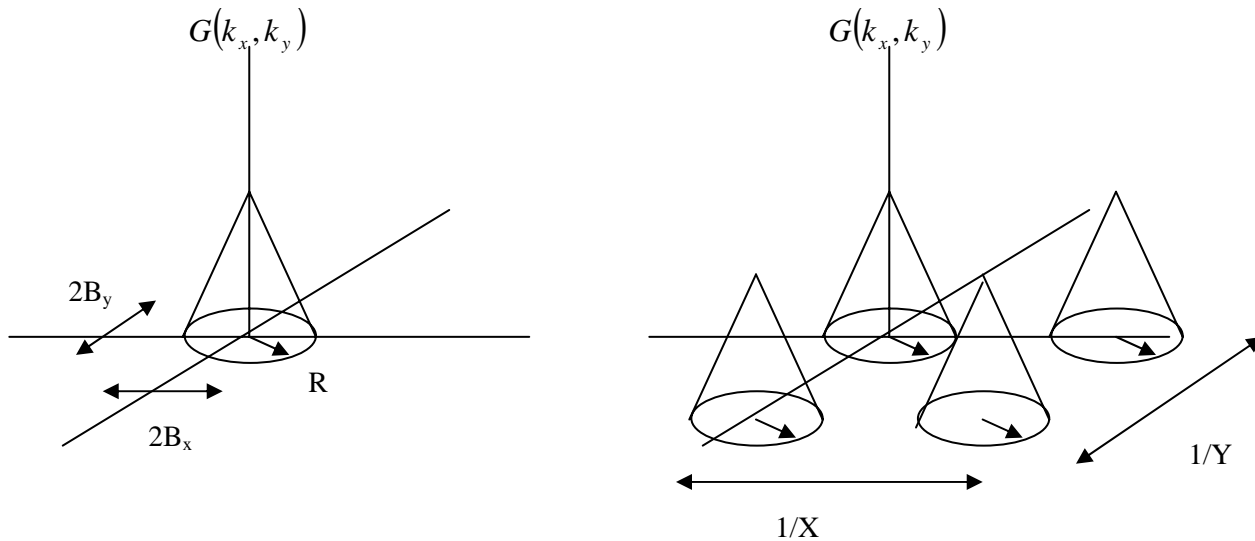


Figure 33 – Representation of $G(k_x, k_y)$

To determine the maximum allowable separation between the samples, let $2B_x$ and $2B_y$ be the widths in k_x and k_y of the smallest rectangle enclosing the region R . Then,

$$X \leq \frac{1}{2B_x}, Y \leq \frac{1}{2B_y}$$

To retrieve $g(x, y)$ from $g_s(x, y)$, we must pass g_s through a filter of a transfer function. One of the possible choices for this transfer function H is:

$$H(k_x, k_y) = \text{rect}\left(\frac{k_x}{2B_x}\right) \text{rect}\left(\frac{k_y}{2B_y}\right)$$

where

$$\text{rect}(x) = \begin{cases} 1, & |x| \leq \frac{1}{2} \\ 0, & \text{elsewhere} \end{cases}$$

therefore,

$$G_s(k_x, k_y) H(k_x, k_y) = G(k_x, k_y)$$

In the spatial domain, this becomes a convolution of $g_s(x, y)$ and $h(x, y)$. In the spatial domain, $h(x, y)$ is:

$$h(x, y) = 4B_x B_y \text{sinc}(2B_x x) \text{sinc}(2B_y y)$$

By working through the convolution given that $g_s(x, y)$ is a comb function, we can obtain the final solution for $g(x, y)$ for this given set of conditions:

$$g(x, y) = \sum_m \sum_n g\left(\frac{n}{2B_x}, \frac{m}{2B_y}\right) \sin c\left[2B_x\left(x - \frac{n}{2B_x}\right)\right] \sin c\left[2B_y\left(y - \frac{m}{2B_y}\right)\right]$$

Cross-sectional reconstruction

Projection Reconstruction

Given any object $g(x,y)$ in spatial coordinates, it is often easier to find its Fourier transform $G(k_x, k_y)$ from most imaging techniques, including CT and MRI. However, since these techniques take projections of multi-dimensional objects, there must be a way of reconstructing the image from the data obtained.

$$G(k_x, k_y) = \iint g(x, y) e^{-2\pi i(k_x x + k_y y)} dx dy$$

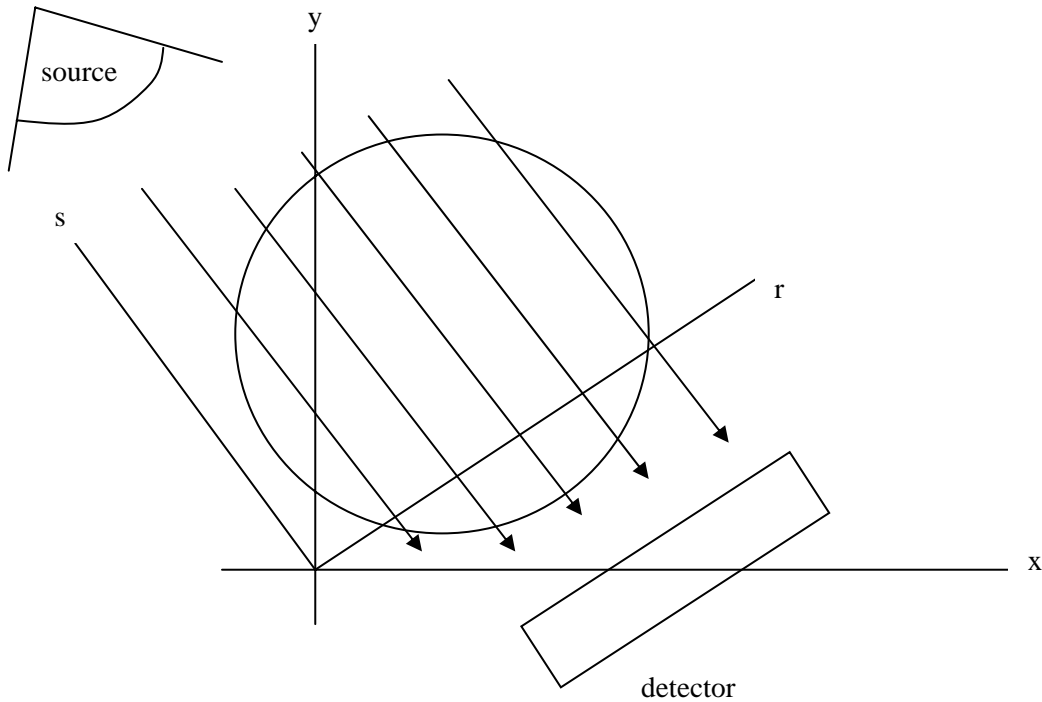


Figure 34 – Projection of a 2-D object onto axis r

The projection of $g(x,y)$ along any axis can be found by evaluating the following integral, for example, along the x-axis: $P(x) = \int_{-\infty}^{\infty} g(x, y) dy$. For any arbitrary angle ϕ , $P(r, \phi) = \iint_{r, \phi} g(x, y) ds$. The Fourier transform of this projection corresponds to a line through $G(k_x, k_y)$ (i.e. $\text{FT}\{P(x)\} = G(k_x, 0)$). To see this, rewrite $G(k_x, k_y)$ in terms of an integral over the axes r and s .

$$G(k_x, k_y) = \iint g_s(x, y) e^{-2\pi i k r} dr ds$$

$$k = \sqrt{k_x^2 + k_y^2} \quad \phi = \tan^{-1}\left(\frac{k_x}{k_y}\right)$$

But as seen above, the integral of $g(x, y)$ over s is simply the projection onto $P(r, \phi)$. Therefore,

$$G(k_x, k_y) = \int P(r, \phi) e^{-2\pi i k r} dr = G(k, \phi)$$

The Fourier transform of each projection therefore defines a ray at angle ϕ in $G(k_x, k_y)$. This is known as the Central Slice Theorem. If enough projections are taken, it is reasonable to assume that we can construct $g(x, y)$, by taking the inverse Fourier Transform of the projections.

This requires that the projection be linear, such that each element along the path contributes equally.

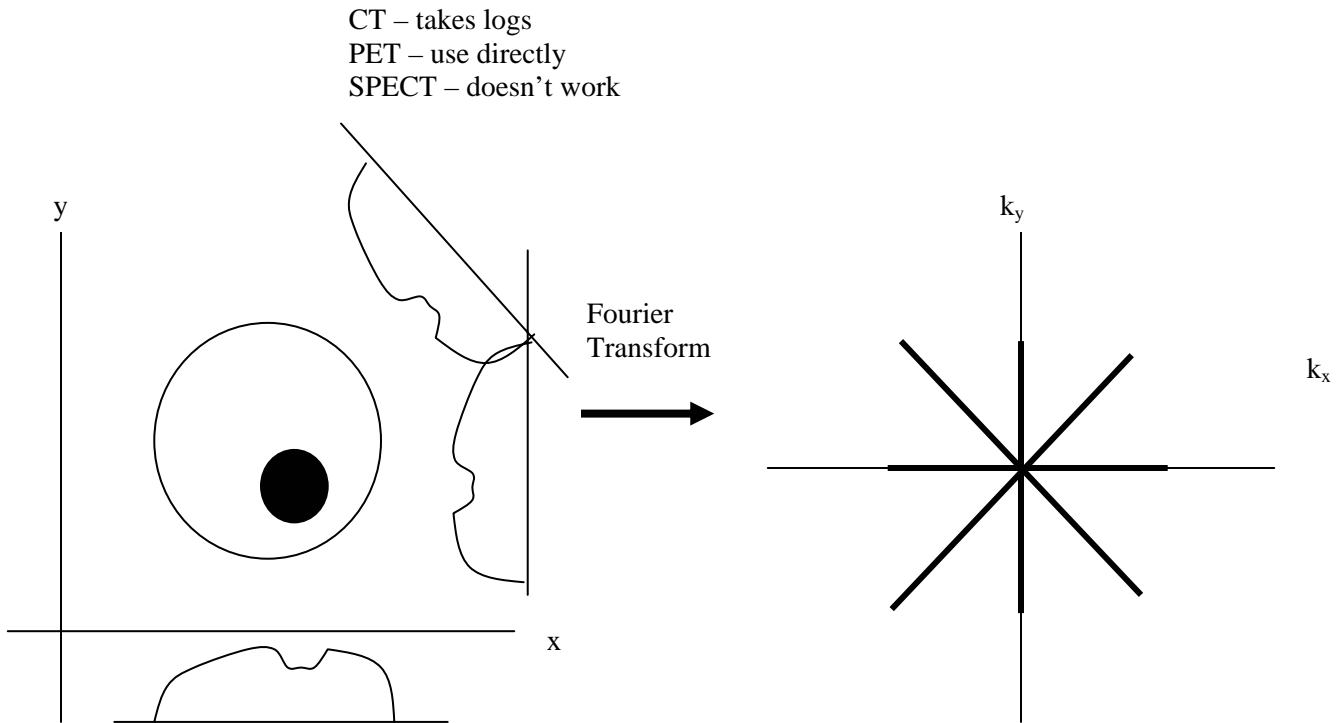


Figure 35 – Central Slice Theorem

Back projections

Instead of building the k -space picture by overlaying the projections through the origin, what if the projections were backprojected throughout the entire k -space domain along their respective angles (see Figure 36). In this fashion, the point response is a star, or equivalently, $PSF \propto 1/r$.

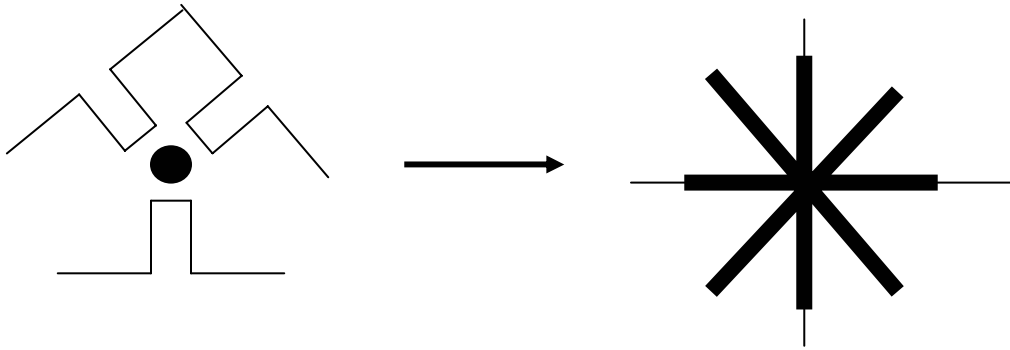


Figure 36 – Backprojection of a Point

The points at low spatial frequencies are oversampled. To obtain a properly weighted image, multiply the backprojected image by a ramp filter $W(k) = |k|$. In real space, this can be achieved by convoluting the projections with the Fourier Transform of $W(k)$.

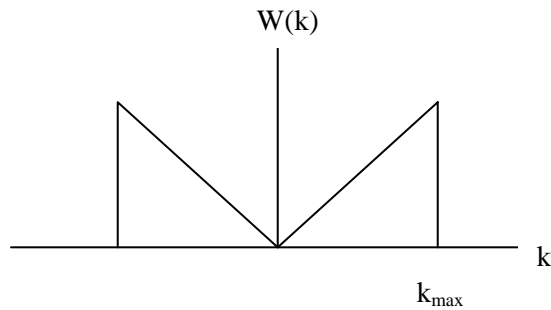


Figure 37 – Convolution Function Used in Backprojection

In practice, the exact convolution will vary and lead to trade-offs in resolution since we don't have a smooth roll-off in frequency to avoid ringing in space.

CHAPTER 7: NMR IMAGING

Now that we have seen how to reconstruct images from their projections, how do we obtain projections using NMR? We can't collimate the RF pulses like we can collimate x-rays because their wavelength is much too long. However, we can apply a linear magnetic field in the desired direction, i.e.:

$$G_z = \frac{dB_z}{dx}$$

$$B_z(x) = (B_o + xG_x)\hat{z}$$

$$\begin{aligned}\omega(x) &= \gamma B(x) = \gamma(B_o + xG_x) \\ &= \omega_o + \omega_x\end{aligned}$$

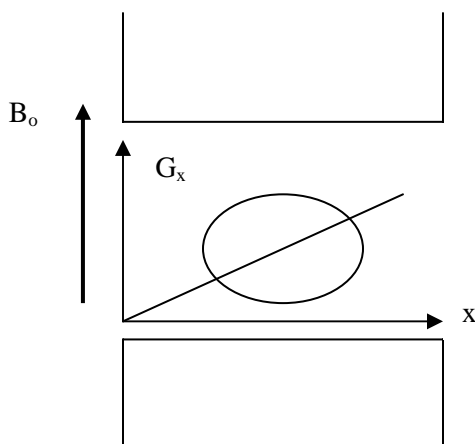


Figure 37 – Linear Gradient in the Magnetic Field

The spins distributed in the object will be precessing at different resonance frequencies which are dictated by the strength of the linear gradient. By examining the spatial distribution of the frequencies, we get a projection of the object along the x direction. The signal can be written as follows:

$S(\omega) \propto P(x) = \int \rho(x, y) dy$ where $\rho(x, y)$ is the object in question. Then the signal as a function of time can be written as:

$$\begin{aligned}S(t) &= \int P(\omega_x) e^{i\omega_x t} d\omega \\ &= \gamma G_x \int P(x) e^{i\gamma G_x t} dx\end{aligned}$$

Now by setting $k_x = \gamma G_x t$ we can see that $S(t)$ is simply the inverse Fourier transform of $P(x)$. This can be generalized to any line in the object by changing the linear gradient. If a combination of gradients in the x and y direction is applied, the projection through the object will be at an angle $\theta = \tan^{-1}\left(\frac{G_y}{G_x}\right)$.

Once the projections have been obtained, the image can be reconstructed by any of the techniques mentioned in the previous chapter.

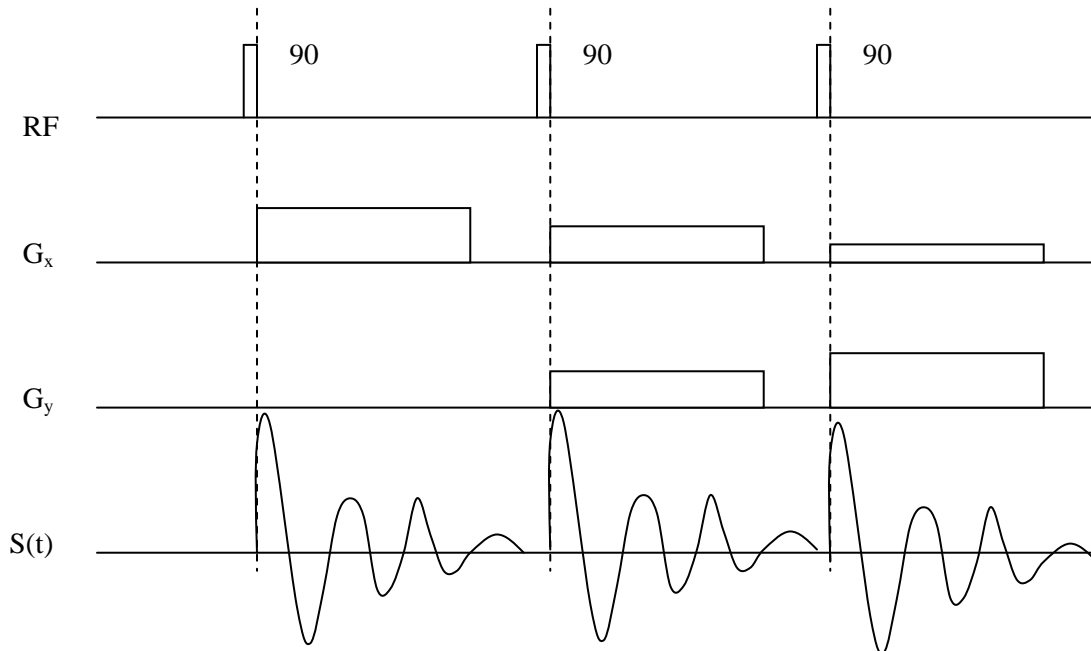


Figure 38 – Example of Pulse Sequence

These techniques can also be applied to reconstruct 3D images, simply by applying a third gradient in the z direction. (*References: Lai & Lauterber, J. Phys, E. 13, 747 (1980); Shepp, JCAT, 4, 94 (1980)*)

Details of Projection

(1) Signal to Noise

In one dimension, $SNR \propto \Delta x \sqrt{N}$, where Δx is the pixel size and N is the number of times the experiment is repeated. In three dimensions, $SNR \propto \Delta V \sqrt{N}$; therefore, to reduce the size of the voxel and maintain the same SNR, we must increase the number of experiments by quite a lot. For example, to reduce the voxel size by 2, the number of experiments must increase by 64!

(2) Gradient Size

The size of the gradient must be large enough to overcome the inhomogeneities in the magnetic field, i.e.:

$$\Delta\omega_{\text{gradient}} > \Delta\omega_{\text{in homogeneities +line width}}$$

However, if the gradient is too big, then noise will be introduced since the signal is too spread out. We need to have a large signal to over a small $\Delta\omega$ to overcome the noise.

(3) Sampling Rate

SI = sampling interval. $\frac{1}{SI} = \Delta\omega = \text{bandwidth} = \gamma G_x \Delta x$

where Δx is the size of the region of interest being imaged, or in other words, the field of view (FOV).

(4) Resolution

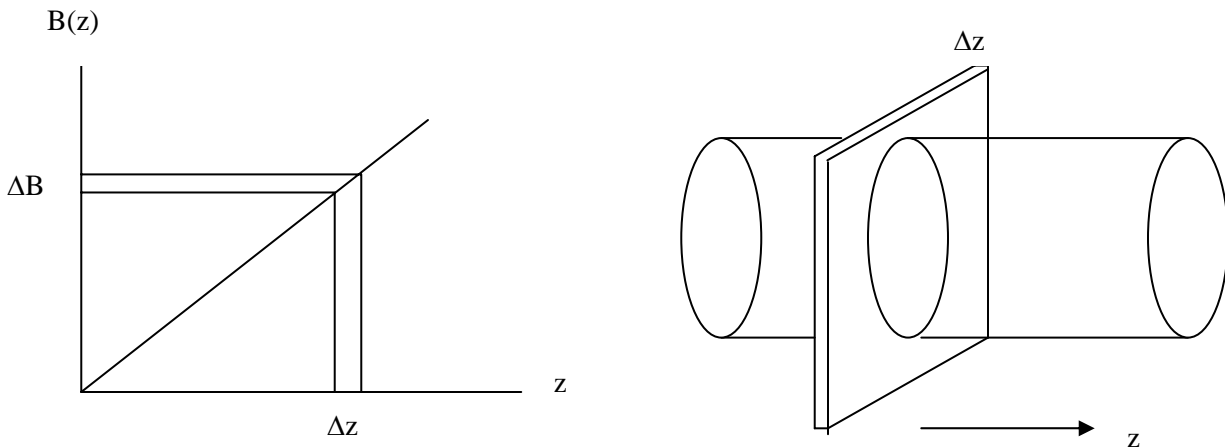
The number of pixels in an image is determined by the number of points that are sampled during one FID. If there are 256 sampled points, then there are 256 pixels in one dimension. The size of the pixels is determined by the FOV and the # of pixels:

$$\begin{aligned} \text{pixel size} &= \frac{FOV}{\# \text{ of pixels}} = \frac{1}{\gamma G_x (\text{SI} \cdot \# \text{ of sampled points})} \\ &= \frac{1}{\gamma G_x (\text{total acquisition time})} \end{aligned}$$

For an image containing $n \times n$ pixels, each acquisition gives us n samples. We therefore require n acquisitions. Similarly, in 3D, we require n^2 acquisitions.

Slice Selection

To define a plane in the z direction of an object, we can apply a gradient in the z direction and use an RF pulse with a well defined frequency range.



$$\Delta B = G_z \Delta z \text{ implies that } \Delta z = \frac{\Delta\omega}{\gamma G_z}, \text{ where } \Delta\omega = \text{RF bandwidth.}$$

To obtain a perfectly rectangular pulse of width, $\Delta\omega$, the pulse must have sinc shape in the time domain. It is impractical however to have a pure sinc function since it cannot be applied from $t = -\infty$ to $t = \infty$. It is necessary to truncate the sinc function, and it is usually limited to one lobe. This truncation causes “ringing” in the RF pulse as seen in the frequency domain.

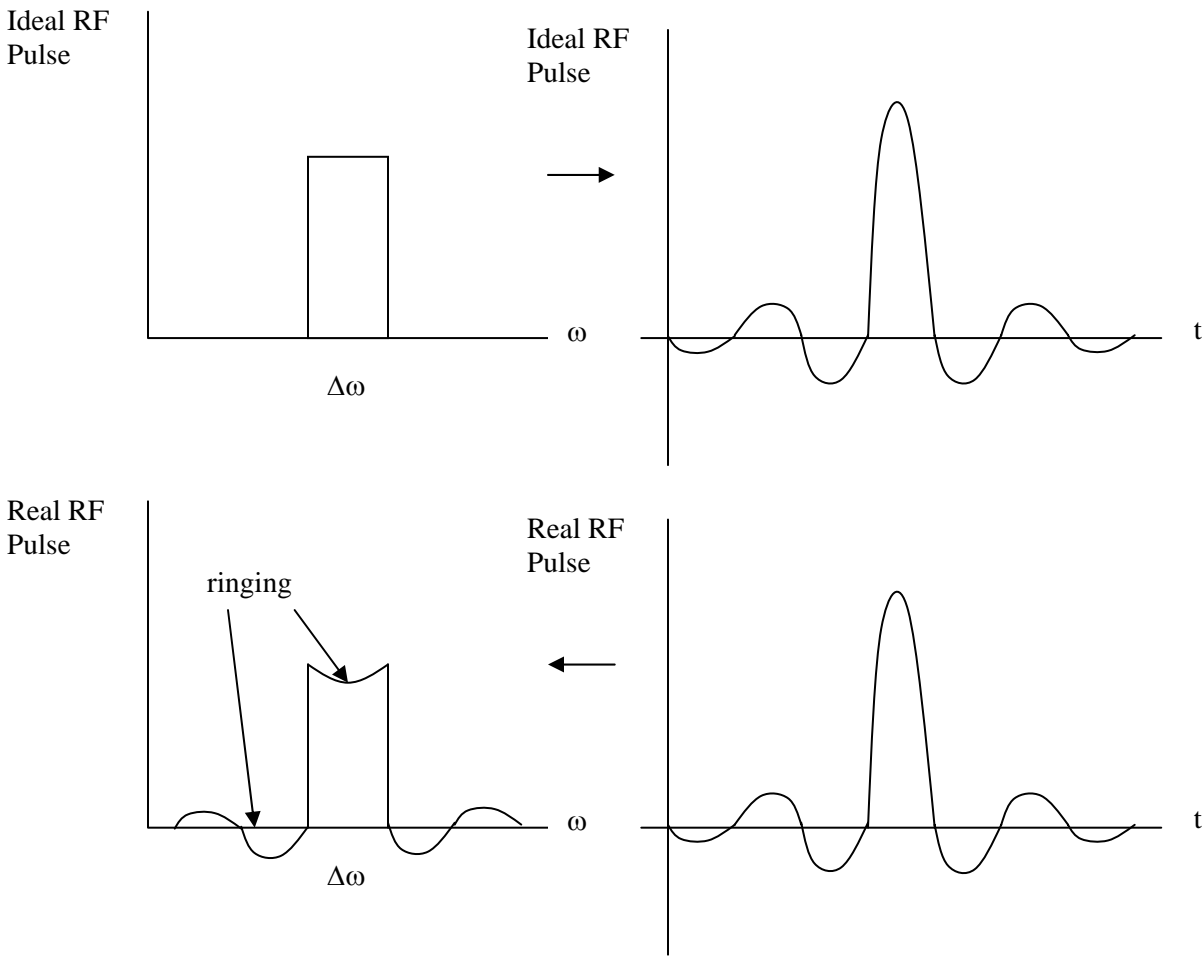


Figure 39 – Ideal and Realistic RF Pulse Shapes

If the gradient is simply applied at the same time as the RF pulse, there will be no signal detected. This is due to the fact that some spins will reach the transverse plane before the RF pulse is turned off. Since the gradient is still on, the spins will be dephased by an amount equal to $\Delta\Phi = \gamma G_z \Delta z \tau$, where τ is the time that the gradient is on and the magnetization vector is in the transverse plane. τ is actually equal to half the total time that the gradient is on. To compensate for this, apply the reverse gradient for a time τ in the z direction to rephase the spins by the amount $\Delta\Phi$. This is called compensatory gradient.

This will give a gradient echo, i.e. when the spins are refocused from the effects of the previous gradients (this will not correct for magnetic inhomogeneities like 180° pulse).

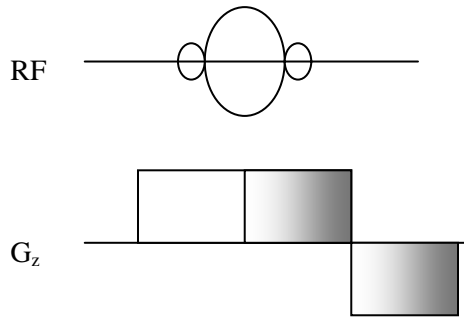


Figure 40 – RF Pulse and Compensatory Gradient

A different gradient G_z could be applied, as long as the angle $\Delta\Phi$ is the same (i.e. a smaller gradient could be applied for a longer time or a stronger gradient could be applied for a shorter time).

Gradient Echo Pulse Sequence

So far we have discussed slice selection and projection formation. Putting all of this together, the following pulse sequence will give us a gradient echo signal for various projections. Once the projections have been obtained, the reconstruction algorithms may be applied.

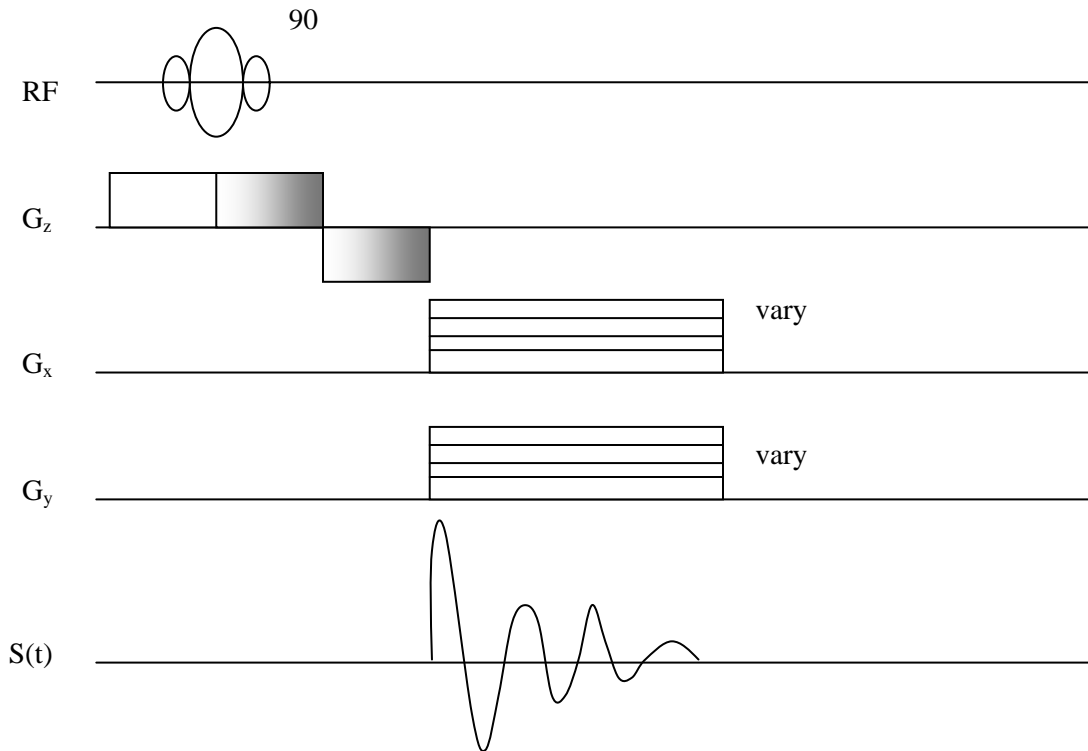


Figure 41 – Gradient Echo Pulse Sequence

Spin Echo Pulse Sequence

To create a spin echo, apply a 180° pulse at time $t = TE/2$. At time TE , the spins will refocus and an echo will be formed. The pulse sequence would look something like this:

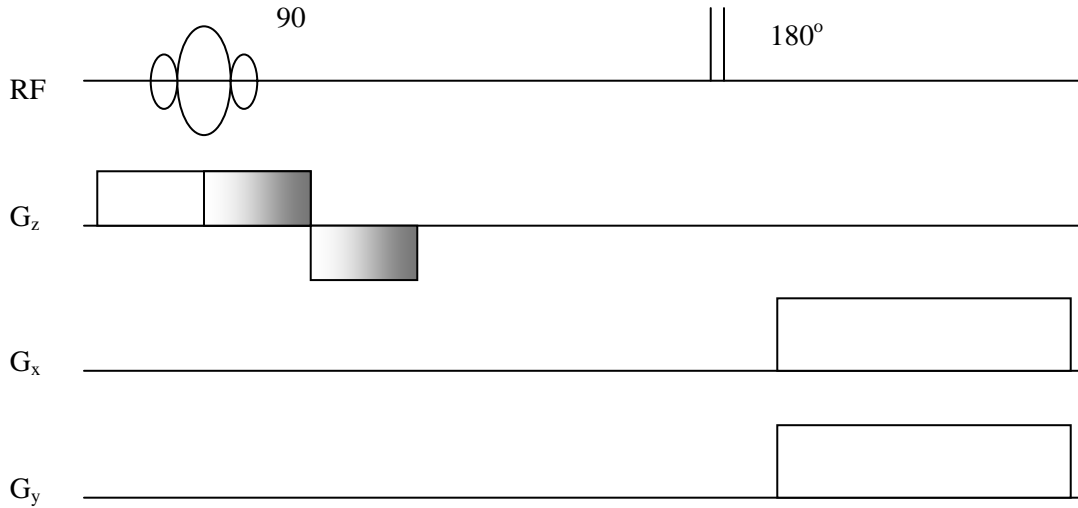


Figure 42a – Incorrect spin echo pulse sequence

This sequence will not produce a signal for the same reason that a compensatory gradient needed to be added to G_z . The first half of the gradients in x and y will dephase the spins as they are attempting to rephase and create the spin echo. To correct for this effect, we must apply a compensatory gradient. This can be done by either applying reverse gradients just before the read-out gradients or we could apply the same gradients before 180° pulse since the 180° pulse will reverse their effect.

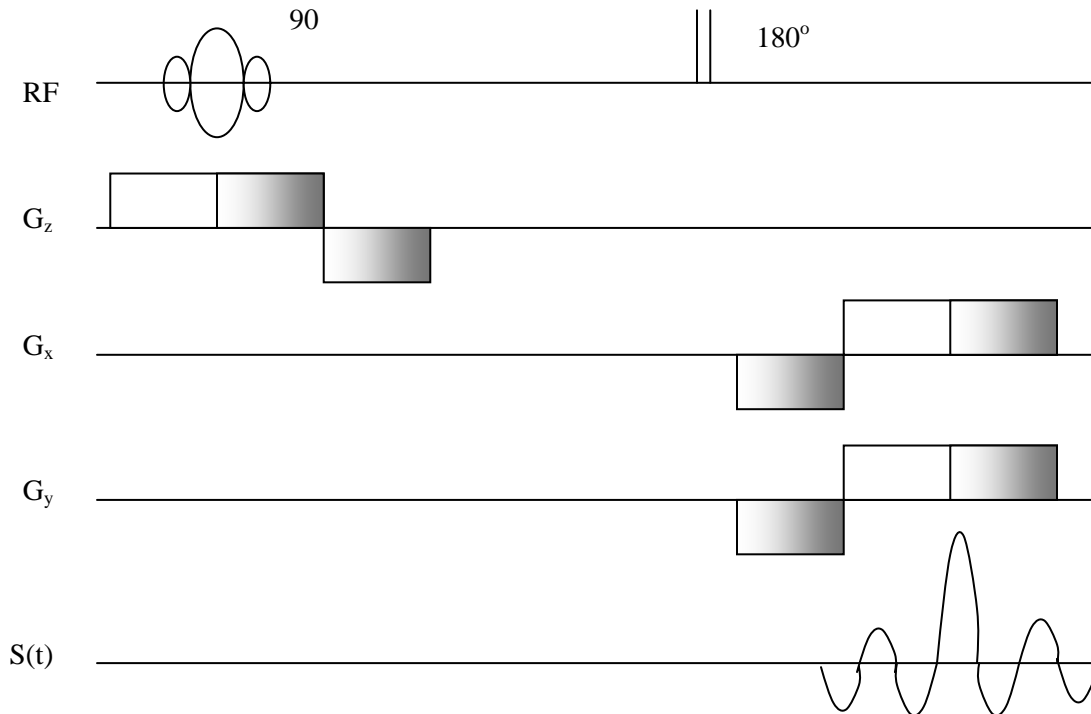


Figure 42b – Correct spin echo pulse sequence

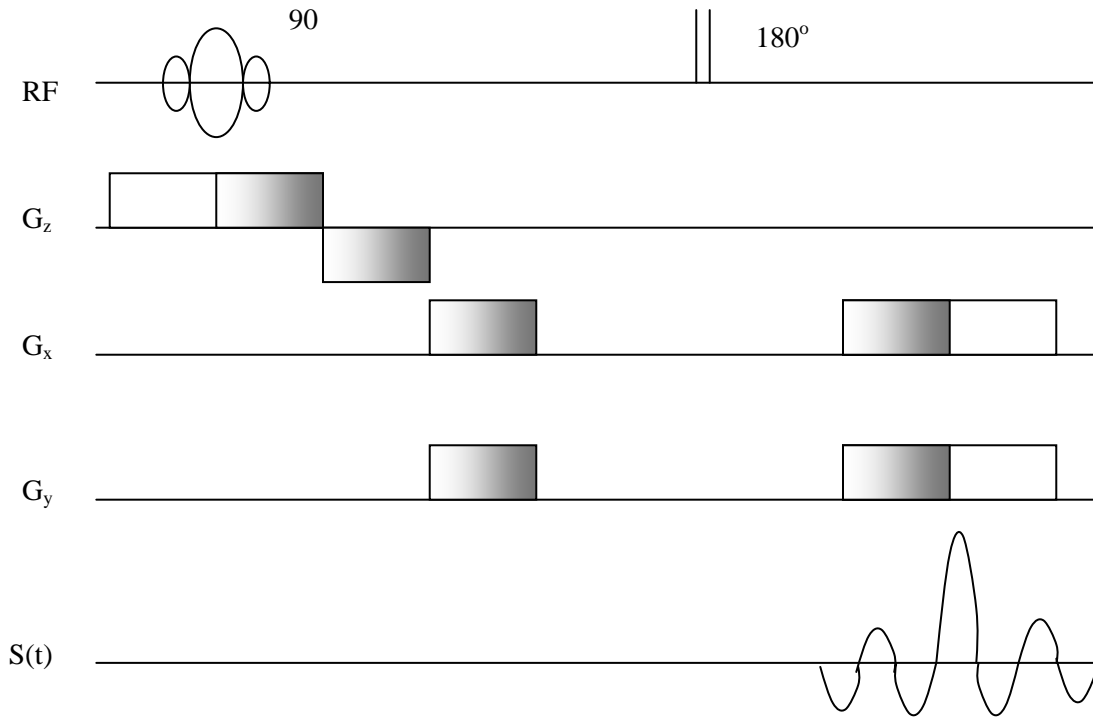


Figure 43 – Correct Spin Echo Pulse Sequence

Phase Encoding

Can we use the gradient dephasing for something useful? If we apply a gradient in the y direction without refocusing the spins, we will obtain information about the frequency distribution of the object in that direction. If the gradient is applied for a constant time τ , then the spins will be dephased by an amount:

$$\Delta\Phi_y = \gamma G_y y \tau$$

The signal can then be represented by:

$$\begin{aligned} S(t, \tau) &= \iint \rho(x, y) e^{i(\gamma G_x x t + \gamma G_y y \tau)} dx dy \\ &= \iint \rho(x, y) e^{i(k_x x + k_y y)} dx dy \end{aligned}$$

where

$$k_x = \gamma G_x t; \quad k_y = \gamma G_y \tau$$

This looks parallel in x and y, but τ is a constant, while t evolves, thus giving us spatial encoding by taking the Fourier Transform. This puts a phase twist in y. One way of looking at this is for each x, we are measuring a single Fourier component of the data along y. To get the whole object, we must sample multiple Fourier components in k_y and then take the inverse Fourier transform. To change k_y , we can either change $G_y \tau$. Each point sampled from the FID gives us one point in k_x at a constant k_y . The entire k-space can be rastered through in a rectilinear fashion by changing the value of k_y and repeating the experiment. Each value of k_y is called a phase encoding step.

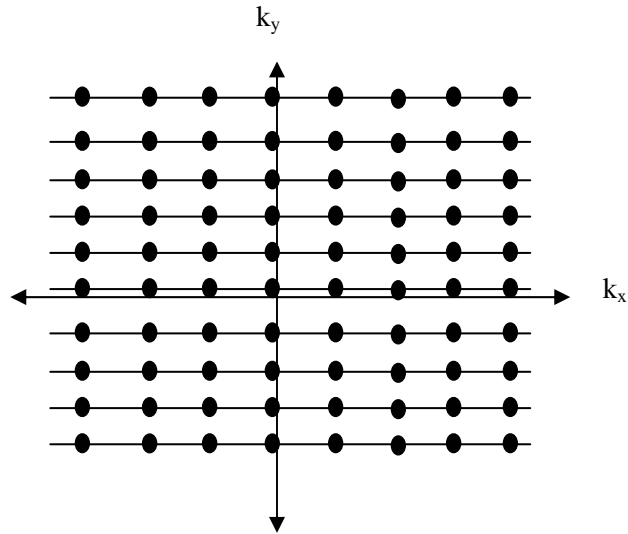


Figure 44 – Digitization of k-space

To obtain an $n \times n$ image, we acquire n points in the FID and then repeat the experiment n times, each time with a different value of k_y . To reconstruct the image, simply inverse Fourier transform the acquired data. This experiment is called spin warp.

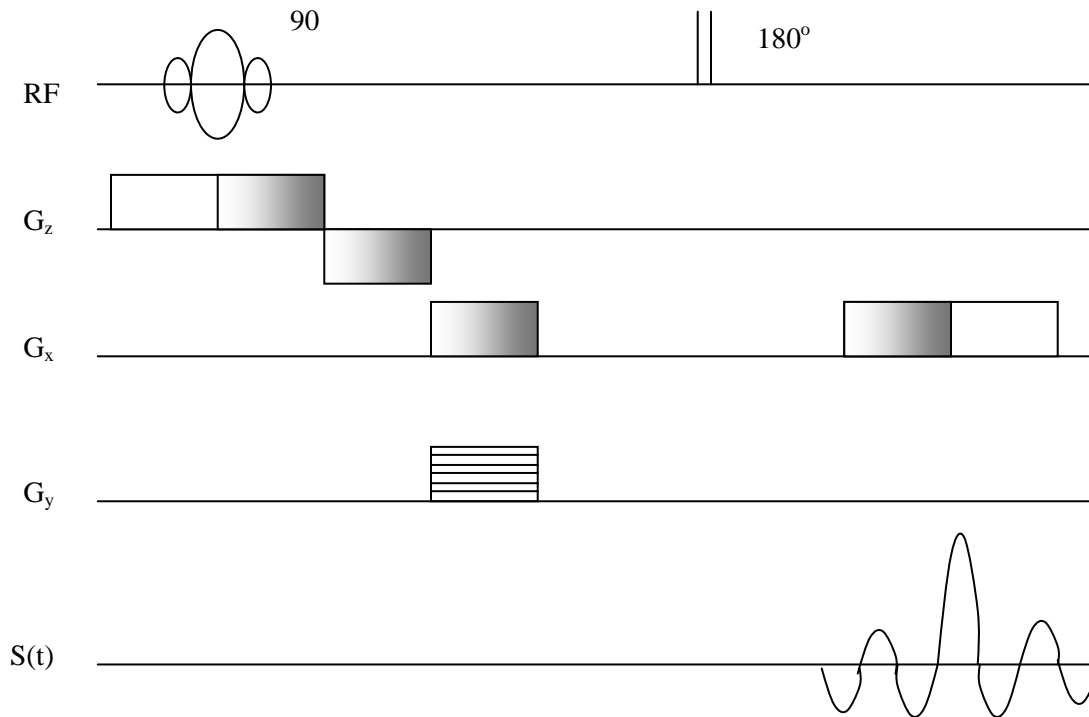


Figure 45 –Spin Warp Pulse Sequence

This method can be applied to 3D imaging as well. Simply add G_z gradient in the same manner that a G_y gradient is applied. If a slice selective G_z is applied as well, we will obtain multiple finer slices within the selected slice.

e.g. If we want 1 mm slices

$$G_z = \frac{\Delta\omega}{\gamma\Delta z} = \frac{3000 \text{ Hz}}{4 \times 10^3 \frac{\text{Hz}}{\text{G}} \cdot 0.1 \text{ cm}} = 7.5 \frac{\text{Gauss}}{\text{cm}}$$

which is a very large gradient. Instead, we can obtain a 15 mm slice (with $G_z = 0.5 \text{ Gauss/cm}$) and use 16 phase encoding steps in z. This is a good way of getting thin slices, but it can be a lengthy experiment.

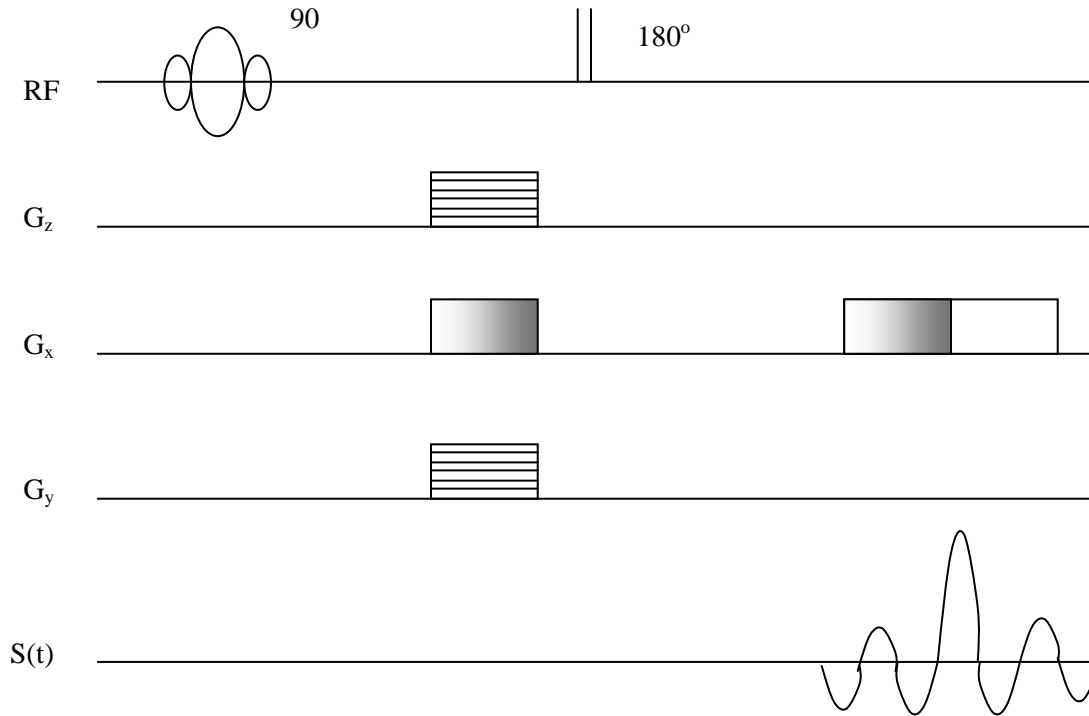


Figure 46 – 3D Spin Warp Pulse Sequence

Multiplanar Imaging

There are long delays in viewing a large 3D objects because each slice must have time to relax before the experiment may be repeated. For example, if we want to obtain a 256x128 image with $N_{ave} = 4$, then if $TR = 300 \text{ ms}$, it takes 4.3 minutes to acquire one slice. If 10 slices are to be acquired, the total experiment requires 3 hours. Is there a way of obtaining stack images faster? Since $T_2 \sim 0.1 T_1$, there is a lot of dead time since TR is on the order of T_1 . We can image other slices during this time by either shimming B_0 or by changing the center frequency of the 90° RF pulse.

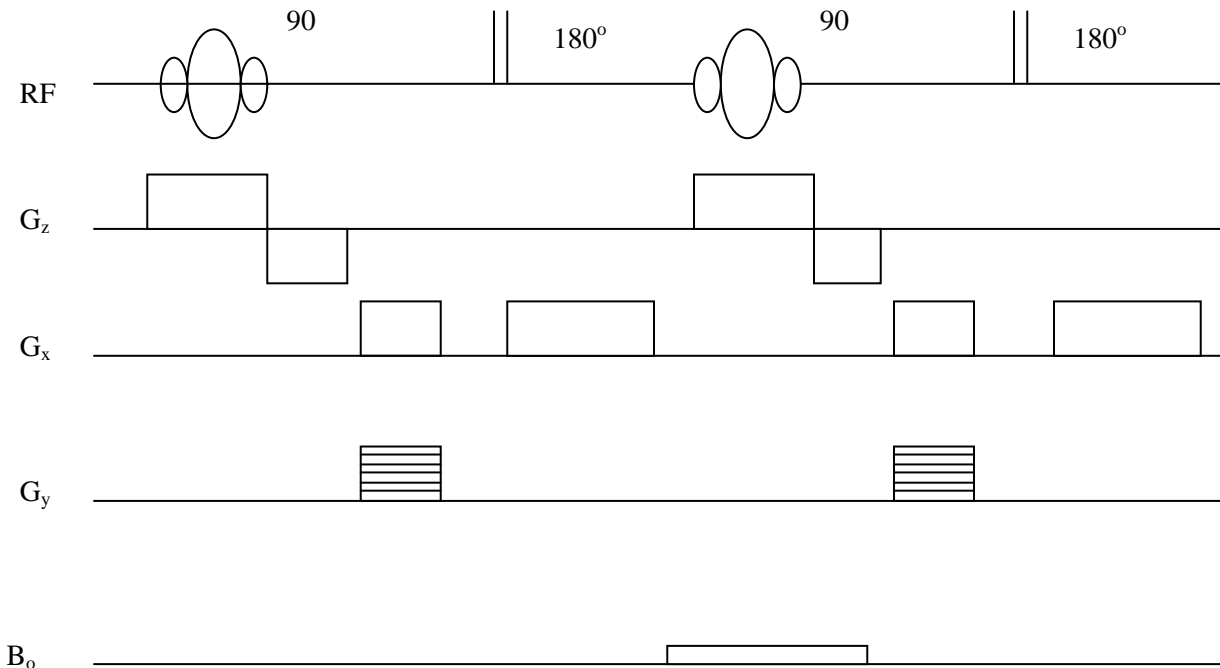


Figure 47 – Incorrect Fast Spin-Echo Pulse Sequence

The 180° pulses are “hard” pulses (i.e. they tip every spin in the sample). To avoid perturbing spins that are not involved in the slice, we must make the 180° pulse a “soft” pulse. It will look like the 90° pulse, will be centered around the same frequency and a slice selective G_z must be applied at the same time. The number of slices which can be obtained from this sequence is now dependent on TE and the total data collection time. The former is determined by the contrast that is desired in the image (as will be shown later) while the latter is dependent on gradient strengths, etc.

The total number of slices collected can be determined from

$$* \text{ of slices} = \frac{TR}{TE + \frac{1}{2}(\text{data collection time}) + F}$$

where F represents any additional time needed for gradients, etc

Example: If data collection time = 15 ms and TE = 30 ms, then the time between slices is ~ 40 ms.

If TR = 500 ms → 12 slices can be collected

If TR = 2000 ms → 50 slices can be collected

Is this more efficient? It all depends on the number of averages (N_{ave}) which are needed to get adequate SNR. If $N_{ave} < \#$ of slices needed, 2D is more efficient than the 3D method. However, the 2D multiscale approach may be less efficient if the total number of slices scanned does not cover the region of interest (small TR) and many slice averages are required. In general, the 2D technique is used. Only when very thin slices are needed or TR is very short is the 3D technique used.

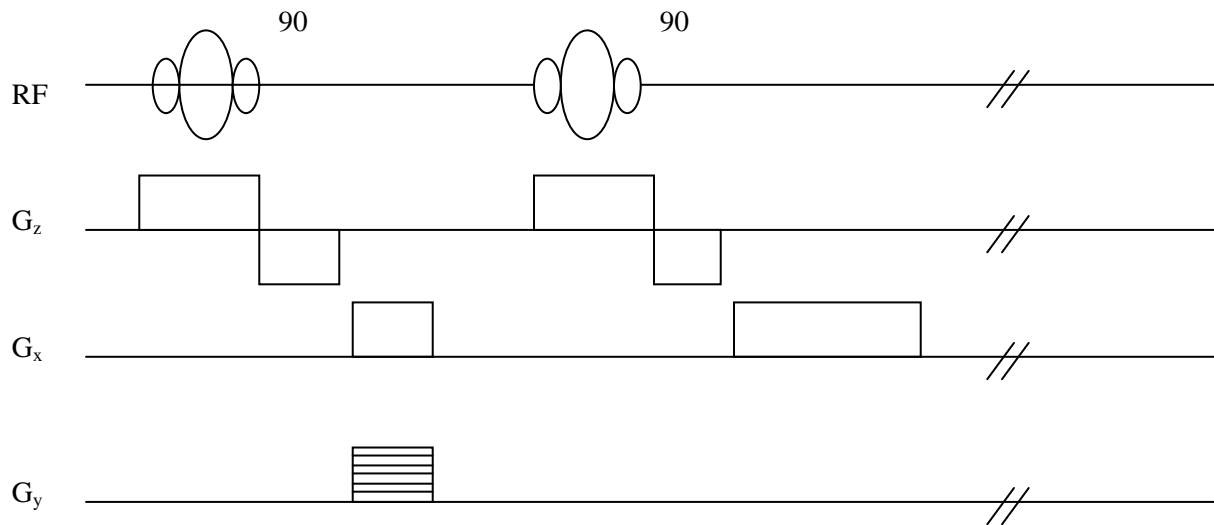


Figure 48 – Correct Fast Spin-Echo Pulse Sequence

Image Contrast

Now that we know how to obtain an image, we need to understand what kind of information these images are providing us. The image is not simply a measure of the proton density of the tissue. The relaxation times will influence the image contrast depending on the TE and TR chosen. To understand these concepts, let's examine the Bloch equations:

$$\frac{dM_z}{dt} = \frac{M_o - M_z(t)}{T_1}$$

$$\frac{dM_x}{dt} = -\frac{M_x(t)}{T_2}$$

$$\frac{dM_y}{dt} = -\frac{M_y(t)}{T_2}$$

Solving these equations in the rotating frame on resonance gives

$$M_x(t) = M_x(0)e^{-\frac{t}{T_2}}$$

$$M_z(t) = M_o \left(1 - e^{-\frac{t}{T_1}} \right) + M_z(0)e^{-\frac{t}{T_1}}$$

T₁ Weighted Images

Since different tissues have different relaxation times, can we use this behavior to our advantage?

To ensure maximum contrast between tissues, it is necessary to optimize TR. If we assume a small difference in tissue T_1 where the largest signal intensity difference?

$$d(SI) = \frac{M_o TR \cdot \left(e^{-\frac{TR}{T_1}} \right) d(T_1)}{T_1^2}$$

Now maximize with respect to TR:

$$\begin{aligned} \frac{d(SI)}{d(TR)} = 0 &= M_o \left(\frac{e^{-\frac{TR}{T_1}}}{T_1^2} - \frac{TR \cdot e^{-\frac{TR}{T_1}}}{T_1^3} \right) d(T_1) \\ 0 &= \frac{e^{-\frac{TR}{T_1}}}{T_1^2} \left(1 - \frac{TR}{T_1} \right) \\ TR &= T_1 \end{aligned}$$

Therefore, when $TR = T_1$, we obtain a maximum contrast between two tissues with small differences in T_1 . Is contrast what we really want to maximize however? It may be best, depending on other imaging constraints (i.e. # of slices) to maximize the **contrast to noise ratio** (or SNR).

Note: This derives from Roses's (1957) concept of features of dots in a background of dots. Using Poisson statistics, he showed that to "see" a feature the difference in the number of dots in the feature and the background must be greater than some factor (he suggested 5) times the expected variation of the number of dots in the feature.

$$(n_2 - n_1)s^2 \geq k\sqrt{n_2s^2}$$

where: n_1 = dots in background/area
 n_2 = dots in feature/area
 s = area
 k = constant ($\cong 5$)

Therefore,

$$\frac{C}{N} = \frac{(n_1 - n_2)s^2}{\sqrt{n_2s^2}} > 5$$

If we reduce TR, we will be able to perform more averages (which reduces the noise) in the same imaging time. However, the decrease in TR will decrease the contrast between the tissues. It is necessary to optimize these two conflicting parameters:

Give: $SNR \propto \sqrt{N}$; $N \propto \frac{1}{TR}$ then

$$SNR \propto \sqrt{\frac{1}{TR}}$$

$$\Rightarrow d(SNR) = \sqrt{\frac{1}{TR}} \frac{TR \cdot e^{-\frac{TR}{T_1}}}{T_1^2} d(T_1) = \frac{\sqrt{TR} e^{-\frac{TR}{T_1}}}{T_1^2} d(T_1)$$

Now maximize with respect to TR:

$$\frac{d(SNR)}{d(TR)} = \frac{e^{-\frac{TR}{T_1}}}{2\sqrt{TR}T_1^2} - \frac{\sqrt{TR}e^{-\frac{TR}{T_1}}}{T_1^3} = 0$$

$$\Rightarrow TR = \frac{T_1}{2}$$

Therefore, to maximize the signal to noise, choose $TR = T_1/2$. For example, for gray-white matter in the brain, choose $TR \sim 800$ ms, since $T_1(\text{gray}) \sim 1700$ ms and $T_1(\text{white}) \sim 1500$ ms.

If we want to measure T_1 , we should measure multiple points in order to get an appropriate fit. We can obtain a nice linear equation to fit T_1 to:

$$SI(TR) = SI(\infty) \left(1 - e^{-\frac{TR}{T_1}} \right)$$

$$SI(\infty) - SI(TR) = SI(\infty) e^{-\frac{TR}{T_1}}$$

$$\ln[SI(\infty) - SI(TR)] = \ln[SI(\infty)] - \frac{TR}{T_1}$$

There remains one question: How do we measure T_1 most efficiently? i.e. for a given total image time, how many points would you measure with how many N_{ave} ? It all depends on the total imaging time, T_1 (sample) and T_1 (range of samples).

Inversion Recovery

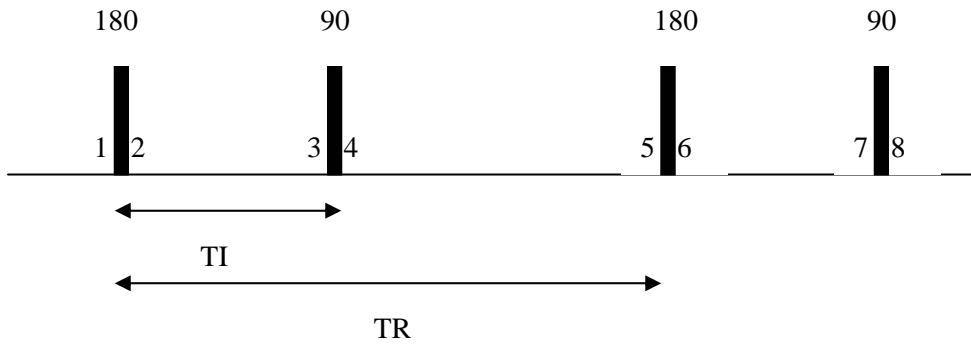


Figure 50 – Inversion Recovery Pulse Sequence

Assume that $TR \gg T_1$

$$M_z(1) = M_o$$

$$M_x(1) = 0$$

$$M_z(2) = -M_o$$

$$M_x(2) = 0$$

$$M_z(3) = M_o \left(1 - e^{-\frac{TI}{T_1}} \right) + M_z(2) e^{-\frac{TI}{T_1}}$$

$$M_x(3) = 0$$

$$= M_o \left(1 - 2e^{-\frac{TI}{T_1}} \right)$$

$$M_z(4) = 0$$

$$M_x(4) = M_o \left(1 - 2e^{-\frac{TI}{T_1}} \right)$$

Since $TR \gg T_1$, $M_x(8) = M_x(4)$ i.e. equilibrium is immediately reached. This is much like the SR equation, however the dynamic range is increased by 2.

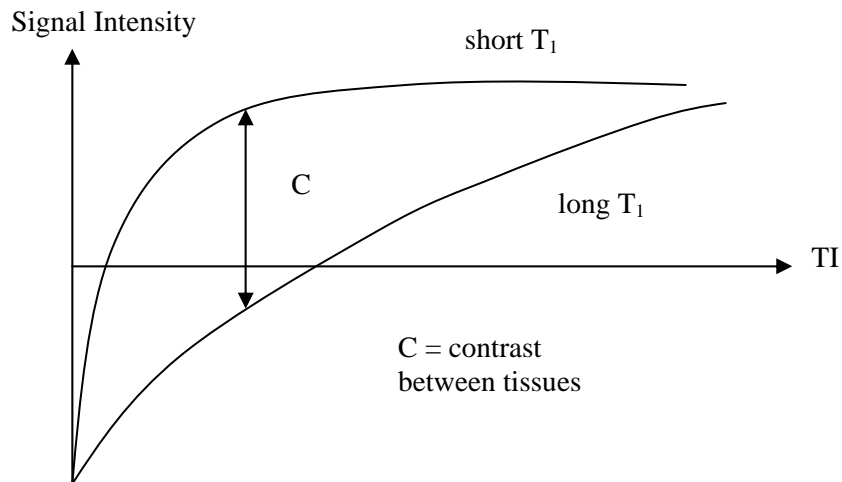


Figure 51 – Signal Intensity as a Function of TI

Again, optimum contrast can be defined. If TR is not $\gg T_1$, things become tricky. Nevertheless, we can use SI(TI) to measure T_1 as in SR. This is traditionally done when total time is not at a premium, as in spectroscopic measurements. We can also make images which reflect T_1 or T_1 rate ($1/T_1$).

T₂ Weighted Images:

To reflect T_2 differences in tissue, do a spin echo experiment

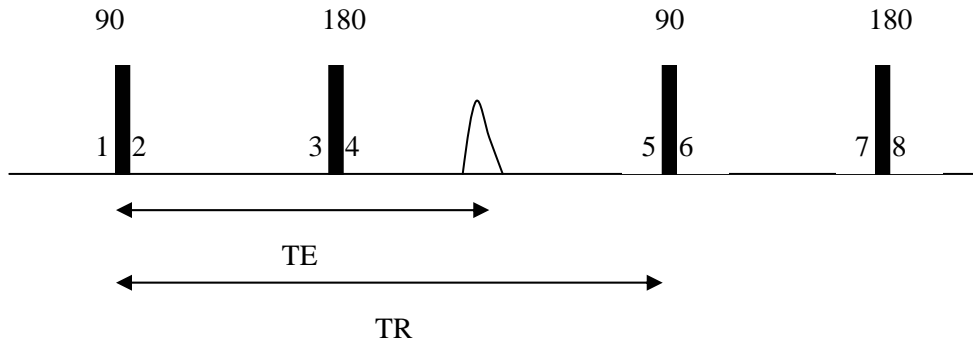


Figure 52 – Spin Echo Pulse Sequence

If $TR \gg T_1$, then

$$SI = kM_0 e^{-\frac{TE}{T_2}}$$

What if TR is not $\gg T_1$?

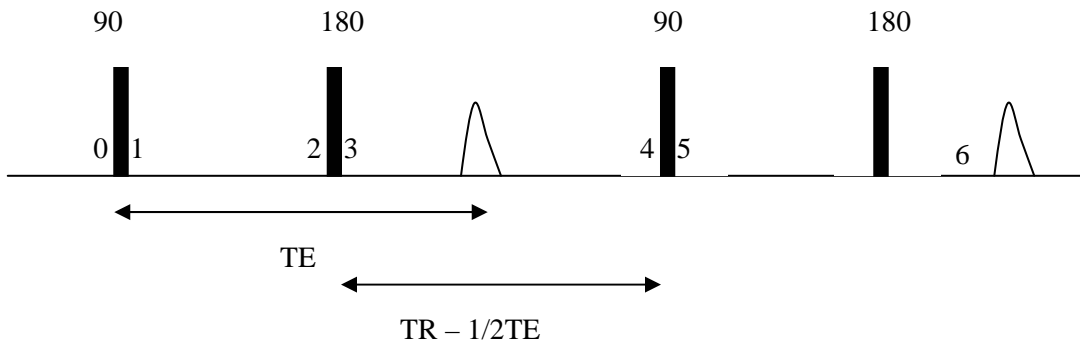


Figure 53 – Spin Echo Pulse Sequence

As before, compute M_z and look at the signal intensity proportional to M_{xy} after the 90° pulse.

$$M_z(2) = M_o \left(1 - e^{-\frac{TE}{2T_1}} \right)$$

$$M_z(3) = -M_z(2) = -M_o \left(1 - e^{-\frac{TE}{2T_1}} \right)$$

$$\begin{aligned} M_z(4) &= M_o \left(1 - e^{-\frac{(TR-TE/2)}{T_1}} \right) + M_z(3) e^{-\frac{(TR-TE/2)}{T_1}} \\ &= M_o \left(1 - 2e^{-\frac{(TR-TE/2)}{T_1}} \right) + e^{-\frac{(TR-TE/2)}{T_1}} \end{aligned}$$

Now compute M_{xy}

$$M_{xy}(5) = M_z(4)$$

$$M_{xy}(6) = M_{xy}(5) e^{-\frac{TE}{T_2}}$$

If $TE \ll TR$, then

$$SI \propto e^{-\frac{TE}{T_2}} M_o \left(1 - e^{-\frac{TR}{T_1}} \right)$$

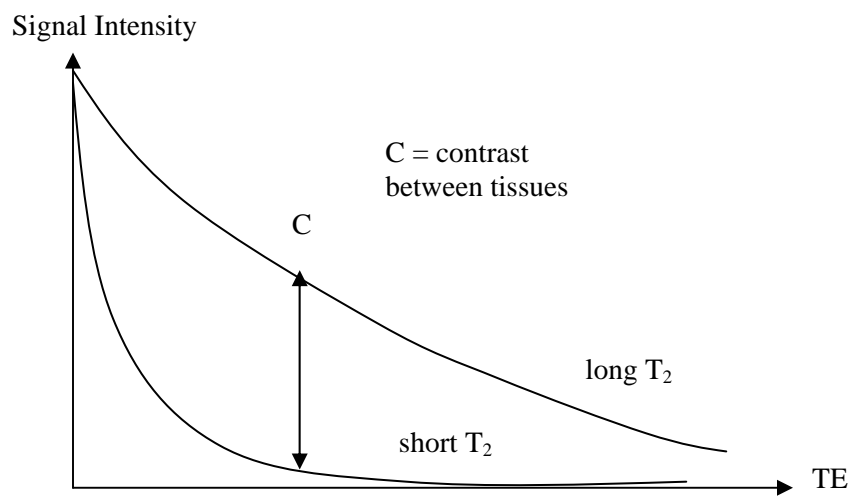


Figure 54 – Signal Intensity as a Function of TE

Therefore, long $T_2 \Rightarrow$ bright image
 short $T_2 \Rightarrow$ dark image

Where is the maximum contrast point?

$$SI \propto M_o e^{-\frac{TE}{T_2}}$$

$$d(SI) = \frac{M_o TE e^{-\frac{TE}{T_2}}}{T_2^2} dT_2$$

$$\frac{d(SI)}{d(TE)} = \frac{e^{-\frac{TE}{T_2}}}{T_2^2} \left(1 - \frac{TE}{T_2} \right) dT_2$$

$$TE = T_2$$

For maximum contrast, choose $TE = T_2$.

What if $TR \approx T_1$? Remember that long $T_1 \Rightarrow$ dark image and a long $T_2 \Rightarrow$ bright image. These are competing contrasts. Often, tissues with long T_2 have long T_1 .

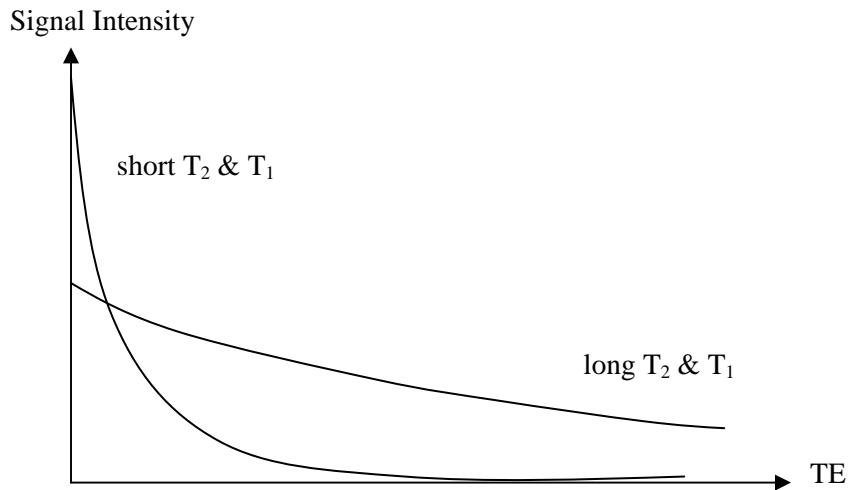


Figure 55 – Signal Intensity for Both Long and Short T_1 and T_2

So for long TE, T_2 will dominate, but for short TE, T_1 will dominate.

Example

$T_1 = 500$ ms $T_2 = 50$ ms
 Set $TR = T_1$ (maximum T_1 contrast)

If TE = 30 ms (typical value), then $\Delta SI \approx 0$

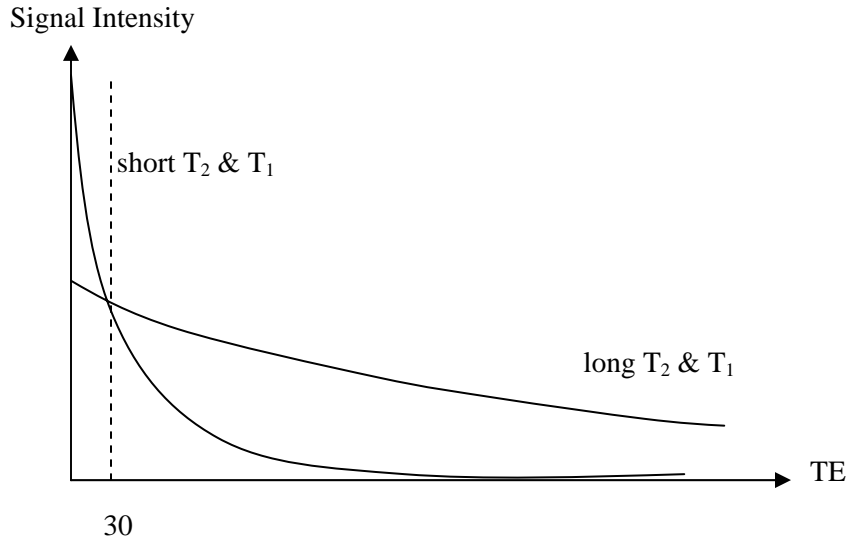


Figure 56 – An Example of Poor Parameter Choices

Thus the maximum contrast T_1 weighted image is in fact a very poor choice if $TE_{min} = 30$ ms. To get maximum T_1 contrast from SE images, you need to set TE_{min} as small as possible.

Time Parameter	T_1 Weighted	T_2 Weighted	ρ Weighted
TR	$T_1/2$	$\gg 3T_1$	$\gg 3T_1$
TE	TE_{min}	T_2	TE_{min}

Small Tip Angle

What if the tip angles are not exactly 90° or 180° ?

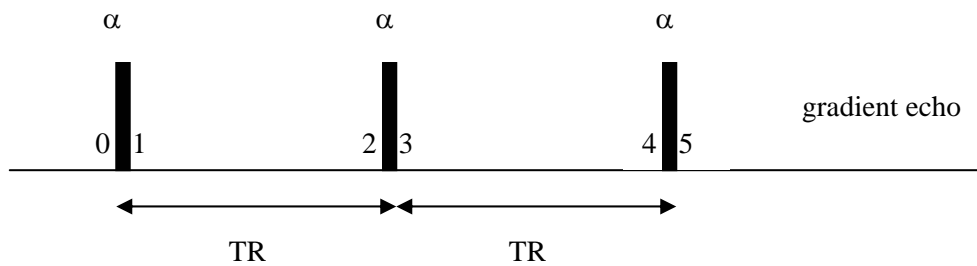


Figure 57 – Small Tip Angle Pulse Sequence

$$\begin{aligned}
 M_z(0) &= M_o & M_x(0) &= 0 \\
 M_z(1) &= M_z(0)\cos\alpha & M_x(1) &= M_z(0)\sin\alpha
 \end{aligned}$$

Now assume that all transverse magnetization (M_x) is lost in TR.

$$\begin{aligned}
M_z(2) &= M_o \left(1 - e^{-\frac{TR}{T_1}} \right) + M_z(1) e^{-\frac{TR}{T_1}} & M_x(2) &= 0 \\
M_z(3) &= M_z(2) \cos \alpha & M_x(3) &= M_z(2) \sin \alpha
\end{aligned}$$

We could march down to 4 and 5, but that would get messy. A better way of looking at this problem is by assuming that there have already been many pulses prior to 0 and that the system has reached equilibrium. In this situation, $M_z(2) = M_z(0)$.

$$M_z(0) = M_o \left(1 - e^{-\frac{TR}{T_1}} \right) + M_z(0) e^{-\frac{TR}{T_1}} \cos \alpha$$

$$M_z(0) = \frac{M_o \left(1 - e^{-\frac{TR}{T_1}} \right)}{\left(1 - e^{-\frac{TR}{T_1}} \cos \alpha \right)}$$

If $\alpha = 90^\circ$, then we recover $M_z(\text{equil}) = M_o \left(1 - e^{-\frac{TR}{T_1}} \right)$. The signal intensity is then given by:

$$SI \propto M_x = M_z(\text{equil}) \sin \alpha$$

$$SI = \frac{M_o \left(1 - e^{-\frac{TR}{T_1}} \right) \sin \alpha}{1 - e^{-\frac{TR}{T_1}} \cos \alpha}$$

We can maximize this expression with respect to α to obtain an expression for α which maximizes M_x for a give TR. This angle is known as the Ernst angle. However, the Ernst angle may not give the maximum T_1 contrast-to-noise ratio. The T_1 contrast is large for large α and is small for small α (SNR drops for both cases).

For a real gradient echo experiment, there is also a T_2^* decay term. The signal intensity is therefore:

$$SI \propto e^{-\frac{TE}{T_2^*}} \frac{M_o \left(1 - e^{-\frac{TR}{T_1}} \right) \sin \alpha}{\left(1 - e^{-\frac{TR}{T_1}} \cos \alpha \right)}$$

This also assumes that $T_2 < TR$. If this is not the case, “steady state” can occur and new expressions are needed.

CHAPTER 8: CHEMICAL SHIFT IMAGING

How can we combine spectral and spatial information? In conventional NMR imaging, there have historically been three models:

- (1) Point methods (e.g. TMR to define a point and then move the point or the object)
- (2) Sensitive lines
- (3) Sensitive planes and volumes

How can we spatially encode without disrupting the chemical shift information? Typically, imaging gradients are on the order of 0.1 – 1.0 G/cm or 1.0 – 10.0 ppm/point, as expected since we need $\Delta\omega_{\text{gradient}} > \Delta\omega_{\text{linewidth}} / \text{pixel}$. If chemical shifts are greater than the line widths, then we have:

$$\Delta\omega_{\text{shift}} > \Delta\omega_{\text{gradient}} > \Delta\omega_{\text{pixel}} > \Delta\omega_{\text{linewidth}}$$

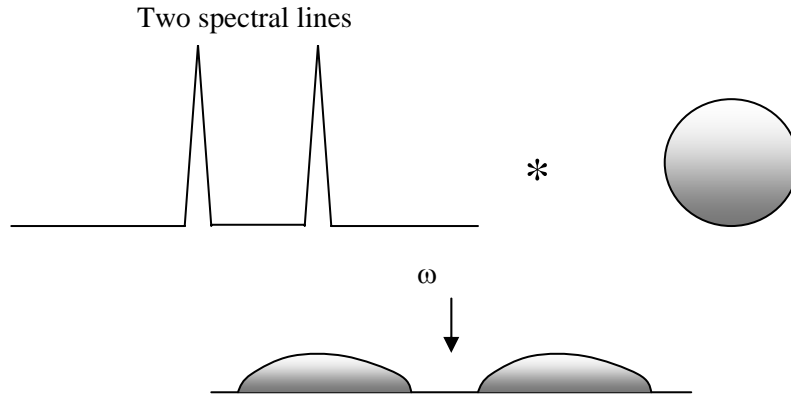


Figure 58 – Convolution of an Object With Two Spectral Lines

We get two separate images, one for each peak. Obviously though, this places severe constraints on homogeneity and requires large chemical shifts and narrow line widths. This is a good technique for an element like Fluorine. For protons, which have a chemical shift of ~ 5 ppm, this is impossible.

Why not then simply deconvolve the spectra with the projection acquired using a larger (relative) gradient?

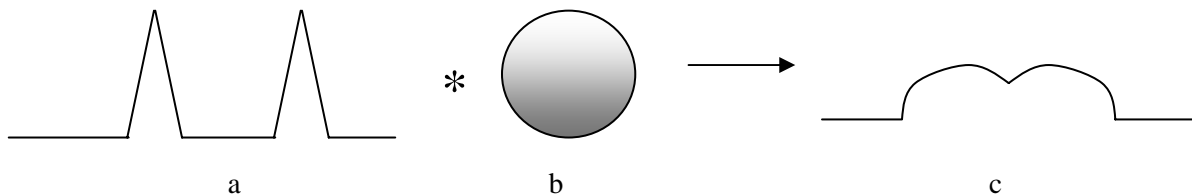


Figure 59 – Chemical Shift Artifact

This can be done, but this supposes that we know (a) in Figure 59 everywhere and of course it is what we are hoping to measure, since it varies across the object. The image (c) which results is exactly what is seen with the **chemical shift artifact**. The shift can be quantified as follows:

In cm	In Pixels
--------------	------------------

$\Delta\omega = \delta_{(ppm)}\omega_o$ $\Delta x = \frac{\Delta\omega}{\gamma G_x}$	$\frac{\Delta\omega}{\text{Hz / point}} = \Delta\omega \cdot TDCT$
--	--

The problem would get very complex for more complex lines shapes as well.

3-D Chemical Shift Imaging

What we would really like to do is read our signal without the presence of a gradient.

$$S(t) = \int \rho(\omega, x, y) e^{i\omega t} d\omega$$

$$S(\omega) = \rho(\omega, x, y)$$

How can we spatially encode? Why not use phase encoding:

$$S(t, n, m) = \iiint \rho(\omega, x, y) e^{i[\omega t + \gamma G_x m + \gamma G_y n]} dx dy d\omega$$

$$FT[S(t, n, m)] = S(\omega, x, y) = \rho(\omega, x, y)$$

This becomes a 3-D object with two spatial dimensions and one frequency dimension. It is possible to perform a 4-D chemical shift image if we also phase encode in the third dimension. The frequency axis in Figure 61 includes both δ and B_o inhomogeneities; therefore, the lines are actually curved. If δ is kept constant (i.e. a vial of water), the inhomogeneities in B_o can be mapped using this technique. It should be noted that this technique is very efficient at low concentrations.

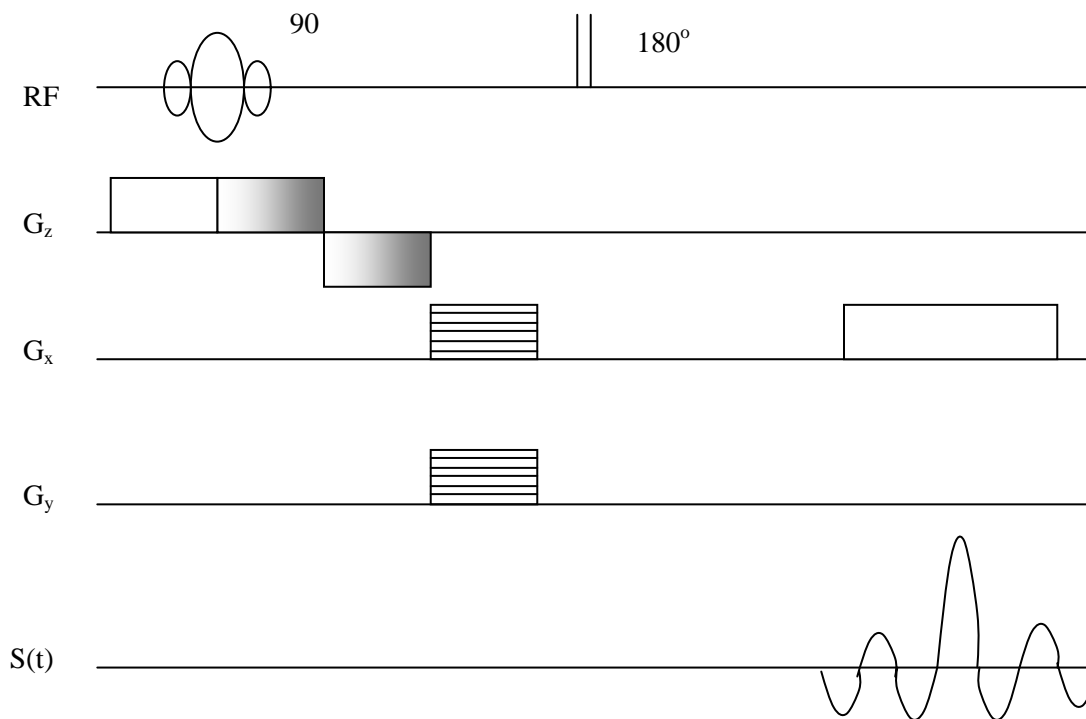


Figure 60 – 3-D Chemical Shift Pulse Sequence

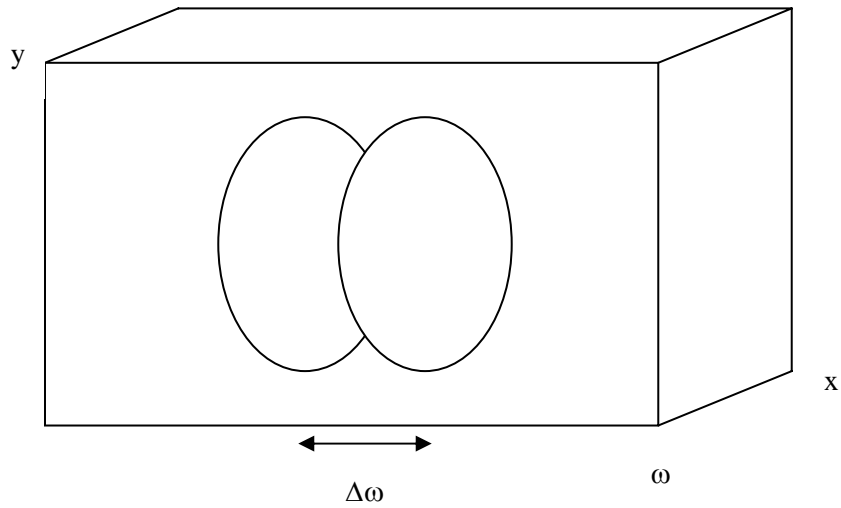


Figure 61 – 3-D Chemical Shift Image

Phase Contrast Imaging

At higher concentrations, it is possible to phase encode the chemical shift instead of the position. This is done by off-setting the spin echo and the gradient echo in a typical spin echo pulse sequence. This can be done by moving the 180° pulse by $\tau/2$. The echo still occurs at $t = TE$ since the gradient echo dominates the inhomogeneities. The spin echo will occur at $TE - \tau$. Since the spin echo refocuses the chemical shifts in an object, different chemical species will pick up different phase shifts during the time τ between the spin echo and the gradient echo.

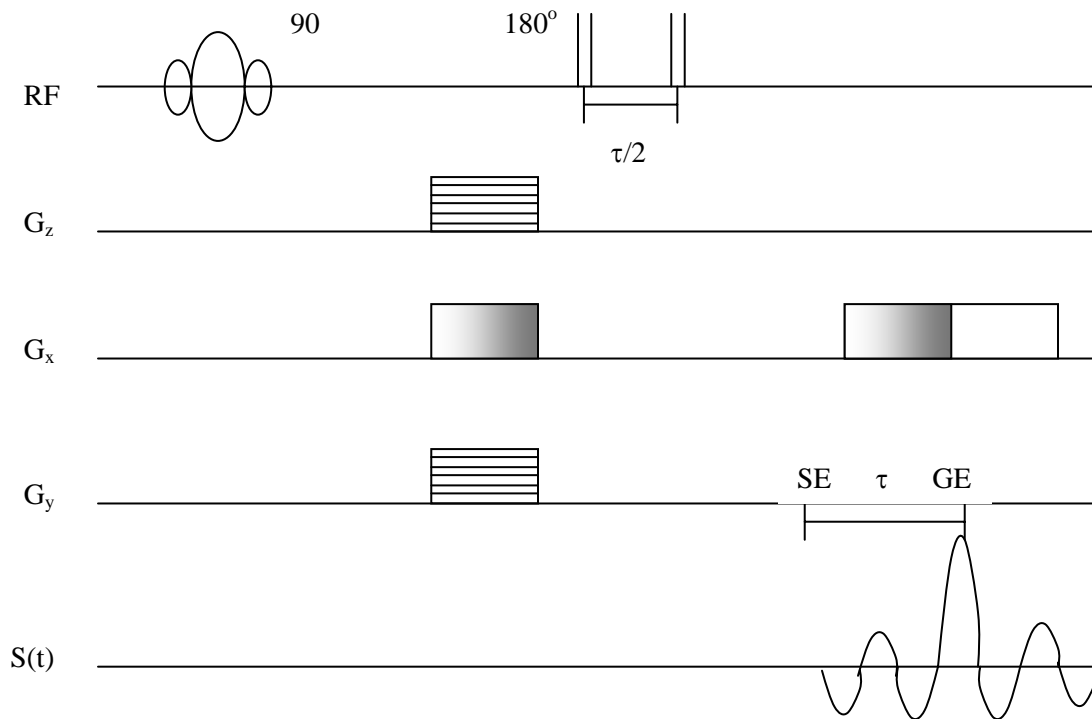


Figure 62 – Phase Encoding Chemical Shift (SHUFFLEBUTT sequence)

$$\Delta\Phi = \tau\Delta\omega = \tau\delta_{(Hz)}$$

Therefore,

$$S(t, n, \tau) = \int \rho(x, y, \delta) e^{i(\gamma G_x x t + \gamma G_y y n + \delta t)} dx dy d\delta$$

By sampling a range of τ values, we can raster through k space. By sampling m different τ steps, we can obtain an m-point frequency spectrum.

This technique gives great spatial resolution but less spectral resolution. This is a valuable when the spectrum is simple (fat and water) since you can keep one “higher resolution” spatial axis. For example, proton imaging is mostly dominated by lipids and water which are 3.5 ppm apart and are present in molar concentrations. In this case, we can further simplify the SHUFFLEBUTT sequence.

Dixon Method

Set $\tau = \frac{1}{2\delta_{(Hz)}}$. This is designed to make lipid and water 180° out of phase: therefore, the image will be

a difference of water and fat (W-F). By taking a conventional “in phase” image where the spin echo and gradient echo occur at the same time, you obtain an image of W+F. Adding these two images will give a pure water image and subtracting the two will give a pure fat image.

Water + Fat	In phase	
<u>Water – Fat</u>	Out of Phase (OOPS)	
Add	2 Water	A pure water image
Subtract	2 Fat	A pure fat image

This technique will work if there are only two spectral lines. We are also assuming that we are looking at the “real” data and not just its magnitude.

Selective Saturation/Excitation

If your spectra is simple, and we have good homogeneity, we could produce a water image by only exciting the water line. This can be done by tuning the RF pulse to the water frequency. Equivalently, we could presaturate the fat line by applying an RF pulse tuned to the fat frequency prior to the experiment. This will cause the fat spins to lie in the transverse plane and as such, when the first slice selective 90° pulse is applied, only the water spins will provide a signal. Inhomogeneities in the magnet will cause the water and fat spectral line to broaden. Due to this line broadening, the pre-saturation pulse may not saturate all of the fat spins but may saturate some of the water spins. To avoid this, the B₀ inhomogeneities must be made as small as possible by shimming the magnet.

This type of chemical shift imaging is important when dealing with very low concentrations, i.e. lactate. In-vivo lactate has a concentration on the order of mM while water has a concentration on the order of 80M. By performing a water suppression pulse, it might be possible to see the lactate. Unfortunately, the chemical shift of lactate is identical to the chemical shift of fat. The lactate line is therefore buried in the 100 M line of fat. We can suppress the lipid line based on the J-coupling.

Binomial Excitation

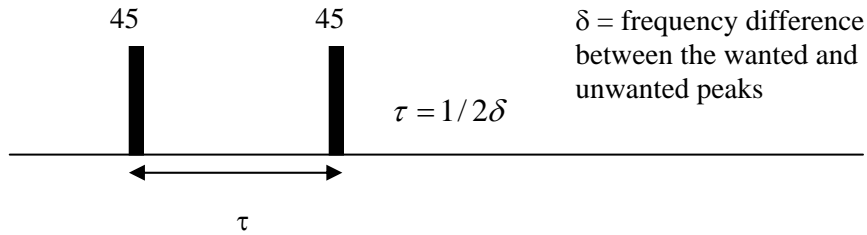


Figure 63 – Binomial Excitation Pulse Sequence

What do we see?

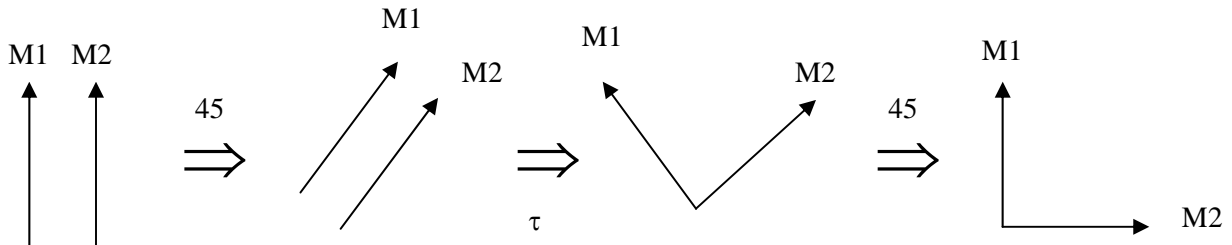


Figure 64 – Schematic of Spins Undergoing Binomial Excitation

If we made the second 45° pulse negative, we obtain a signal from M1 as opposed to M2. We can only see one peak IF we can clearly separate each peak over the whole object (i.e. small inhomogeneities). This kind of water suppression is needed to do in-vivo proton CSI (3-D). We can also perform higher order binomial excitations (1:2:1, 1:3:3:1, etc.), to give more precise excitations.

STIR – Short TI Inversion Recovery

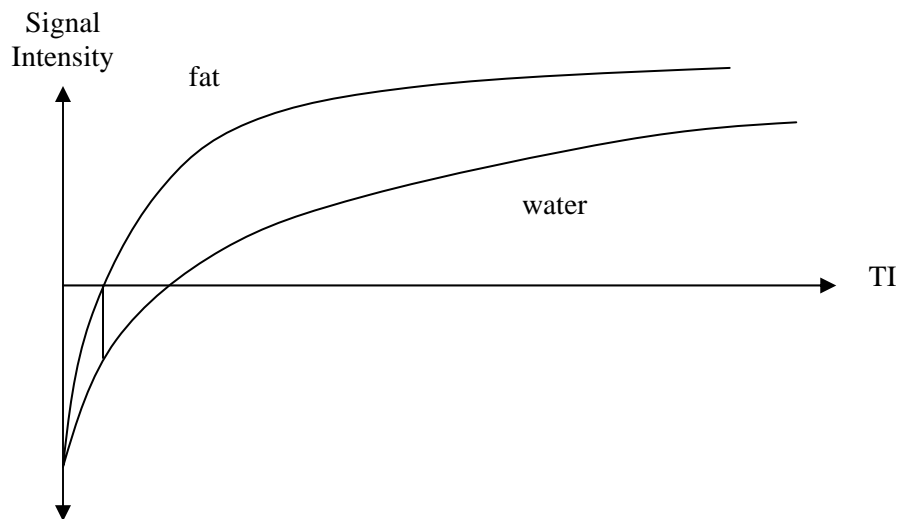


Figure 65 – Null Point TI

By performing an inversion recovery sequence, we can choose TI such that the fat signal is passing through its null point. This method is very dependent on the values of T₁.

CHAPTER 9: FLOW IMAGING

(1) Time of Flight (TOF) or Flow Related Enhancement (FRE)

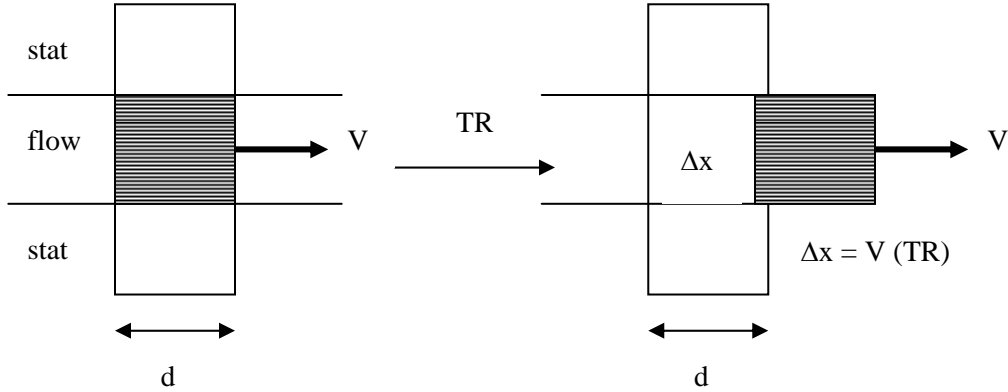


Figure 66 – Imaging Spins Flowing With Speed V

What is the signal for stationary and flowing spins? (assume a $90^\circ - 90^\circ$ pulse sequence)

(a) stationary: $SI \propto \rho \left(1 - e^{-\frac{TR}{T_{1-stat}}} \right) d$

(b) moving: $SI \propto \begin{cases} \rho \left(1 - e^{-\frac{TR}{T_{1-flow}}} \right) (d - V \cdot TR) + \rho \cdot V \cdot TR & V \cdot TR < d \\ \rho \cdot d & V \cdot TR > d \end{cases}$

The signal will actually fall off at high V leading to “flow void”: absent signal within fast moving blood vessels (Figure 67). This is due to the fact that during a spin echo, the spins will move out of the slice during $TE/2$: $V > 2d/TE$.

(2) Phase Velocity Imaging

If we turn on a gradient during the experiment, the spins will accumulate some phase. If the gradient is turned on immediately after the 90° pulse for a time t , then the phase that is accumulated is:

$\Delta\phi = \int \gamma \Delta B dt$. In a constant gradient, if two spins are located at $x = 0$, one is stationary and one is moving at velocity V , then $\Delta B = G_x x$.

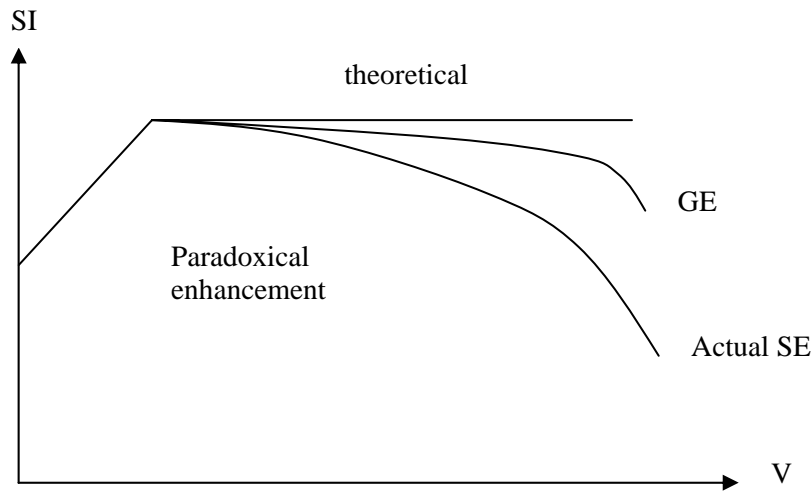


Figure 67 – Signal Intensity as a Function of Velocity

$$\Delta B_{stationary} = 0$$

$$\Delta B_{moving} = \int_0^t \gamma G x dt = \int_0^t \gamma G V t dt = \frac{1}{2} \gamma G V t^2$$

For a spin echo experiment, the phase accumulated before the 180° pulse is reversed and the phase accumulated after the 180° pulse is additive:

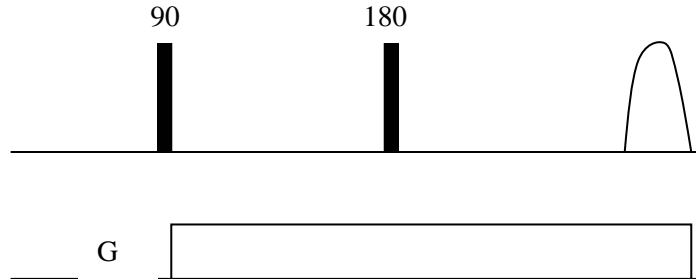


Figure 68 – Spin Echo With Gradient

$$\begin{aligned} \Delta \phi_{SE}(TE) &= - \int_0^{TE/2} \gamma G V t dt + \int_{TE/2}^{TE} \gamma G V t dt \\ &= -\frac{1}{2} \gamma G V \left[-\left(\frac{1}{2} TE\right)^2 + TE^2 - \left(\frac{1}{2} TE\right)^2 \right] \end{aligned}$$

$$\boxed{\Delta \phi_{SE}(TE) = \frac{1}{4} \gamma G V t^2}$$

For a multi-echo experiment,

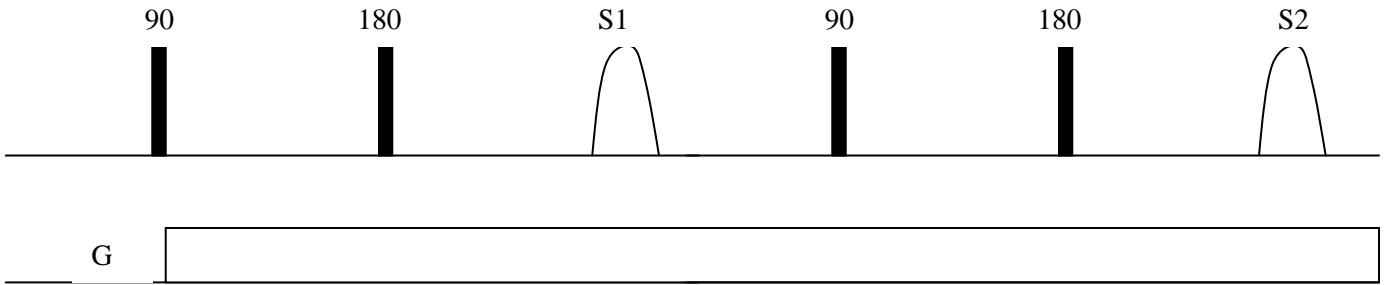


Figure 69 – Multi-echo Experiment

We know what the phase accumulation is for S1. What about for S2?

- (1) Phase accumulated before the first 180° pulse is positive since it is “flipped” twice.
- (2) Phase accumulated between the 180° pulses is reversed.
- (3) Phase accumulated after the second 180° pulse is positive again.

$$\begin{aligned}
 \Delta\phi &= \int_0^{TE/2} \gamma GVt dt - \int_{TE/2}^{3TE/2} \gamma GVt dt + \int_{3TE/2}^{2TE} \gamma GVt dt \\
 &= \frac{1}{2} \gamma GV \left[\left(\frac{1}{2} TE \right)^2 - \left[\left(\frac{3}{2} TE \right)^2 - \left(\frac{1}{2} TE \right)^2 \right] + \left[(2TE)^2 - \left(\frac{3}{2} TE \right)^2 \right] \right] \\
 &= \frac{1}{2} \gamma GV \left[\frac{1}{4} TE^2 - 2TE^2 + \frac{7}{4} TE^2 \right] \\
 &= 0
 \end{aligned}$$

There is no net phase accumulation on the second echo (assuming constant V). This is actually true for all even echoes. Moving spins show no phase shift on even echoes. We still have a net phase shift on all odd echoes.

Is it useful? Look at a geometric interpretation of even echo rephasing.

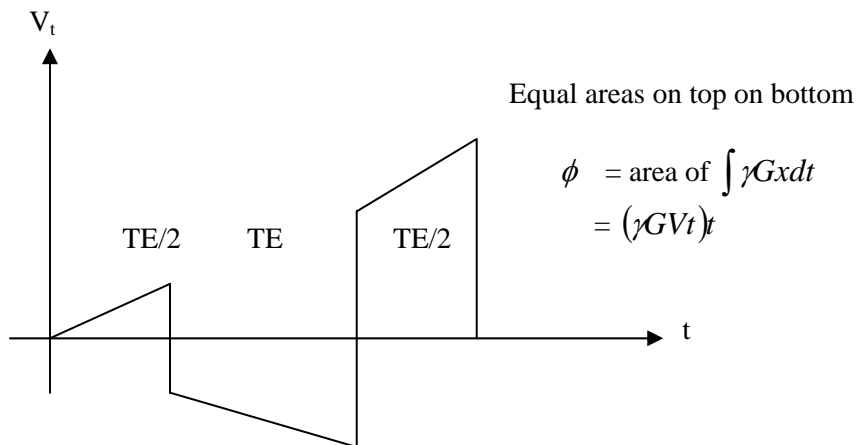


Figure 70 – Geometric Interpretation of Even Echo Rephasing

How can we use this? Lot of ways! $\phi = \left(\frac{1}{4}\gamma TE^2\right)GV$

(1) Phase encode

Note that (again!) we have a phase term proportional to a gradient and a quantity of interest (velocity) ... why not phase encode! (Figure 71)

$$S(t, n, m) = \int \rho(x, y, V) e^{i\left(\gamma G_x x t + \gamma G_y y m + \left(\frac{1}{4}\gamma G_V \tau^2\right) m V\right)} dx dy dV$$

This gives us a 3-D object with the third dimension being the z-axis velocity.

(2) Zebra Imaging

2-D FT imaging gives a phase-velocity relationship: $\Delta\phi \propto kV_x TE^2$, where k depends on the duration and amplitude of G_x . Other gradients (G_z and G_y) affect the signal to a lesser extent since they are on less long. If the flow is laminar, then the phase shift is proportional to velocity.

In a magnitude image, we are insensitive to phase. We can display the “imaginary” component of the signal to get:

$$SI \propto \sin(\phi)$$

(a) for a small ϕ , $SI \propto \phi \propto V$

(b) for a large ϕ , we get redundancy

How can we clear this ambiguity?

1. Put on a “first order” phase shift mX , such that $\phi = kx$. We can do this by displacing the echo in the data collection period – a translation in $t =$ phase shift in w . If we have moving spins, their phase shift is additive with the stationary phase shift, such that $\phi = kx + k'V$ (Figure 72). We can now see large phase shifts and if there are slower flow rates, there is no ambiguity. If we know k, we can measure V.

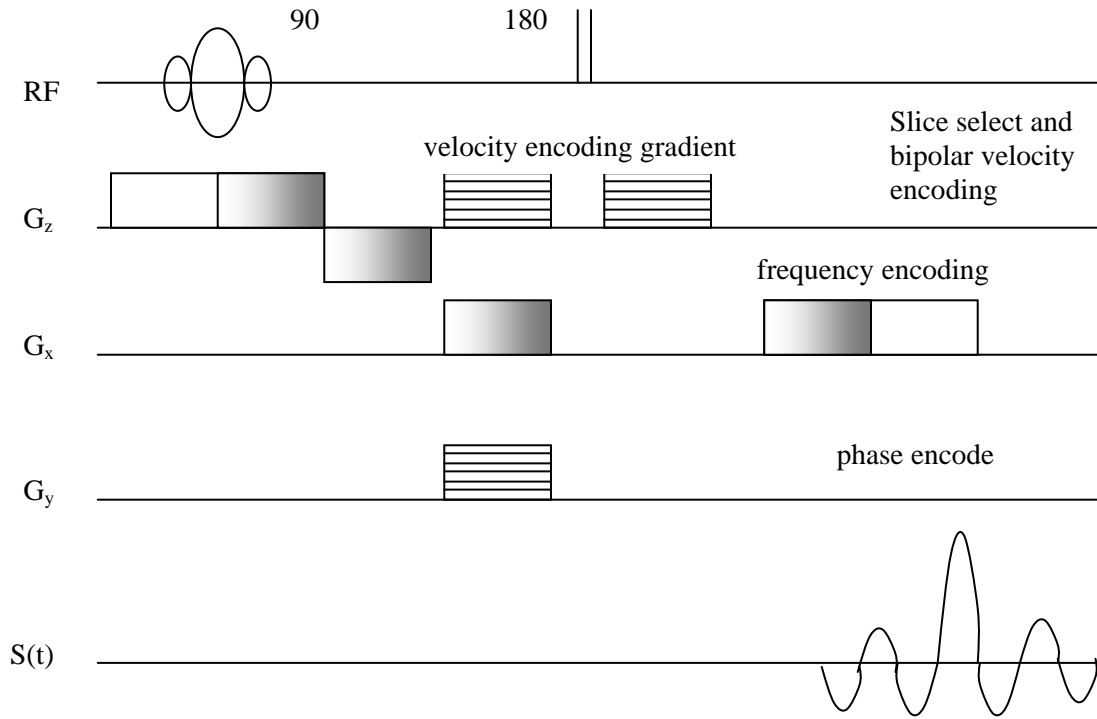


Figure 71 – Velocity Encoding Pulse Sequence

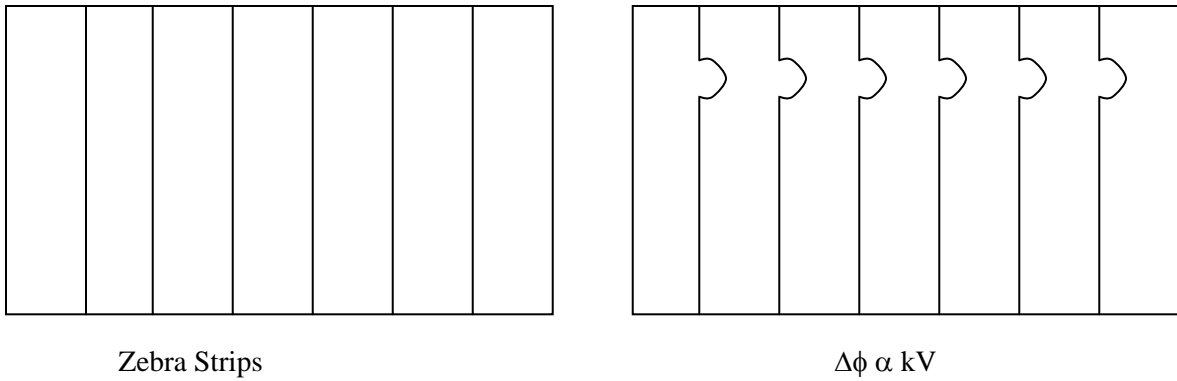


Figure 72 – Zebra Imaging

(3) Projective Imaging

Vessels do not lie in a plane often. In order to see them, we need to take projections, either in acquisition or post-processing.

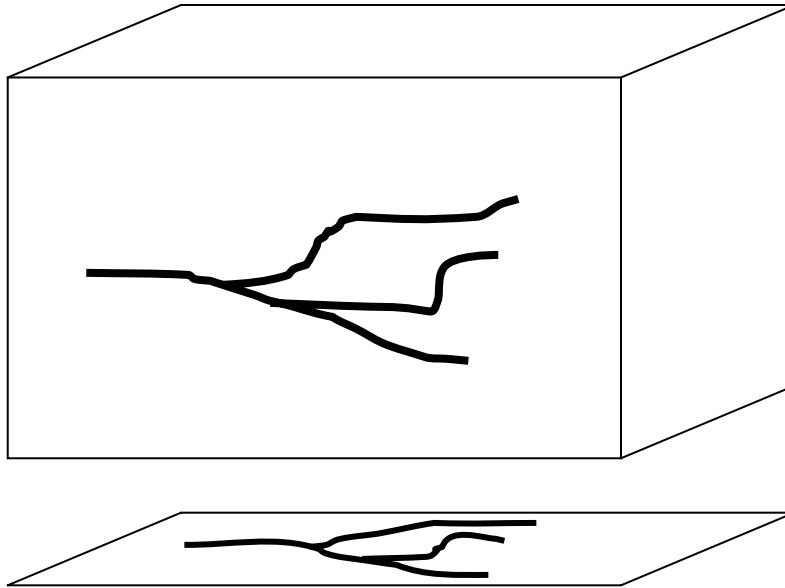


Figure 73 – Projection Image Along z

To do this with MR, simply turn off the slice selective gradient and use hard pulses. It is also possible to acquire a 3-D data set and project in post-processing. How can we “pick out” the blood vessels? In conventional x-ray angiography, inject a lot of x-ray dye with iodine to absorb x-rays. In Digital Subtraction Angiography (DSA), use less x-ray dye but subtract a background image. All that is left is what change which will be the blood vessels (without dye in background image and with dye in second image). In MR, we use the concept of phase contrast.

1. If we take an “imaginary” image ($SI \propto \sin \phi$), then $SI_{stationary} = 0$ and $SI_{moving} \propto V$ for small V (or k). If we took an “imaginary” projective image, we would have a flow projective image (an MR arterio/venogram). However, this assumes a good phase stability across the whole object which is hard to get at high field strengths.
2. How about a subtraction? If k or V is large, we get large phase twists across the vessel.

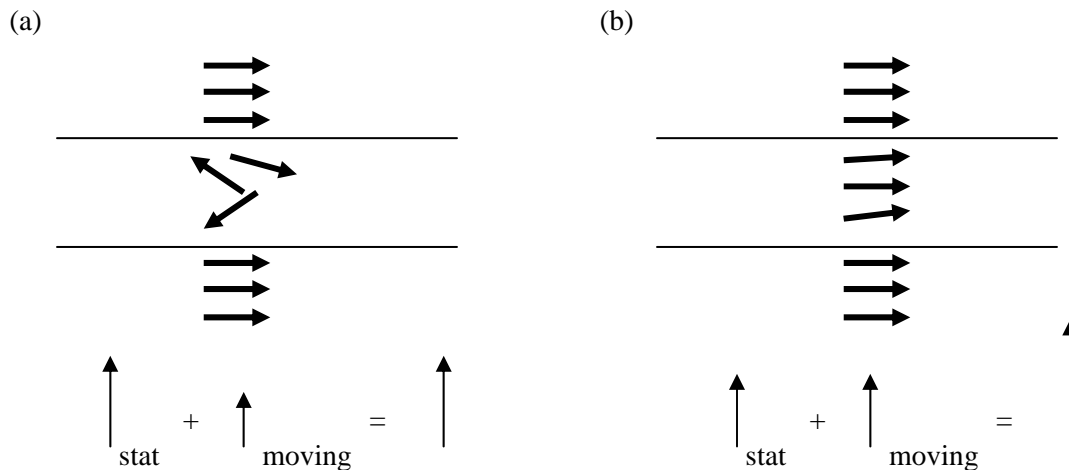


Figure 74 – Fast vs. Slow Moving Spins

Subtract a from b = Flow image.

1. large vs. small V – diastolic/systolic gating
2. large vs. small k – change the gradient waveform

(4) Flow Compensation Gradients

Let's start with a 2 echo experiment. We know that the second echo is rephased (i.e. $k = 0$). Now play some games!

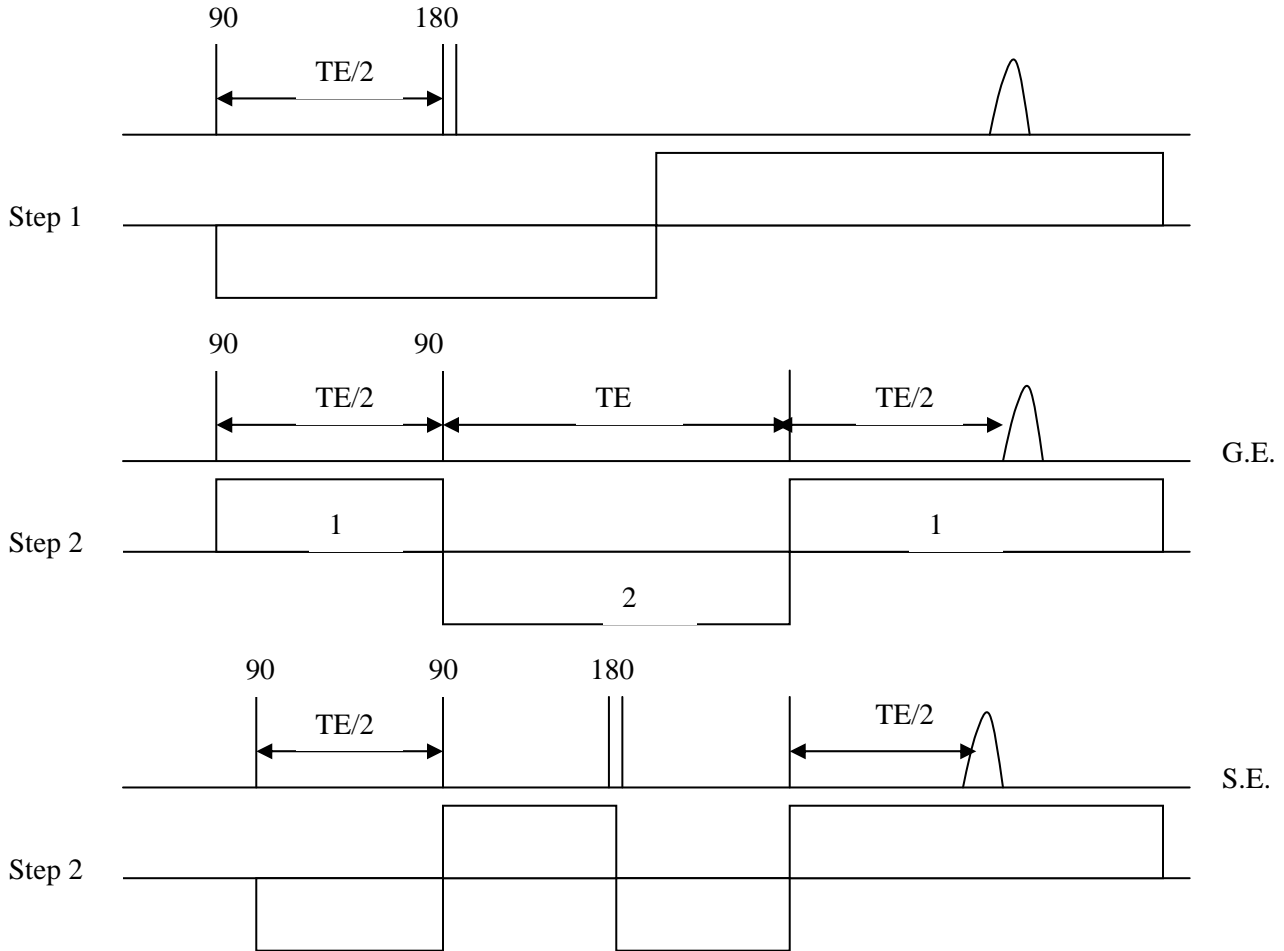


Figure 75 – Gradient Moment Nulling

A bipolar readout gradient will have $k = 0$ for a S.E. A binomial 1:2:1 readout will have $k = 0$ for a G.E. If the gradients are not exactly so balanced, then $k \neq 0$. Higher order binomial gradient pulses null $\Delta\phi$ for higher order motions (e.g. acceleration is nulled with a 1:3:3:1 sequence). Therefore, another way of doing subtraction angiography is to interleave sequences with different k , ($k = 0$ and $k \neq 0$). Subtracting one image from the other will provide flow information.

CHAPTER 10: MICROSCOPIC MOTIONS

Is it possible to measure the diffusion of water with MR? Assume a random walk model. In this situation, there is no average displacement, i.e. $\langle x \rangle = 0$. But, $\langle x^2 \rangle = 2Dt$, where D = diffusion coefficient. In 3-D, $\langle x^2 \rangle = 6Dt$, ($D = \text{cm}^2/\text{s}$). Thus, $\sqrt{\langle x^2 \rangle} \propto \sqrt{t}$. How does this affect the MR signal? What is the phase accumulation of one spin?

$$\begin{aligned} \phi &= \gamma \int_0^{\delta} G(t)x(t)dt \\ &= \gamma g \int_0^{\delta} x(t)dt \\ &= \gamma g \langle x \rangle \delta \\ &= 0! \end{aligned}$$

There is no net phase accumulation because the average is zero. However, if we look at higher order terms:

$$\begin{aligned} \langle \phi^2 \rangle &= \gamma^2 g^2 \delta^2 \langle x^2 \rangle \\ &= \gamma^2 g^2 \delta^2 2D\delta \\ &= 2\gamma^2 g^2 \delta^3 D \end{aligned}$$

For random walk, we get a Gaussian distribution of displacements (x), leading to a Gaussian distribution of phases. Therefore,

$$\begin{aligned} S &= S_o e^{-\frac{\langle \phi^2 \rangle}{2}} \\ &= S_o e^{-\gamma^2 g^2 \delta^3 D} \end{aligned}$$

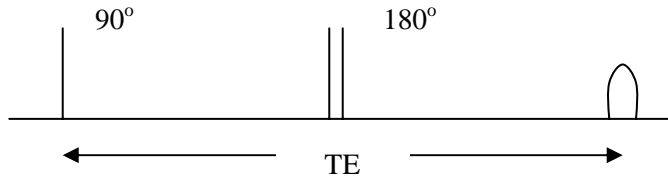
We can obtain a measure for D now: $D = -\frac{\ln\left(\frac{S}{S_o}\right)}{\gamma^2 g^2 \delta^3}$. Diffusion effects vary as $1/t^3$. This is different from T_2 effects which vary as $1/t$. It is therefore possible to separate T_2 effects from diffusion effects.

For a typical spin echo experiment, the 180° pulse does not completely refocus diffusion effects, because the inhomogeneities aren't static. For a spin echo with constant gradient g ,

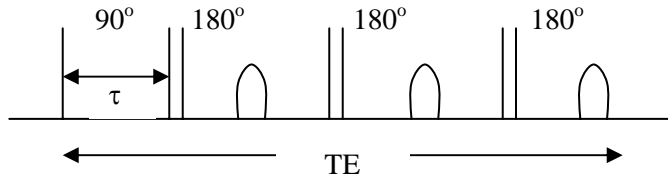
$$\boxed{\ln\left(\frac{S}{S_o}\right) = -\frac{1}{12} \gamma^2 g^2 TE^3 D}$$

How does this predict Hahn vs. CPMG?

Hahn



CPMG



$$\ln\left(\frac{S}{S_o}\right) = \frac{1}{3} \gamma^2 g^2 \tau^2 TE \cdot D$$

Figure 76 – Hahn vs. CPMG Pulse Sequence

For a multiecho sequence, # of echoes $n = \frac{TE}{2\tau}$. Therefore:

$$\ln\left(\frac{S}{S_o}\right)_{CPMG} = -\frac{1}{12} \frac{\gamma^2 g^2 D \cdot TE}{n^2}$$

and the attenuation goes down as n increases. So for large n: $\ln\left(\frac{S}{S_o}\right) = -\frac{TE}{T_2}$ and for n = 1:

$$\ln\left(\frac{S}{S_o}\right) = -\left(\frac{TE}{T_2} + \frac{1}{12} \gamma^2 g^2 TE^3 D\right). \text{ We can separate D from } T_2 \text{ by subtraction.}$$

It is also possible to change the gradient strength or the duration of the gradient. Look at pulsed sequence:

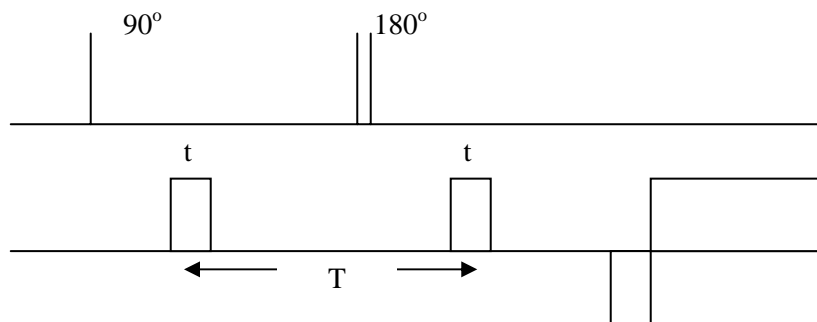


Figure 77 – Stejskal-Tanner Sequence

$$\ln\left(\frac{S}{S_o}\right) = -D \gamma^2 g^2 t^2 \left(T - \frac{t}{3}\right)$$

This is known as the Stejskal-Tanner equation. It can be used in imaging if the read gradient is small or if it is explicitly corrected for.

What happens if $\langle x^2 \rangle \neq 2Dt$? This could happen if barriers prevented free diffusion. This is observed in tissue and is labeled restricted diffusion. In vivo, we may actually get retarded diffusion.

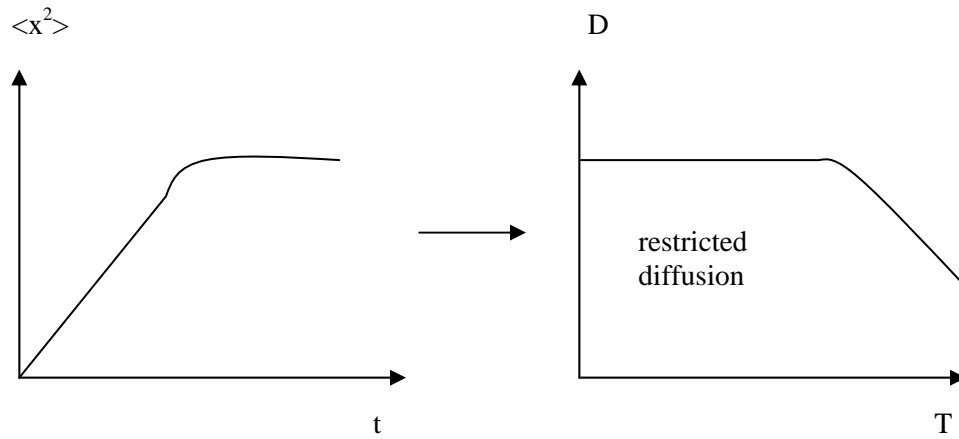


Figure 78 –Restricted Diffusion

CHAPTER 11: RAPID IMAGING

Imaging time = $TR \frac{PES}{PES / excitation} N_{ave}$ where PES = Phase Encoding Steps. To reduce this time, we must reduce one of the factors.

- (1) To reduce N_{ave} (NEX) implies high SNR, an increased B_0 and decreased resolution.
- (2) “Half Fourier” or “half NEX”: Since the object is a real function, its Fourier Transform shows conjugate symmetry:

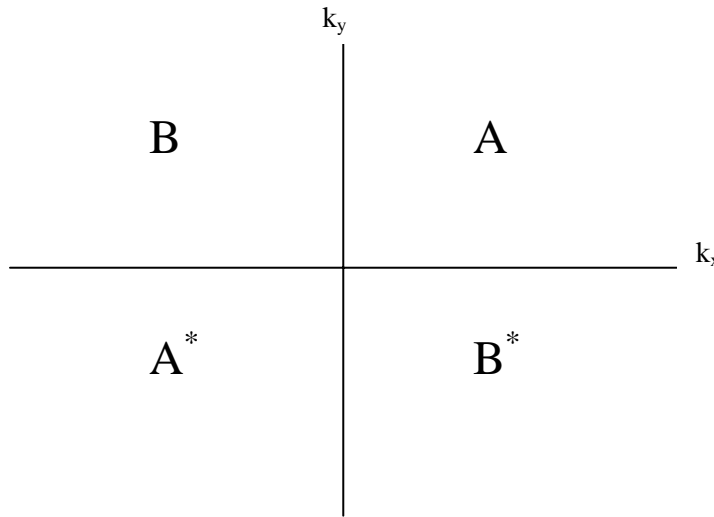


Figure 79 – Conjugate Symmetry of k-space

So in principle, half of k-space is conjugate.

- (a) half in time \Rightarrow short TE's
- (b) half in pseudo time \Rightarrow lower imaging time (labeling half NEX)

3a) Reduce TR – FLASH/GRASS –

- Implies gradient echoes to avoid M_L inversion
- Small tip angles
- Steady state or “spoiled”

3b) “Turbo” FLASH – Very short TR/TE (but this leads to little T_1/T_2 contrast) – To improve the contrast, perform magnetization preparation:

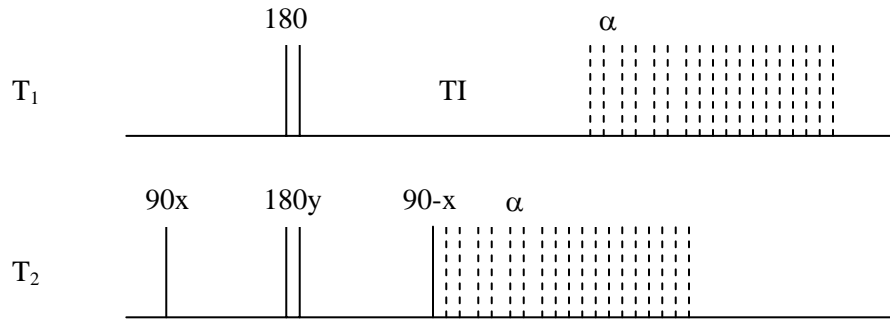


Figure 80 – IR Turbo Flash

(4) Increase # of PES/RF excitation

(a) RARE or “Fast Spin Echo” – Do a CPMG with addition of PES during each echo

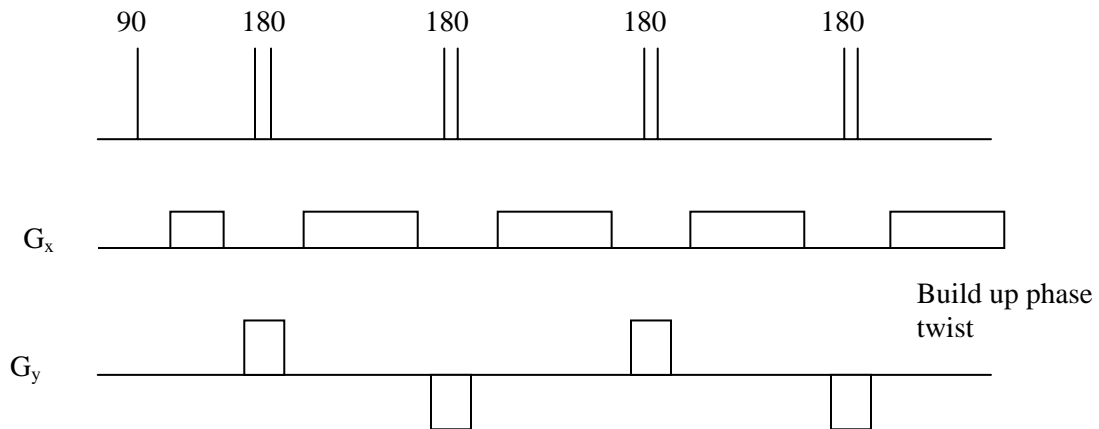


Figure 81 – Fast Spin Echo Sequence

Currently, there are 8-32 180° pulses per excitation. The advantage is that this is 8-32 times faster than conventional T_1 and T_2 contrast images. The disadvantage is that lots of 180° pulses produce RF heating over a long acquisition.

(b) Spiral Scan:

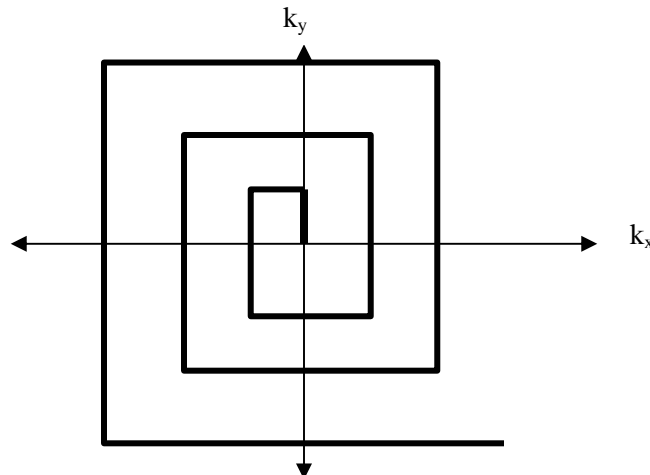


Figure 82 – Spiral Scan Through k-Space

Currently, interleave 8 such scans to cover k-space.

(c)

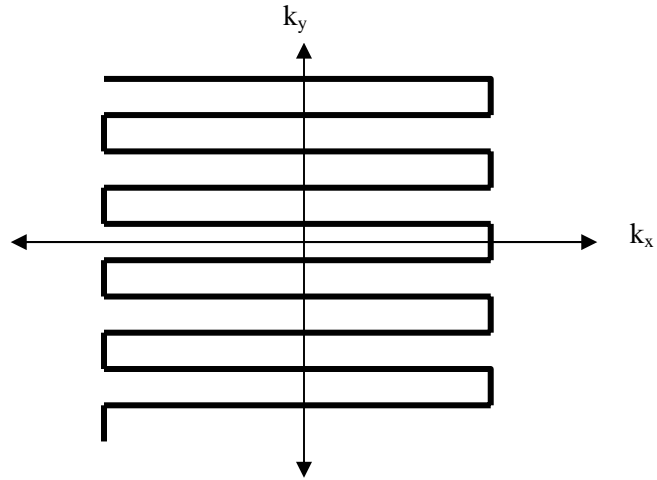


Figure 83 – EPI Scan Through k-space